

2008

The study of compensatory motions while using a transradial prosthesis

Stephanie Lutton Carey
University of South Florida

Follow this and additional works at: <http://scholarcommons.usf.edu/etd>

 Part of the [American Studies Commons](#)

Scholar Commons Citation

Carey, Stephanie Lutton, "The study of compensatory motions while using a transradial prosthesis" (2008). *Graduate Theses and Dissertations*.
<http://scholarcommons.usf.edu/etd/160>

This Dissertation is brought to you for free and open access by the Graduate School at Scholar Commons. It has been accepted for inclusion in Graduate Theses and Dissertations by an authorized administrator of Scholar Commons. For more information, please contact scholarcommons@usf.edu.

The Study of Compensatory Motions While Using a Transradial Prosthesis

by

Stephanie Lutton Carey

A dissertation submitted in partial fulfillment
of the requirements for the degree of
Doctor of Philosophy
Department of Chemical and Biomedical Engineering
College of Engineering
University of South Florida

Major Professor: Rajiv V. Dubey, Ph.D.
M. Jason Highsmith, DPT
William E. Lee, III, Ph.D.
Craig Lusk, Ph.D.
Murray E. Maitland, Ph.D.

Date of Approval:
March 20, 2008

Keywords: biomechanics, amputee, motion analysis, kinematics, activities of daily living

© Copyright 2008, Stephanie L. Carey

Acknowledgements

I would like to thank my advisor, Dr. Rajiv Dubey, for providing me great opportunities to teach, research and present at conferences and sharing his knowledge on these subjects. I would also like to express my gratitude to Dr. Jason Highsmith for taking time to find volunteers, collect data, edit my manuscripts and encourage me. I would also like to thank the rest of my committee, Dr. Murray Maitland, Dr. Craig Lusk, and Dr. Bill Lee for valuable advice and guidance throughout this doctoral process.

I would like to thank Greg Bauer, president of Westcoast Brace and Limb for recruiting volunteers and Dr. Sam Phillips, Dean of the St. Petersburg College of Orthotics and Prosthetics for technical advice.

I sincerely thank my husband, Craig Carey, for his unconditional love and support and for taking care of our children and home. I am grateful to my in-laws, Don and Audrey Carey, and Colette Carey Swingle, for raising such a wonderful son and brother. I would like to acknowledge my children, Jack Donald and Amelia Joan Carey, who greet me, daily with smiles.

I would like to thank my mother, Dr. Joan Drody Lutton, the first person I knew with a doctoral degree. She has taught me perseverance and independence. I would like to express my gratitude to my father, Stephen C. Lutton, who doted on my children while I studied and worked. My parents have taught me to love learning and always supported me and my endeavors.

I would like to send a big “Yahoo” out to my brothers, Andy Lutton and Don Lutton, for making me laugh at least every Friday, for providing me with good music to listen to while studying and for helping me to take my life less seriously. I will always appreciate my sister-n-laws, Lorraine Lutton and Jennifer Lutton for showing me it is possible to be a successful mother and career woman.

I would like to sincerely acknowledge Theresa Nolla and Derek Lura for helping me collect and analyze motion analysis data.

Note to Reader

The original of this document contains color that is necessary for understanding the data. The original dissertation is on file with the USF library in Tampa, Florida.

Table of Contents

| | |
|---|------|
| List of Tables | vi |
| List of Figures | viii |
| Abstract | xi |
| Chapter 1: Introduction | 1 |
| 1.1 Research Motivation | 1 |
| 1.2 Objectives | 4 |
| 1.3 Hypotheses | 5 |
| 1.4 Dissertation Outline | 6 |
| Chapter 2: Background | 8 |
| 2.1 Technical Background | 8 |
| 2.1.1 Newton's Laws of Motion | 8 |
| 2.1.2 Biomechanics and Anthropometrics | 9 |
| 2.1.3 Euler Angles | 10 |
| 2.1.4 Newton-Euler Inverse Dynamics Method | 10 |
| 2.2 Anatomy and Biomechanics of the Human Arm | 11 |
| 2.2.1 Shoulder Complex | 11 |
| 2.2.2 Elbow and Forearm Complex | 13 |
| 2.2.3 Wrist | 14 |
| 2.3 Upper Limb Prosthesis | 15 |
| 2.3.1 Terminal Devices | 15 |

| | | |
|------------|---|----|
| 2.3.2 | Wrist Units | 16 |
| 2.3.3 | Control Devices | 16 |
| 2.3.4 | Current Approaches for Fitting an Upper Limb Prosthesis | 17 |
| 2.4 | Prior Research | 18 |
| 2.4.1 | Gait Analysis and Prosthetic Design | 18 |
| 2.4.2 | Upper Limb Motion Analysis | 19 |
| 2.4.3 | Upper Limb Research for Orthotic and Prosthetic Design | 20 |
| Chapter 3: | Design of Experiment | 22 |
| 3.1 | Introduction | 22 |
| 3.2 | Participants | 23 |
| 3.3 | Activities of Daily Living | 24 |
| 3.4 | Test Protocol | 26 |
| 3.4.1 | Subject Measurements | 26 |
| 3.4.2 | Marker Placement | 26 |
| 3.4.3 | Experimental Trials | 27 |
| Chapter 4: | Experimental Instrumentation and Set-up | 29 |
| 4.1 | Introduction | 29 |
| 4.2 | Testing Apparatus | 29 |
| 4.3 | Vicon™ Motion Analysis System | 31 |
| 4.3.1 | Hardware | 31 |
| 4.3.2 | Software | 31 |
| 4.4 | ATI™ Force/Torque Transducer | 32 |
| 4.5 | Calibration | 33 |

| | |
|---|----|
| 4.5.1 Calibration of the Cameras | 33 |
| 4.5.2 Calibration of the ATI TM Transducer | 34 |
| Chapter 5: Kinematic Model | 35 |
| 5.1 Introduction | 35 |
| 5.2 Determining Local Coordinate Systems | 35 |
| 5.2.1 Introduction | 35 |
| 5.2.2 Torso Segment | 37 |
| 5.2.3 Upper Arm Segment | 38 |
| 5.2.4 Forearm Segment | 38 |
| 5.2.5 Wrist Segment | 39 |
| 5.2.6 Hand Segment | 39 |
| 5.3 Calculation of Joint Angles | 40 |
| Chapter 6: Kinetic Chain and Inverse Dynamics | 42 |
| 6.1 Introduction | 42 |
| 6.2 Segment Hierarchy Description | 43 |
| 6.3 Kinetic Chain While Opening a Door | 45 |
| 6.4 Kinetic Chain While Lifting a Box | 46 |
| 6.5 Adjusted Inertial Properties for an Upper Limb Prosthesis | 46 |
| 6.6 Adjusted Inertial Properties with Added Mass | 49 |
| Chapter 7: Data Analysis | 52 |
| 7.1 Validation | 52 |
| 7.2 Reliability | 55 |
| 7.3 Kinematic Outcome Measures | 56 |

| | |
|--|----|
| 7.4 Kinetic Outcome Measures | 56 |
| 7.5 Statistical Analysis | 57 |
| 7.5.1 Power Calculation to Determine Sample Size | 57 |
| 7.5.2 Between Subject Analysis | 58 |
| 7.5.3 With-In Subject Analysis | 59 |
| Chapter 8: Descriptive Observations | 60 |
| 8.1 Control Subjects | 60 |
| 8.2 Prosthesis Wearing Subjects | 62 |
| 8.3 Case Study of Prosthesis User Subject # 3 | 63 |
| Chapter 9: Experimental Results | 67 |
| 9.1 Range of Motion Results | 67 |
| 9.1.1 Between Group Results | 67 |
| 9.1.1.1 Drinking from a Cup | 68 |
| 9.1.1.2 Opening a Door | 69 |
| 9.1.1.3 Lifting a Box | 72 |
| 9.1.1.4 Turning a Steering Wheel | 75 |
| 9.1.2 Braced Group With-In Subject Results | 77 |
| 9.1.3 Prosthesis Wearing Group With-In Subject Results | 79 |
| 9.2 Kinetic Results | 81 |
| 9.2.1 Between Group Kinetic Results | 82 |
| 9.2.2 Prosthesis Wearing Group With-In Subject Results | 86 |
| Chapter 10: Discussion | 91 |
| 10.1 Limitations of the Study | 91 |

| | |
|--|----------|
| 10.2 Comparison of Results to Similar Studies | 94 |
| 10.3 Discussion of Results | 96 |
| 10.3.1 Drinking from a Cup | 97 |
| 10.3.2 Opening a Door | 98 |
| 10.3.3 Lifting a Box | 98 |
| 10.3.4 Turning a Steering Wheel | 100 |
| 10.3.5 Review of Hypotheses | 101 |
| 10.4 Recommendations | 102 |
| Chapter 11: Summary and Conclusions | 105 |
| 11.1 Contributions | 105 |
| 11.2 Future Studies | 105 |
| 11.2.1 Biomechanical Model | 106 |
| 11.2.2 Prosthetic Component Design Testing | 108 |
| 11.3 Conclusions | 108 |
| List of References | 110 |
| Appendices | 115 |
| Appendix A: Bodybuilder™ Software Program for Upper Limb Calculations | 116 |
| Appendix B: Solution to an Open Chain 2D Example Problem | 125 |
| About the Author | End Page |

List of Tables

| | |
|---|----|
| Table 3.1. Descriptions of the transradial prosthesis users. | 23 |
| Table 3.2. Descriptions of the tasks analyzed. | 25 |
| Table 3.3. Descriptions of the subject measurements collected prior to testing. | 26 |
| Table 3.4. Marker placement and code names of markers used in programming. | 27 |
| Table 6.1. Inertial properties from a typical TRMP calculated from a suspension test. | 49 |
| Table 6.2. Adjusted inertial properties of the prosthesis users with added mass. | 51 |
| Table 7.1. Measurements of shoulder and elbow angles from the goniometer and the Vicon™ system. | 54 |
| Table 7.2. Measurements of elbow flexion of skeleton model. | 54 |
| Table 8.1. The maximum, minimum and range of motions (in degrees) during each task for Subject # 3 of prosthesis users. | 65 |
| Table 9.1. Average and standard deviation (SD) peak wrist flexion and extension and peak forearm pronation and supination of right (dominant) side (in degrees) of control group during the four tasks. | 67 |
| Table 9.2. The maximum and range of motion of the glenohumeral (GH) joint and the elbow joint of the three groups while drinking from a cup. | 68 |
| Table 9.3. Maximum and total range of motion of shoulder and elbow of the reference, braced and prosthetic side while drinking from a cup. | 70 |
| Table 9.4. Average maximum (Max) and range of motion (ROM) of the three groups while lifting a box. | 73 |
| Table 9.5. Average maximum (Max) and range of motion (ROM) of the three groups while turning a steering wheel to the affected side. | 76 |
| Table 9.6. Maximum and range of motions of braced group while drinking from a cup during three mass conditions. | 78 |

| | |
|---|----|
| Table 9.7. Maximum and range of motions of the braced group while opening a door during three mass conditions. | 78 |
| Table 9.8. Maximum and range of motions of braced group while lifting a box during three mass conditions. | 78 |
| Table 9.9. Maximum and range of motions of braced group while turning a steering wheel during three mass conditions. | 79 |
| Table 9.10. Maximum and range of motions of prosthesis users while drinking from a cup at three mass conditions. | 80 |
| Table 9.11. Maximum and range of motions of prosthesis users while opening a door at three mass conditions. | 80 |
| Table 9.12. Maximum and range of motions of prosthesis users while lifting a box at three mass conditions. | 81 |
| Table 9.13. Maximum and range of motions of prosthesis users while turning a steering wheel at three mass conditions. | 81 |
| Table 10.1. A review of statistically significant findings during the unilateral tasks. | 96 |
| Table 10.2. A review of statistically significant findings during the bilateral tasks. | 97 |

List of Figures

| | |
|---|----|
| Figure 2.1. Movement of the glenohumeral joint. | 12 |
| Figure 3.1. Brace used to restrict forearm and wrist motion. | 28 |
| Figure 4.1. Testing apparatus used to complete the tasks. | 30 |
| Figure 4.2. The steering wheel used for the turning task. | 30 |
| Figure 4.3. ATI TM Gamma transducer connected to the door knob. | 33 |
| Figure 4.4. L-frame and wand used for the calibration of the Vicon TM motion analysis system. | 34 |
| Figure 5.1. Local coordinate systems of defined segments. | 40 |
| Figure 6.1. Marker placements on the box during the bilateral lifting task. | 46 |
| Figure 6.2. Suspension test on a typical TRMP to determine inertial properties. | 49 |
| Figure 6.3. Depiction of the forearm (FA) with mass added at the elbow and at the wrist. | 50 |
| Figure 7.1. Linear regression between the goniometer and Vicon TM for shoulder flexion. | 53 |
| Figure 7.2. Average shoulder flexion with standard deviations shaded areas of one subject opening a door three times showing repeatability. | 55 |
| Figure 8.1. a. Torso right side bend during the door task. | 65 |
| Figure 8.1. b. Elbow flexion during the door task. | 65 |
| Figure 9.1. Average range of motion of the glenohumeral (GH) joint in the sagittal plane of the three groups while drinking from a cup. | 68 |
| Figure 9.2. Average range of elbow flexion of the three groups while drinking from a cup. | 69 |

| | |
|---|----|
| Figure 9.3. Average range of shoulder rotation of the three groups while opening a door. | 70 |
| Figure 9.4. Average range of elbow flexion of the three groups while opening a door. | 71 |
| Figure 9.5. Torso side bending (toward affected side) of one subject from each group while opening a door. | 71 |
| Figure 9.6. Average torso bending (affected side +; unaffected side -) during door opening of the three groups. | 72 |
| Figure 9.7. Average torso bending (forward + / backward-) while lifting a box. | 73 |
| Figure 9.8. Average range of torso bending (Right side +; Left side -) while lifting a box. | 74 |
| Figure 9.9. Degree of asymmetry during the box lift for each of the three groups. | 74 |
| Figure 9.10. Right (affected) and left shoulder flexion of one subject during the non-braced and braced conditions while turning a steering wheel to the affected side. | 75 |
| Figure 9.11. Average range of elbow flexion of the reference, braced and prosthetic side while turning a steering wheel to the affected side. | 76 |
| Figure 9.12. Degree of asymmetry of range of motions during the steering wheel right turn. | 77 |
| Figure 9.13. Degree of asymmetry of elbow flexion while lifting a box during four conditions. | 79 |
| Figure 9.14. The peak external joint forces of the non-braced (NB) group and the prosthesis user (PROS) group while opening a door. | 82 |
| Figure 9.15. The peak shoulder joint forces of the non-braced (NB) group and the prosthesis user (PROS) group while lifting a box. | 83 |
| Figure 9.16. The peak elbow joint forces of the non-braced (NB) group and the prosthesis user (PROS) group while lifting a box. | 83 |
| Figure 9.17. The peak wrist joint forces of the non-braced (NB) group and the prosthesis group (PROS) group while lifting a box. | 84 |
| Figure 9.18. Degree of asymmetry of the peak shoulder joint forces between the non-braced (NB) group and prosthesis wearing (PROS) group. | 84 |

| | | |
|--------------|--|-----|
| Figure 9.19 | Degree of asymmetry of the peak elbow joint forces between the non-braced (NB) group and prosthesis wearing (PROS) group. | 85 |
| Figure 9.20. | Degree of asymmetry of the peak wrist joint forces between the non-braced (NB) group and prosthesis wearing (PROS) group. | 85 |
| Figure 9.21. | Shoulder (Sh) and elbow (El) joint moments between the non-braced (NB) group and prosthesis wearing (PROS) group while opening a door. | 86 |
| Figure 9.22. | Peak joint forces while opening a door during three mass conditions. | 87 |
| Figure 9.23 | Peak shoulder (Sh) and elbow (El) moments while opening a door during three mass conditions. | 87 |
| Figure 9.24. | Peak external forces acting on the shoulder joint while lifting a box during three mass conditions. | 88 |
| Figure 9.25. | Peak external forces acting on the elbow joint while lifting a box during three mass conditions. | 88 |
| Figure 9.26. | Peak external forces acting on the wrist joint while lifting a box during three mass conditions. | 89 |
| Figure 9.27. | Peak moments acting at the shoulder while lifting a box during three mass conditions. | 89 |
| Figure 9.28. | Peak moments acting at the elbow while lifting a box during three mass conditions. | 90 |
| Figure 11.1. | Schematic of biomechanical simulation model for compensatory motion of transradial prosthesis users created by Derek Lura. | 107 |
| Figure B.1. | A free body diagram of the arm. | 125 |

The Study of Compensatory Motions While Using a Transradial Prosthesis

Stephanie Lutton Carey

ABSTRACT

Improvement of prostheses requires knowledge of how the body adapts. A transradial prosthesis without a dynamic wrist component may cause awkward compensatory motion leading to fatigue, injury or rejection of the prosthesis. This work analyzed the movements of shoulder, elbow and torso during four tasks: drinking from a cup, opening a door, lifting a box and turning a steering wheel.

The main purpose of this study was to determine if using a basic transradial prosthesis that lacks motion of the forearm and wrist would cause significant compensatory motion of the shoulder, elbow and torso during the tasks. The second purpose of the study was to determine if the location of added mass would affect compensatory movements during these tasks.

A group of able-bodied participants were asked to complete the tasks, without and with a brace, simulating a basic transradial prosthesis to determine if bracing is an appropriate way to study prosthetic use. Transradial prosthesis wearers also completed the tasks without and with added mass at the elbow or at the wrist to determine if distribution of mass has an effect on the motions. Using a motion capture system movements of the shoulder, elbow and torso were analyzed. For the bilateral tasks, the degree of asymmetry (DoA) was calculated for each subject. Statistical analysis was

completed within subject comparing the mass interventions and between subjects comparing the control, braced and prosthesis wearing groups.

While opening a door and lifting a box, prosthesis users compensated predominantly by bending the torso sideways toward affected side. During the steering wheel task, amputees used more elbow flexion to accommodate for the lack of forearm rotation. While drinking from a cup, compensation occurred by bending the cervical spine, although this was not measured. Adding mass increased the joint forces and moments during the box lift.

This research can be used for transradial prosthesis design improvements as well as improving methods of prosthesis fitting and therapeutic training by providing quantitative data of compensatory motion. The data from this study is being used to develop a model for an upper limb prosthesis.

Chapter 1: Introduction

1.1 Research Motivation

According to 1996 survey conducted by the Amputee Coalition of America, approximately 1,285,000 persons in U.S. have an amputation excluding finger and toes [1]. Due to the present war in Iraq and Afghanistan, the numbers of amputees including upper limb amputees will most likely increase. According to the Department of Veteran's Affairs (VA), since Feb. 2006 over 400 soldiers have suffered an amputation because of the casualties of war [2]. According to the Veteran Affairs Department's survey of traumatic amputees, 22% perceive a prosthesis as "not good for anything" [3]. Amputees often choose not to wear a prosthesis due to marginal performance or may settle for a prosthesis that offers only a cosmetic improvement, but that lacks function [4]. In the United States, rejection rates for upper limb prostheses have been shown to be as high as 50% [5]. Poor function of an upper limb prosthesis may cause awkward compensatory motion. These awkward motions have been cited as an explanation for the discontinuation of prosthetic use [5]. Quantification of these compensatory motions can help to test design changes and training methods of the upper limb prosthesis.

The majority of upper extremity amputations occur below the elbow and are referred to as transradial amputations[6]. The terminal device of a transradial prosthesis can be controlled by excursion of the shoulder via cables (body powered) or controlled by muscle contractions in the residual limb (myoelectric). This study is limited to the use of a transradial myoelectric prosthesis (TRMP).

Current research on the optimal designs of TRMPs includes advanced technology in control systems and electronic circuitry that allow for human motion mimicking of and prosthesis function movement. Often times these improvements require large amounts of power, circuitry and excess mass distally along the prosthesis that may require greater effort from the user. The increased weight of the myoelectric prosthesis is a common cause for complaints among users [5, 7-10] [11][12].

Persons using a myoelectric upper limb prosthesis are forced to decide if the extra function provided by the advanced electronics is worth carrying the extra mass which may cause fatigue, socket issues and greater stress on the remaining joints. An example is the wrist rotator component of the TRMP which may allow greater function and reduce compensatory motion, but adds mass distally, potentially causing greater torques on remaining joints. It may also be important to consider the distribution of weight. The human hand, forearm and upper arm each weigh a certain percentage of the total arm that seems to result in minimal effort across a wide variety of tasks.

Pronation and supination of the forearm are important in normal completion of many activities of daily living [13]. According to surveys, users would like the wrist component of the prosthesis to perform more movements particularly drinking from a glass and opening a door [14]. This suggests that the wrist component of an upper limb prosthesis is important. Surveys are a useful tool to determine specific needs of a given population, but there is also a need for evidence-based research when setting guidelines for design, fitting and training techniques for the TRMP.

In March 2005, the Defense Sciences Office of the Defense Advanced Research Projects Agency (DARPA) announced a Prosthesis 2007 program to advance the research

in upper limb prosthetic design. The goal of the project is to improve the capabilities of the upper limb prosthesis. DARPA listed 17 desired characteristics for an upper arm prosthesis system, which included inertial properties that matched the lost limb, wrist flexion strength of up to 1.67 ft-lbs, 2-degrees of freedom at the wrist and humeral rotation [15]. This dissertation attempts to address this particular subset of the characteristics deemed by the Department of Defense to be of great importance in upper limb prosthetic design improvement. The study discussed in this dissertation considered how the joint angles and torques were affected by mass added at different locations. It may also be of interest to determine how inertial properties of the TRMP alter torques at the interface between the prosthesis and the residual limb, but this concept was not explored here.

The evolution and improvements of lower limb prostheses have often been made on the basis of studying gait pattern studies. These studies determine common parameters that constitute a normal gait, and lower limb prostheses are often designed to mimic 'normal' gait as characterized by these parameters. Many studies have analyzed the speed, energy costs, and efficiency of gait. These gait analysis studies have included kinematic studies determining the joint angles, angular velocity and acceleration during different phases of a gait pattern. Kinetics or the forces, moments and powers of the various joints required for walking have also been thoroughly studied. The parameters obtained from these tests enable designs to be adjusted to match expected normal values. In depth gait analysis also provides a tool to properly test and compare prosthetic performance. Detailed examples of gait analysis studies will be discussed in Chapter 2.

This type of detailed motion benchmarking of the upper limb is often lacking in the literature. A review of the limited current publications in this area is discussed in Chapter 2. The essential difficulty is that the lower extremity is used for one stereotypical motion whereas the upper extremity is used in numerous skilled ways. Part of the rationale for this study is the need to obtain benchmark motion data for the upper limb in order to improve prosthetic design, fitting and training techniques. During this study, special attention was given to the wrist component of upper limb prosthesis. The benchmarks obtained in this dissertation will improve upper limb prosthetic prescription and training. Proper prescription and training may reduce the number of patients who reject their prosthesis.

1.2 Objectives

This dissertation describes the importance of the need to improve upper limb prosthetic design, prescription and training. Improvement of prosthetic design often requires knowledge of how the human body works and adapts. There were three main objectives or goals in performing this study.

The first objective was to create normal profiles of upper limb motions that can be used for prosthetic performance evaluation. Normal profiles were created for four activities of daily living: drinking from a cup, opening a door, lifting a box, and turning a steering wheel. The profile of these motions included shoulder, elbow and wrist joint angles and the associated forces and torques.

The second objective was to quantify the compensatory motion caused by the limitations of a TRMP lacking a powered wrist component during the four common

tasks. This objective was first approached by testing healthy subjects who wore a brace in a way that simulated TRMP use. This was done to determine if TRMP use can be appropriately simulated with non-amputee subjects who are easier to recruit for research studies. Second, tests were also performed on actual amputee subjects. Quantification of compensatory motion could be used to create a mathematical model of a transradial prosthesis to be used for fitting, training and evaluation.

The final objective was to determine if location (distally or proximally) of a mass equivalent to the mass of a wrist rotator of a TRMP affects the compensatory motion during the four common tasks. With the information regarding the motions of healthy subjects, braced subjects, and prosthesis users some general design, fitting and training guidelines were made.

1.3 Hypotheses

This was a scientific study that used statistical analysis to accept or reject hypotheses. The following hypotheses were considered for this study:

- The ranges of motion of the shoulder, elbow and torso will be significantly different between the non-amputee group (N-BR), the braced group (BR) and the transradial myoelectric prosthesis user group (PROS). This hypothesis was tested using a one-way analysis of variance between subjects. Since the N-BR and the BR group contained the same subjects a repeated measure analysis of variance was also completed between these groups.
- The range of motion of the shoulder, elbow and torso of the TRMP wearing group will be significantly different during three conditions: with prosthesis (PROS),

prosthesis with added mass at the elbow (P-EL) and prosthesis with added mass at the wrist (P-WR). This hypothesis was tested using a repeated measure analysis of variance.

- The shoulder and elbow joint forces and torques of PROS group will be significantly different during the three conditions mentioned above while completing one unilateral task (opening a door) and one bilateral task (lifting a box). This hypothesis was tested using a repeated measure analysis of variance.

1.4 Dissertation Outline

Background information is presented in Chapter 2. This includes technical background describing forces, torques, anthropometrics and biomechanics. The details of the anatomy of the upper limb that pertain to this study are also described. An exploration of prior research on the subjects of motion analysis, gait analysis, prosthetics, and activities of daily living is offered in Chapter 2.

The study methodology is discussed in Chapter 3. The design of the experiment and a description of the participants, the activities of daily living studied and the testing protocol are given in this chapter.

In Chapter 4, the experiment instrumentation and set-up are described. This includes the testing apparatus, the motion analysis system and the force transducer used to collect data. An explanation of the calibration methods and the subject measurements is also stated in this chapter

Chapter 5 explains the development of a kinematic model, specifically; how segments of the arms and torso are determined and joint angles are calculated.

In Chapter 6, a description of the kinetic chain while opening a door and lifting a box was determined and how inverse dynamics is used to determine joint forces and torques. This chapter also explains how the differences between inertial properties of a prosthesis and a forearm with added mass were reconciled.

Chapter 7 explains the outcome measures that were compared and the statistical analysis used to determine significance and test the hypotheses. Chapter 8 observationally describes the motions of the three groups: non-braced, braced and the TRMP wearing group. This chapter also looks at a case study of one prosthesis users comparing the motions of prosthetic side to the sound side while completing the tasks.

The results such as the maximum and the range of the joint angles, the forces, and the torques are presented in Chapter 9. Chapter 10 compares and discusses the results, explains limitations of the study and presents recommendations for upper limb prosthetic design, training and evaluation.

The final chapter, Chapter 11, summarizes the conclusions of the study. This chapter also suggests how information from this research will lead to future studies and funding.

Chapter 2: Background

2.1 Technical Background

2.1.1 Newton's Laws of Motion

Basic physics principles guide the study of how the body moves. Sir Isaac Newton first published his laws of motion in a work written in Latin and titled *Philosophiæ Naturalis Principia Mathematica* in 1687. Newton's first law (the law of inertia) explains that inertia is the resistance of an object to changing its motion. A particle will stay at rest or in constant velocity unless acted upon by a force. Newton's second law describes the effect of a resultant force vector on the relative acceleration of an object:

$$F = ma \quad (2.1)$$

where F is the force vector, m is the mass of the object and a is the linear acceleration vector (time derivative of velocity) of the object.

Newton's second law can also be described in terms of angular momentum which is described in Euler's equations of motion (Eq. 2.2). Angular inertia also known as moment of inertia describes an object's resistance to change its rotational motion. The moment of inertia of an object is affected by mass and its distribution of mass as described by:

$$M = I\alpha \quad (2.2)$$

where M is the resultant moment of all forces acting on the object, I is mass moment of inertia and α is the angular acceleration of the object. The greater the distance of an

object from its axis of rotation, the larger its moment of inertia will be. For example, moving the heavy electronics and motors associated with an electric wrist closer to the elbow joint would decrease the moment of inertia, and thus require less torque from the user to perform a task involving elbow flexion.

Newton's third law states that for every action there is an equal and opposite reaction. It also determines how forces and moments propagate with a solid body, and determines the internal forces and moments that the body experiences. This becomes important when a segment of the body comes in contact with another object such as the ground or a door knob.

2.1.2 Biomechanics and Anthropometrics

Biomechanics applies classical mechanics described by Newton's laws of motion to biology and physiology. Biomechanical properties of tissue such as bone, cartilage, tendons, ligaments, muscles and nerves can be studied. This dissertation is concerned with applied biomechanics or segmental motion analysis. Kinematics is a branch of motion analysis that describes movement without reference to the causes of those movements. In humans, kinematic studies can include descriptions of range of motion of the joints, as well as, position, velocity and acceleration of the body segments. Kinetics as applied to humans is the study of forces and moments acting on the segments both statically (at rest) and dynamically (in motion).

Anthropometrics is the study and measurement of human physical dimensions. Anthropometric tables of the human body give average data such as segment lengths, weights, center of mass and radius-of-gyration data based on numerous cadaver

experiments [16, 17]. The radius of gyration describes the distribution of mass of an object or in this case of a segment of the body about a particular axis. The moment of inertia of body segments with respect to an axis of rotation can be estimated using data from anthropometric tables and the following equation:

$$I = k^2 m \quad (2.3)$$

where k is the numerical value of the radius of gyration

I is the moment of inertia

m is the mass of the object

2.1.3 Euler Angles

In order to describe how one object in space is oriented in relation to another object, Euler angles can be used. Each object's orientation is defined by a local coordinate system using vectors. Euler angles are a set of three rotations performed on a moving (as opposed to a fixed) system. Each rotation is performed about an axis whose location is determined by the previous rotation [18]. To describe the orientation of each upper limb segment relative to another, Euler angles were computed. Each Euler-angle rotation represented a particular joint movement such as flexion, abduction or rotation. Details of how each joint angle was calculated using Euler angles are written Chapter 5.

2.1.4 Newton-Euler Inverse Dynamics Method

The Newton-Euler Inverse Dynamics Method is used to estimate the applied forces and moments at the joints using the Newton (linear) and the Euler (angular)

equations of motion and the kinematic data. In order to solve these equations of motions at each joint, the following assumptions are made about the human body:

- Segments are rigid bodies with the mass distributed about the center of mass.
- Joints are frictionless joints.
- There is no co-contraction of agonist and antagonist muscles.
- Air friction is minimal.

2.2 Anatomy and Biomechanics of the Human Arm

2.2.1 Shoulder Complex

The shoulder complex is made up of several joints and articulations that allow for a wide range of mobility. While the sternoclavicular joint, the acromioclavicular joint, and the scapulothoracic articulation are all essential to upper limb function, the glenohumeral joint (GH) often plays the most important role. The scapular motion is hard to measure, so scapulothoracic and glenohumeral rotations are often combined during calculations of the shoulder motions. For this reason and to simplify calculations, the GH joint will be the main focus of this description of shoulder biomechanics.

The GH joint lies where the head of the humerus connects to the glenoid fossa of the scapula. There is little bony constraint in the GH joint, making its motion almost purely rotational [19]. Dislocation or inferior subluxation is prevented by the slight superior inclination of the proximal humerus articulation with the glenoid fossa. With an incline superiorly of about 5° relative to the plane of the scapula a great degree of geometric stability is created [19]. Structures such as the glenoid labrum, the

glenohumeral joint capsule, the rotator cuff muscles, and the glenohumeral and coracohumeral ligaments provide much of the stability in the shoulder joint complex.

The GH joint allows for three types of pure motions: flexion/backward extension ($120^{\circ}/60^{\circ}$), abduction/adduction in standard position ($120^{\circ}/0^{\circ}$), hyperadduction ($10-15^{\circ}$), and internal/external rotation ($70^{\circ}/90^{\circ}$) [20] (Figure 2.1). Other combination motions of the shoulder complex include horizontal flexion/extension, shoulder girdle elevation/depression and protraction/retraction, and combined glenohumeral and scapulothoracic motion. Although activities of daily living often require a complex combination of these motions, for research purposes it is appropriate to study the pure movements separately. To test range of motion of shoulder flexion, the humerus resides in the sagittal plane, and the straight arm is raised forward with palm down. For abduction of the shoulder, the humerus is in the frontal plane and the straight arm is lifted away from the body. Internal and external rotation is tested with the humerus at the side with rotation occurring around the long axis of the humerus in the transverse plane.



Figure 2.1. Movement of the glenohumeral joint.

2.2.2 Elbow and Forearm Complex

The joints at the elbow allow for two types of motions: flexion/extension (10° to 145°) in the sagittal plane and pronation/supination of the forearm ($71^{\circ}/81^{\circ}$) [20, 21]. The hinge joint at the elbow allows for the flexion and extension of the forearm that occurs at the humeroulnar (or ulnohumeral) articulation where the spool-shaped surface of the trochlea on the distal end of the humerus articulates with the ulna. The capitulum, also located distally on the humerus, articulates with the radius creating the humeroradial joint which also allows for the flexion and extension movement. The olecranon fossa, a depression located on the dorsal distal end of the humerus just above the trochlea, accepts the olecranon process of the ulna when the arm is fully straightened. Upon complete flexion, the coronoid process of the ulna moves into the coronoid fossa located also above the trochlea but on the ventral side of the humerus. The semilunar notch of the ulna and the precise markings of the trochlea prevent any lateral movement at this joint making it predominately uniaxial.

The radius rotates relative to the humerus and ulna during pronation and supination at the proximal radioulnar articulation. As the distal radius rotates around the distal ulna in a cone-shaped arc during pronation and supination, the forearm is rotating around a longitudinal axis. This axis passes through the center of the capitulum, the rounded protrusion at the distal end of the humerus, the radial head and the distal ulnar articular surface [19]. The supinator muscle, the biceps brachii, brachioradialis and wrist extensors are responsible for rotating the radius during supination and the pronator teres, pronator quadratus, brachioradialis and wrist flexor muscles pronate the forearm at the superior and inferior radial ulnar joints. Most of these muscles are multiarticular and so

the motion and forces at one joint are directly interrelated to other joints in the upper extremity.

The medial and lateral epicondyles of the distal end of the humerus are the prominent attachment sites for many muscles responsible for movements of the forearm and fingers. For this study the epicondyles will also serve as bony landmarks used for marker placement and to estimate the location of the elbow joint center when calculating flexion and extension of the elbow during common tasks.

2.2.3 Wrist

The wrist is made up of eight carpal bones. The proximal row contains the scaphoid, the lunate, the triquetrum and the pisiform. The distal row of carpal bones is made up of the trapezium, the trapezoid, the capitate and the hamate. The primary joints of the wrist are at the radiocarpal joints, where the radius articulates with the proximal carpals and the metacarpal joints where the proximal and distal carpal rows articulate. The intercarpal joints create a sliding motion between carpal bones adding to the wrist motion in a less considerable way [22].

The wrist joint allows for flexion and extension ($80^{\circ}/75^{\circ}$) in the sagittal plane as well as in radial and ulnar deviation ($25^{\circ}/45^{\circ}$) in the frontal plane. Small combinations of these movements as well as insignificant amounts of axial rotation can occur at the wrist in some individuals, but for this study axial rotation of the hand is considered to occur from pronation and supination of the forearm. The range of motion of flexion and extension is split between the radiocarpal joint and the metacarpal joints. The scaphoid articulates with the radius at the scaphoid fossa, the lunate articulates with the lunate

fossa of the radius and partly with the ulnar soft tissue to allow for the flexion/extension of the wrist. During radial deviation the proximal carpal row, led by the scaphoid, flexes, and the opposite occurs during ulnar deviation. The distal carpal row follows the finger rays during both directions of deviation [19].

2.3 Upper Limb Prosthesis

An upper limb prosthesis can be either transradial (below the elbow) or transhumeral (above the elbow) or through the elbow. This dissertation concentrates on the transradial prosthesis because it can be simulated with a less complicated bracing system. The below elbow prosthesis consists of a terminal device (TD), a wrist unit, a forearm section, a socket with some type of suspension to attach the prosthesis to the remaining limb and some type of control device to operate the TD [23].

2.3.1 Terminal Devices

There are passive functioning terminal devices often used for cosmetic purposes and for simple tasks such as opposition or stability. Active terminal devices can be controlled by a body-powered harness system or by external power which is most often a myoelectric system. A combination of these two controls is also found in some upper limb prostheses and is referred to as a hybrid system. The choice of a TD shape is usually limited to a hook which can be more functional or a hand shape which is more cosmetically pleasing [7]. Active hand shaped TDs are typically more bulky and heavier than hooks [23].

2.3.2 Wrist Units

The wrist unit is attached to the terminal device of the prosthesis and is responsible for positioning of the TD. Some wrist units are fixed which limits the position of the TD. Other wrist units can be manually adjusted such as a Motion Control (Salt Lake City, UT) wrist or moved by an external power such as a myoelectric system [23]. A quick disconnect wrist unit allows for exchange of a terminal device easily. A locking wrist unit provides safety by locking in place while the TD is used for grasping or lifting [23]. Liberating Technologies (Boston, MA) and Otto Bock (Duderstadt, Germany) are companies that sell powered wrist rotators that allow for complete rotation of the TD, but do not provide wrist flexion or extension. In contrast to the anatomical wrist and forearm, these wrist units cause rotation about a transverse axis. The Otto Bock wrist rotator is the lightest wrist rotator currently available and weighs 96 grams.

2.3.3 Control Devices

Upper limb prostheses are divided in two main control types: body-powered and externally powered. As mentioned previously myoelectric control is the most common form of external power although electrical switches with an on/off button and hybrid controls are also used. Body powered systems use either a figure eight or a figure 9 harness to control opening and closing of a terminal device by a mechanical cabling system. Commonly shoulder flexion or scapular abduction is used to create and relax tension on the cable allowing for the TD to be opened or closed [24].

The myoelectrical control system uses electrical signals from muscle activation to control the TD. This requires muscle strength and muscle training for adequate function.

The myoelectrical control system is battery powered and requires control circuitry that has to be fitted into the forearm section of the prosthetic limb [24].

2.3.4 Current Approaches for Fitting an Upper Limb Prosthesis

It is difficult to explain a common and current fitting technique for fitting amputees with an upper limb prosthesis. The fitting practice is often subjective and individualized for the patient by the prosthetist. According to Fillauer (Chattanooga, TN), a leading manufacturer of prosthetic products that includes the Motion Control branch (Salt Lake City, UT), there are many issues to consider when fitting a transradial amputee with a prosthesis. The patient is interviewed to determine goals and expectations of the prosthesis especially in terms of function. An evaluation of the residual limb and joints is conducted to determine range of motion, muscle and joint strength, and in the case of a myoelectrically controlled prosthesis, electrode placement. A plaster cast is made of the residual limb. From the cast, the prosthetist will be able to construct a socket of the prosthesis that should fit closely around the residual limb. Proper socket fit is essential to the user's comfort which may determine the amount of prosthesis use. Often a trial fitting with a diagnostic or "check" socket and components is completed to improve function for the user and justify expenses to a funding source [25].

Advanced Arm Dynamics Inc. (Redondo Beach, CA), a Center of Excellence for Upper Extremity Prostheses, offers services that include expedited delivery, advanced socket design, occupational and physical therapy, psychological counseling as well as rehabilitation planning, insurance assistance services and expert witness testimony. Advanced Arm Dynamics breaks down the prosthesis fitting process into three phases:

Interface Phase, Controls Phase and Alignment Phase. After an initial patient assessment (Patient Evaluation Phase) during the Interface Phase, a socket is made by the prosthetist. During the Controls Phase, myoelectric or body-powered control is chosen. For the myoelectric prosthesis, optimal electrode placement on the residual limb is determined. During the Alignment Phase, a rigid frame is fabricated and all components are attached to the prosthesis and cosmetics are added. After the completion of the three phase fitting process, the patient develops skills for optimal prosthetic use during the Interim Therapeutic Phase. During this phase, minute modifications may be made by the prosthetist to optimize comfort and function of the prosthesis. Even with expedited delivery, Advanced Arm Dynamics requires 1-3 days for fitting with the patient then receiving the prosthesis in 7-10 days [26, 27].

2.4 Prior Research

There have been several studies detailing the use of infrared cameras and motion analysis systems to study human movement. There have also been many articles showing how gait analysis has led to the improvement of lower limb prosthetic design. There is a limit amount of documentation regarding the motion of the upper limb especially in regards to improving prosthetic design.

2.4.1 Gait Analysis and Prosthetic Design

There are many examples throughout scientific literature showing how gait analysis has led to the improvement of lower limb prosthetic design criteria [28, 29]. In 2003, Twiste et al. conducted a literature review on rotation and translation during

prosthetic gait. The abstract from this review mentions that more accurate gait analysis showing optimized gait patterns could help manufacturers design prosthetic components to mimic these patterns [29]. Another study compared the adaptations during gait initiation between able-bodied subjects and amputees wearing a prosthesis. It was determined that since the prosthetic foot could not generate as much force, the amputees were required to increased stance duration to generate force over a longer period of time [30]. This is an example of how gait analysis of healthy subjects was compared to prosthesis wearers to determine how amputees compensate for the limitations of the prosthesis. This same idea was used in this study to compare compensation methods in upper limb motions.

2.4.2 Upper Limb Motion Analysis

There have also been studies involving upper limb motion, but they are few in number [31]. Anglin and Wyss have reviewed studies involving the motion analysis of the upper limb in terms of motions, tasks, methods and kinematic models [31].

Kinematic and trajectory patterns of upper arm reaching have been evaluated [32, 33]. The range of motion of the upper limb of healthy subjects performing activities of daily living such as eating, drinking, [34, 35], jar opening, carton pouring [36], and zipping a jacket [37] have been recorded and analyzed. Wrist, elbow, and shoulder joint kinetics such as external joint forces and moments have been studied during various everyday tasks including reaching, eating, and drinking [35] ; lifting a block and answering a telephone [38]; lifting a 5 kg box and carrying a suitcase 10 kg [39]. Motivations for these studies vary but include definition of normal motion and collection

of input for a biomechanical arm model. In contrast to the cyclic and often predictable motion of normal lower extremity tasks such as gait and running, upper limb tasks are varied and difficult to analyze.

2.4.3 Upper Limb Research for Orthotic and Prosthetic Design

Motion analysis of twenty-two upper limb motions has been used to develop an upper limb power orthosis [40]. First by collecting motion analysis data on unaffected subjects, then using the data to create a simulation program to assist design optimization, and finally clinically assessing actual users by completing motion analysis again [40]. A seven degree of freedom upper limb powered exoskeleton has been designed for applications in rehabilitation medicine and virtual reality simulation [41]. A kinematic database from one subject completing 24 activities of daily living was completed for use in the design of this exoskeleton, although only details from five motions were reported [42].

Developing upper extremity prostheses, and understanding the movement patterns imposed by these mechanisms can be facilitated by comparisons with people with normal upper extremities where movement restrictions have been controlled. Motion analysis of activities of daily living of braced subjects simulating prosthesis use have been performed to determine optimal wrist alignment of an upper limb prosthesis [37, 43]. These studies support the validity of braced subjects as a means of simulating prosthesis users. Studies have also examined common unilateral task completion of an upper extremity while wearing a wrist splint [44]; while using a body powered upper-limb prosthetic simulator during object manipulation [45] and kayaking [46]. Potential energy during work related

activities such as folding, cutting and hammering was measured from three transradial prosthesis users [47].

Chapter 3: Design of Experiment

3.1 Introduction

This study looked at between subjects and with-in subjects comparisons. The first hypothesis was to determine if the range of motion of the shoulder, elbow and torso would be greatest in the prosthetic group (PROS) that required compensatory motion due to loss of degrees of freedom of the wrist and forearm. It was predicted that the braced BR would be significantly the same as the PROS group and that the non-braced (N-BR) would use significantly less range of motion to complete the tasks. The second and third hypotheses were tested with a with-in subjects comparisons of motion predicting that the added mass at the wrist would cause greater compensatory motion than no added mass or added mass at the elbow. For the control group three conditions were compared:

- braced (BR)
- braced with added mass at the elbow (BR-EL)
- braced with added mass at the wrist (BR-WR).

For the transradial myoelectric prosthesis wearing group three conditions were compared:

- with prosthesis (P)
- with prosthesis with added mass at the elbow (P-EL)
- with prosthesis with added mass at the wrist (P-WR).

3.2 Participants

Two groups of subjects were used for this study. There were ten healthy non-amputee adult volunteers with no previous upper limb injury. In this group there were 6 men, 4 women; mean age 28 years old (SD 7.4). In addition there were 7 transradial prosthesis wearers. The group using upper limb prosthetics consisted of 6 men, 1 woman with a mean age of 36 years (SD 10.1). All the non-amputee participants were right hand dominant. Details of the prosthesis wearing subjects are shown in Table 3.1. All participants gave informed consent prior to participation. The experimental procedures were approved by the Institutional Review Board of the University of South Florida prior to data collection.

Table 3.1. Descriptions of the transradial prosthesis users.

| Subject | Sex | Age (years) | Dominant Hand | Year of amputation | Prosthesis side | Time of current prosthesis use (years) | Mass of prosthesis (kg) |
|---------|-----|-------------|---------------|--------------------|-----------------|--|-------------------------|
| 1 | M | 43 | Right | 1999 | Right | 7 | 1.5 |
| 2 | M | 43 | Right | 2003 | Left | 3.5 | 1.5 |
| 3 | F | 53 | Right | Congenital | Left | 16 | 1.2 |
| 4 | M | 31 | Right | 2007 | Left | 0.25 | 1.4 |
| 5 | M | 27 | Left | 2001 | Left | 5 | 1.0 |
| 6 | M | 26 | Right | 1991 | Left | 16 | 1.2 |
| 7 | M | 31 | Right | 2003 | Left | 1 | 1.8 |

Recruitment of transradial prosthesis wearing subjects was difficult. All of the prosthesis wearing subjects used a two channel transradial myoelectric prosthesis with a Sensor Speed Hand® (Otto Bock, Germany). One subject's prosthesis included a humeral half cuff, step up hinges and a split socket. The prosthesis also contained a 3 mm gel liner and pin lock. These additions at the elbow joint were incorporated to

protect the short residual limb from hyperextension and to give a mechanical advantage by exchanging range of motion for increased lift support.

3.3 Activities of Daily Living

Subjects completed four simulated activities of daily living in a laboratory environment: drinking from a cup, opening a door, lifting a box and turning a steering wheel. Two unilateral and two bilateral ADLs were chosen based on surveys of amputees in the literature [14]. Drinking from a cup has been analyzed kinematically in other studies [34, 37] and was used for comparison. Opening a door and turning a steering wheel require obvious movement of the forearm and wrist, so these tasks were chosen to determine compensation when restricting these movements. The box lift was chosen since it was a bilateral task and required moving a mass. Table 3.2 describes the steps of each task.

For the cup task, subjects were asked to start holding by the cup with the elbow at approximately 90 degrees, bring the cup to the mouth and return to the starting position. For the door task, the subjects were asked to open the door without taking a step. For the box lift task, the subjects were asked to bilaterally lift a 2.27 kg box from one shelf (height: 0.91m) and place it on to the higher shelf (0.4572 m above lower shelf) without taking a step. These heights represent the average height of a kitchen counter and cabinet respectively. For the steering wheel task, the subjects were asked to place hands at the “10 and 2” positions on the steering wheel and turn the wheel as far to affected side (right side for non-amputee subjects; prosthetic side for amputees) as possible without moving their hands and then return the steering wheel to the starting position. Before each task,

the subjects were allowed to practice until familiar enough with the task to complete it correctly without instruction or feedback. While braced, subjects were given the same instructions for each task, but were not instructed on how to overcome the restrictions of the brace to perform the ADL. Similarly, the prosthesis wearers were given the basic instructions but not told how to compensate. The non-amputee subjects completed the unilateral tasks with the dominant (right in all cases) hand. The amputee subjects completed the unilateral task with the prosthesis that in most cases (5 of 7) was the non-dominant hand prior to amputation. The effect of hand dominance was not accounted for in this study.

Table 3.2. Descriptions of the tasks analyzed.

| |
|--|
| Drinking from a cup: <ul style="list-style-type: none"> • Standing • Start at neutral position – elbow flexed at approx. 90 ° • Lift the cup to mouth and tilt to simulate drinking • Return to neutral position |
| Opening a door <ul style="list-style-type: none"> • Stand in front of door • Start at neutral position – hands straight down by side • Open the door |
| Turning a steering wheel <ul style="list-style-type: none"> • Sitting in front of steering wheel at comfortable height • Place hands on steering wheel at 10 and 2 • Turn steering wheel to affected side as far as able without removing hands • Return steering wheel to starting position |
| Box lift <ul style="list-style-type: none"> • Standing at counter • Start at neutral position – hands, straight down by side • Lift 5 lb box off lower shelf without stepping • Place box on higher shelf |

3.4 Test Protocol

Prior to each data collection the motion analysis system including the force transducer on the door was calibrated. The calibration process is explained in Section 4.5.

3.4.1 Subject Measurements

Anthropometric measurements were recorded from each subject prior to testing (Table 3.3). These measurements were used in the kinematic and kinetic calculations that will be described in Chapter 5 and 6.

Table 3.3. Descriptions of the subject measurements collected prior to testing.

| Measurement | Units | Instrument Used | Description |
|-----------------|-------|--|---|
| Mass | kg | Professional Health o meter [®] scale | Weight of subject |
| Height | cm | Professional Health o meter [®] scale | Height of subject |
| Shoulder depth | cm | Cloth tape measure | Vertical offset from the base of the acromion marker to shoulder joint center |
| Elbow width | cm | Cloth tape measure | Width of elbow along flexion axis between the distal epicondyles of the humerus |
| Wrist thickness | cm | Caliper | Anterior/Posterior thickness of wrist |
| Hand thickness | cm | Caliper | Anterior/Posterior thickness of the hand |

3.4.2 Marker Placement

Spherical reflective markers approximately 14 mm in diameter were placed on the bony landmarks of the upper limbs and torso of the subjects as described in Table 3.4. In the case of the braced and prosthesis wearing groups, the elbow, wrist and hand markers were placed on the brace or prosthesis.

3.4.3 Experimental Trials

A static trial was collected to allow proper calculations of measurements required for the kinematic program and to expedite marker identification. During the static trial, the subject was instructed to keep arms to the side, the pinky away from body, palms down, and standing perpendicular to the door on the testing apparatus. Once an adequate static trial was collected, the medial elbow markers were removed prior to collection of the dynamic task trials.

Table 3.4. Marker placement and code names of markers used in programming.

| Code name | Marker description | Marker placement |
|-----------|-------------------------------------|---|
| C7 | 7 th Cervical vertebrae | Spinous process of the 7 th cervical vertebrae |
| T10 | 10 th Thoracic vertebrae | Spinous process of the 10 th thoracic vertebrae |
| CLAV | Clavicle | Jugular notch where the clavicles meet the sternum |
| STRN | Sternum | Xiphoid process of the sternum |
| RBAK | Right back | Middle of the right scapula (asymmetrical) |
| RSHO | Right shoulder | Right acromio-clavicular joint |
| RUPA | Right upper arm | Right upper arm between the elbow and shoulder markers |
| RELB | Right elbow | Right lateral epicondyle approximating elbow joint axis |
| RELBM | Right elbow medial | Right medial epicondyle approximating elbow joint axis (static trial only) |
| RWRA | Right wrist A | Right wrist thumb side |
| RWRB | Right wrist B | Right wrist pinkie side –on the pisiform |
| RFIN | Right finger | On the dorsum of the hand just below the head of the right third metacarpal |
| LSHO | Left shoulder | Left acromio-clavicular joint |
| LUPA | Left upper arm | Left upper arm between the elbow and shoulder markers |
| LELB | Left elbow | Left lateral epicondyle approximating elbow joint axis |
| LELBM | Left elbow medial | Left medial epicondyle approximating elbow joint axis (static trial only) |
| LWRA | Left wrist A | Left wrist thumb side |
| LWRB | Left wrist B | Left wrist pinkie side |
| LFIN | Left finger | On the dorsum of the hand just below the head of the left third metacarpal |

The non-amputee participants completed each task during the following interventions: (1) no intervention (N-BR) (2) braced restricting forearm and wrist motion (Figure 3.1), (BR) (3) braced with 96 g (mass of average prosthetic wrist rotator) added near the elbow (BR M-EL), (4) braced with 96 g added near the wrist (BR M-WR). The brace restricted pronation and supination of the forearm as well as wrist movement, but allowed the full range of motion of the elbow. The amputee subjects completed the tasks during the following interventions: (1) wearing a myoelectric transradial prosthesis (PR), (2) prosthesis with 96 g added near the elbow (PR-EL) and (3) prosthesis with 96g added near the wrist (PR-WR). Three trials were collected for each experimental test condition. These three trials were averaged as a representative for each subject. The order of the tests was randomly assigned for each subject.



Figure 3.1. Brace used to restrict forearm and wrist motion.

Chapter 4: Experimental Instrumentation and Set-up

4.1 Introduction

The objectives of this dissertation were to create normal profiles of upper limb motion, quantify compensatory motion caused by lack of wrist and forearm movement and to determine how prosthesis wearers compensate for added mass during several common tasks. Motion analysis was used to determine if prosthesis wearers compensated differently than control subjects wearing a brace and if shoulder and elbow joint angles or resultant forces increased at different mass locations. Video based motion analysis requires defining segments so that joint angles and forces can be calculated.

4.2 Testing Apparatus

A testing apparatus was built to allow for the completion of the four activities of daily living in a controlled situation (Figure 4.1). The apparatus combined an interior door, a steering wheel and shelving system into one unit. The door was a pre-hung interior door measuring 71.12 cm x 203.2 cm (28in x 80in). The door handle was a conventional interior style locking knob. The base of the steering wheel was approximately 78.31cm (31in) off the floor and about 38.1 cm (15in) above the seat of the chair. The steering wheel was angled at 72° relative to the horizon which is typical of a compact car (Figure 4.2). The shelving system was used for the box lift task. The lower shelf was 91.44cm (36in) above the floor which is the standard height of a kitchen countertop and the higher shelf was approximately 45.72 cm (18in) above the lower

shelf. This is the standard height for the bottom shelf of a cabinet above a typical kitchen counter. The box weighed 2.27 kg (5 lb).



Figure 4.1. Testing apparatus used to complete the tasks.



Figure 4.2. The steering wheel used for the turning task.

4.3 Vicon™ Motion Analysis System

4.3.1 Hardware

The Vicon™ motion analysis system allows for the collection and analysis of movement data. It consists of 8 cameras with infrared lights and a Vicon™ 612 datastation computer that is used to collect and preprocess the data from the cameras. The cameras are linearized to correct distortions that may be present in the camera lens and to correct small variations that may exist in the internal mounting of the CCD image sensor. Reflective markers are placed on bony anatomical landmarks of the subjects. Two-dimensional image points of the reflective markers from each camera are digitized and converted to real metric units in three dimensions using direct linear transformation (DTL) [48]. A Canon™ digital video camera was also used to film standard video of the subjects. A Dell™ computer took the information from the datastation and ran programs to analyze the data.

4.3.2 Software

The Vicon™ motion analysis system provides three software platforms to collect and analyze movement data. The Vicon Workstation™ module allows for the calibration of the system through a proprietary technique called DYNCAL™, the collection of the trajectories of the markers and the assigning of names or labeling of these markers.

The Vicon Bodybuilder™ language allows the user to create programs using the positions (X,Y,Z) of the markers to calculate kinematic and kinetic results such as velocities, accelerations of segments, center of rotations of segments, joint angles, joint forces and joint torques.

The Vicon Polygon™ program is a report writer that creates graphs and hyperlinks to explain and present results of data collection. Graphs of each of the outcome measures ,explained in details in the following chapters, were created using Polygon and the maximum and minimum values were extracted.

4.4 ATI™ Force/Torque Transducer

An ATI™ Gamma Force/Torque transducer (F/T transducer) was purchased and implemented onto the door knob in order to get information about forces and torques during the door opening task (Figure 4.3). The Gamma model is 2.97 in. in diameter, 1.31 in. in height and weighs 0.56 lbs. The F/T transducer was connected to a control box which powers, amplifies and calibrates it. A cable was fabricated to send analog data from the control box to the analog to digital converter (A/D) board and then to the Dell™ computer so that the transducer data could be collected simultaneously with the Vicon™ motion analysis data.

The transducer was instrumented with six silicon strain gages. The resistance of the strain gage changes as a function of the applied strain. Six channels of analog data were collected from the transducer representing the six components of force and moments (F_x , F_y , F_z , M_x , M_y , M_z) at the door knob. In order to convert the Volt information from the strain gages into meaningful force information, a scale factor was calculated using the following equation:

$$\text{Scale Factor} = \frac{\text{Input Range (V)}}{\text{Digits}} * \frac{1}{(\text{Sensitivity})(\text{Bridge Excitation})(\text{Amplifier Gain})} \quad (4.1)$$

The 16-bit analog card used on the analog to digital converter had an input parameter set to +/- 10 V (20 V dynamic range) which corresponds to 65535 possible

output values (digits). The sensitivity of the transducer was provided by ATITM and is equal to 6.4 N/V. The bridge excitation and gain were set in the amplifier of the transducer. A similar scale factor was used for the moment data with the additional factor of 10^{-3} added to the denominator since the ViconTM system measures distances in millimeters rather than meters. The sensitivity of the ATITM transducer was given as 0.5 Nm/V. These scale factors were used in the ViconTM software to extract force and moment data.



Figure 4.3. ATITM Gamma transducer connected to the door knob.

4.5 Calibration

Calibration of the ViconTM system and the ATITM transducer was completed at the beginning of each testing session.

4.5.1 Calibration of the Cameras

Prior to calibration, the eight cameras were positioned to ensure that a marker held at any location within the data collection volume was seen by at least two cameras. A four marker calibration frame (L-frame) (Figure 4.4) with known distances between

markers was used during the collection of the static calibration trial to define the location of origin and direction of axes of the global coordinate system. A two marker wand (Figure 4.4) also with a known distance between markers was waved around in the data collection volume to complete the dynamic portion of the calibration. The DYNACAL™ program extracted the locations of the markers on the wand from each camera view and automatically calculated the camera positions and orientations relative to each other. Information from the calibration was used to properly reconstruct the individual 2-D camera data to 3-D data.



Figure 4.4. L-frame and wand used for the calibration of the Vicon™ motion analysis system.

4.5.2 Calibration of the ATI™ Transducer

The ATI transducer was connected to a control box mentioned in Section 4.4. Prior to testing, a button was pressed on the control box that automatically calibrated and zeroed the transducer. The analog signal from the transducer to the Vicon™ system was also calibrated and zeroed with-in the Vicon™ Workstation software.

Chapter 5: Kinematic Model

5.1 Introduction

A kinematic model describes how the segments of the body are defined and quantified in a three dimensional space. From the position data of the markers placed on the segments and captured during the movement, coordinate systems are defined and joint angles are calculated.

5.2 Determining Local Coordinate Systems

5.2.1 Introduction

In order to calculate joint angles, and other information in 3-D space it is important to define a local coordinate system or the orientation for each segment of the arm and torso. As mentioned earlier, in order to avoid a complicated mathematical solution, it was assumed that the segments of the arm and torso were rigid bodies.

For this study the segments of interest were the torso, the upper arm (humerus), the forearm and the hand. At least three non-collinear markers are required to define a segment and its orientation. More markers can be used to assure that a segment is captured by the cameras. Since markers could not be placed directly at the joint centers, or points of rotation of the segments, joint centers had to be determined from the marker placements and the subject measurements.

The joint center located at the distal end of each segment was used as the origin for the local coordinate system assigned to the segment. After the origin was defined, the

other markers were used to determine the x, y, z axes of the local coordinate system of each segment. In the Vicon BodyLanguage™, the code for segment definition is as follows:

$$\text{Segment name} = [\text{origin, defining line 1, defining line 2, token}] \quad (5.1)$$

The first defining line is the direction between two points on the segment and in the model created here coincident to the first segment axis. The second defining line is also defined by two points of the segment. The second segment axis is defined by the cross product of the second defining line with the first. The third segment axis is created by crossing the first segment axis with the second segment axis using the right hand rule.

When writing the defining line in code, two markers were used to describe the line. The line was defined in the direction from the second marker to the first marker. The token labels which segment axis correspond with which lettered axis (x, y, z). For the labeling of the segment axes the right hand rule must be followed. The equations (5.2-5.4) below summarize this general explanation of defining segments or the local coordinate systems in the Vicon Bodybuilder™ Software.

$$\text{SA1} = \text{DL1 (passing through the origin)} \quad (5.2)$$

$$\text{SA2} = \text{DL2 X DL1 (passing through the origin)} \quad (5.3)$$

$$\text{SA3} = \text{SA1 X SA2} \quad (5.4)$$

where SA = segment axis (1, 2, 3) and DL = defining line (1, 2).

The joint centers and segments of the right and left arm were determined using the same orientation for the local coordinate system and therefore are described below in general without reference to a particular side. However, sign (+/-) adjustments in the

software were made in the angle calculations to describe the movement of the right and left arm in an anatomically correct way. This is described in Section 5.3:

Each segment definition is described in detail in the following sections. Figure 5.1 shows the local coordinate system of each segment while subject is standing in a neutral position. The BodyLanguageTM code created to define these segments is shown in Appendix A.

5.2.2 Torso Segment

Markers placed on C7, T10, the sternum (STRN) and the clavicles (CLAV) were used to define the torso segment. Since only three markers are needed to define a segment, a macro was used within the software to replace any missing marker in the set of four allowing for a greater chance of calculating the torso segment constantly even with marker blockage.

For the torso segment, the upper torso, defined as half the distance between the C7 and CLAV marker, was used as the origin of the local coordinate system. The first defining line representing the z-axis was described from the lower torso to the upper torso. The lower torso was calculated as half the distance from STRN marker to the T10 marker. The second defining line was described from the lower torso to the C7 marker. This line is crossed with the first defining line to define the x-axis of the torso segment. The x-axis of the torso is defined using the right hand rule crossing the z-axis with the y-axis.

5.2.3 Upper Arm Segment

Defining the upper arm (humerus) segment or local coordinate system required the calculation of two joint centers. First, the elbow joint center (EJC) was used as the origin. The EJC was determined during a static trial, with markers placed on the medial and lateral epicondyles of the elbow. After collecting the static trial, the distance between these two markers was calculated to give the joint center of the elbow. The medial epicondyle marker was removed for dynamic trials because it is often blocked and may have disturbed movements. A temporary reference frame was used in the software to give directions to the EJC during dynamic trials without the use of the medial marker. The first defining line of the upper arm was determined from the EJC to the shoulder joint center (SJC) and represented the z-axis of the upper arm segment. The SJC was defined as the glenohumeral (GH) which position was calculated from the marker placed on acromio-clavicular joint and the shoulder depth measurement taken by the researcher for each subject. The second defining line was EJC to the upper limb marker (UPA) and was crossed with the z-axis to define the x-axis of the upper arm segment. Finally, the z-axis and the x-axis of the upper arm were crossed (cross-product) using the right hand rule to define its y-axis.

5.2.4 Forearm Segment

For the forearm segment, the wrist joint center (WJC) was used for the origin of the local coordinate system. The WJC was calculated as half the distance between the wrist marker on the radial side (WRA) and the wrist marker on the ulnar side (WRB). The first defining line was determined from the direction of the WJC to the EJC and

represented the z-axis of the forearm local coordinate system. The second defining line was described from the SJC to the EJC and was crossed with the z-axis to define the x-axis. Again to determine the remaining forearm segment axis, the y-axis, the right hand rule was used and the z-axis was crossed with the x-axis.

5.2.5 Wrist Segment

The wrist segment is a dummy segment set up to determine the first defining line of the hand segment. The WJC was also used as the origin to define the wrist segment. The first defining line was calculated from the direction of the WJC to the EJC and defined the z-axis. The second defining line was from marker WRB to marker WRA and was crossed with the z-axis of the forearm segment to define the x-axis. Following the right hand rule, the z-axis was crossed with x-axis to determine the y-axis of the forearm segment.

5.2.6 Hand Segment

The hand segment was also defined using the WJC for the origin. The first defining line used the third axis (y-axis) of the wrist segment and also represented the y-axis of the hand segment. The second defining line was determined from the WJC to the hand joint center (HJC) and represented the x-axis. The HJC was estimated using the finger marker, the subject hand thickness and the marker diameter. The details of this calculation can be found in the software program shown in Appendix A. The y-axis was crossed with the x-axis while adhering to the right hand rule to determine the z-axis of the hand segment.

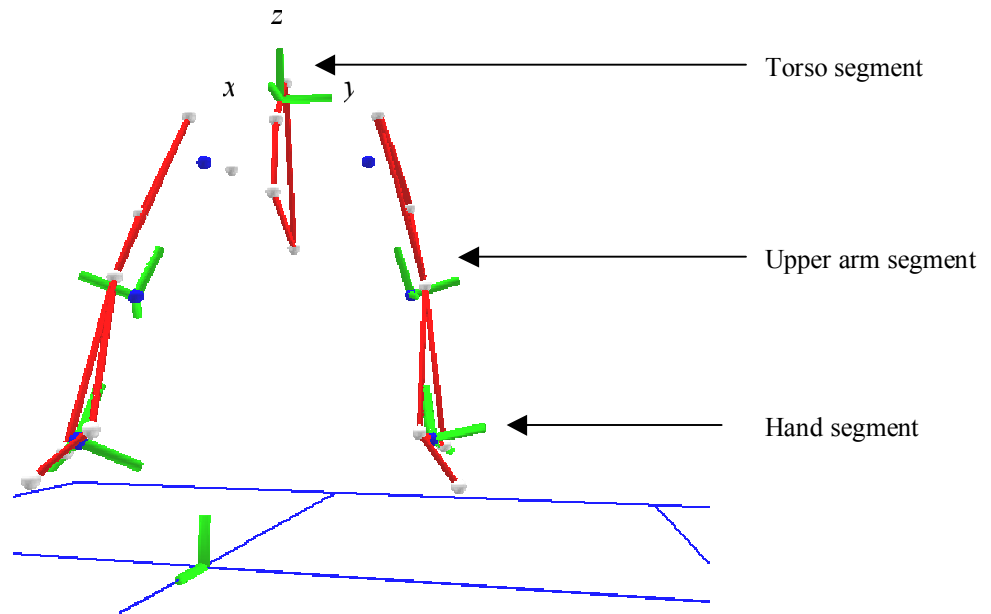


Figure 5.1. Local coordinate systems of defined segments.

5.3 Calculation of Joint Angles

Once local coordinate systems or segments have been defined, relationships between the segments can be determined using Euler angles as described in Chapter 2. Joint angles can be described as the relative orientation of two coordinate systems of segments next to each other. The torso angles were determined by how the torso segment moved relative to the global coordinate system. Torso bending to the right was defined in the positive direction and to the left in the negative direction. Torso forward bending (+) and backward bending (-) were calculated. The glenohumeral joint angles were determined by how the upper arm segment moved in relationship to the torso segment. The glenohumeral joint movement was calculated in the sagittal plane (GHsag) representing the flexion (+) and extension (-) angle, the frontal plane (GHfront) representing the abduction (+) and adduction (-) angle and the transverse plane (GHtran) representing internal rotation (+) and external rotation (-). The elbow joint angles were calculated from the relationship of the upper arm segment to the forearm segment.

The Bodybuilder™ software code used to compute the joint angles is shown in Appendix A. In general, the software will compute the floating point Euler angles between defined segments by using the following syntax:

$$\text{EulerAngles} = -\langle \text{ParentSegment}, \text{ChildSegment}, \text{token} \rangle$$

The EulerAngles describe the relative ParentSegments orientations as three rotations about the axes of the moving ChildSegment. An arbitrary sequence of rotations is used to align the axes of the rotations. By convention, the rotation with the largest assumed angular displacement is the first rotation. Basically the angles between the two moving local coordinate systems are determined. As described in Section 5.2.1, the token is the order definition, in this case the order of rotation. For the shoulder, elbow and wrist angles the yxz token was used with y representing flexion (+)/extension(-) movement, ax representing the abduction (+)/adduction(-) movement and z representing the internal (+)/external (-) rotation movement.

Chapter 6: Kinetic Chain and Inverse Dynamics

6.1 Introduction

Inverse dynamics is used to determine the kinetics or reaction forces and moments at each joint responsible for the joint motion from the kinematic data. The link-segment model or kinetic chain is a mathematical model that uses Newton-Euler equations explained in Chapter 2 to determine the kinetics. Also explained in Chapter 2 are the assumptions made about the human body to simplify calculations. By calculating backwards from the terminal segment, the applied forces and moments of each segment of the human kinetic chain, in this case the upper arm, can be determined. Forces can be due to gravity or from forces applied to a segment by another object.

An open kinetic chain has no resistance at the terminal segment so the equations of motion of each segment based on the effects of gravity can easily be solved using the kinematic data of the segments. From the positions acquired from the markers during the movement and from anthropometric tables (Section 6.2). The positions of center of mass of each segment were extracted from the marker position data and the anthropometric tables (Section 6.2). The second derivatives of segmental center of mass locations and of the joint angles are used to calculate the joint reaction forces (including those due to gravity) and the joint moments of inertia. There is some inherent filtering completed during this process since it is digitally accomplished. A moving average filter of width 0.5 seconds was also applied since the derivatives are taken from the current frame and frames +/- 0.25 from the current frame [49]. In simpler terms, the BodyBuilder™

software linear and angular velocity and acceleration are calculated using three samples of the segments position and orientation, centered on the current frame. Using these three samples allows the segment movement calculations to be significantly greater than any error that may occur from noise or marker positioning. Spikes caused during the reconstruction process were also removed during the filtering process.

When the terminal segment comes into contact with another object such as a door knob or a box, the kinetic chain is considered a closed chain and the force between the obstructing object and the terminal segment has to be measured. Calculating joint forces and torques is an arduous task for the upper limb, due to the difficulty of quantifying the forces acting on the terminal segment. For this reason, the joint kinetics involved during the steering wheel turn were not calculated.

Appendix B shows a simple 2-D calculation of the force and moment of the shoulder joint in one plane using inverse dynamics considering only the force of gravity. This example is an illustration of how the kinetic chain and Newton-Euler equations are used to determine forces and moments at each joint. However, the kinetic data were determined for this study by using the Vicon BodyBuilder™ software written in BodyLanguage™ code in three dimensions.

6.2 Segment Hierarchy Description

The scope of this study concentrates on the upper limb, so the hierarchy of the upper limb will be described. A hierarchical description of the physical interconnection of the segments described in modeled in Chapter 5 must be defined in the BodyLanguage™ of the BodyBuilder™ software. To describe how each segment is

connected to other segments and its anthropometric characteristics the following notation is used in BodyLanguage™:

SegmentName = [Segment, Parent Segment, Attachment Point, Anthropometric Data]

The Segment is also called the child segment. The Parent Segment is higher up in the kinetic chain than the child segment and is connected to the child segment through the attachment point defined in the global space. The Anthropometric Data was entered into the script as a table for each segment (Appendix A). The anthropometric table consists of four numbers:

- the segment mass as a proportion of the total body mass of the subject (%BodyMass)
- the center of mass point as a proportion of the length of the principal (long) segment axis
- the transverse radius of gyration around the center of mass as a proportion of the segment length used for calculations around both transverse axes
- the longitudinal radius of gyration around the center of mass as a proportion of the segment length used for calculations around the principal (long) axis

The upper arm segment was connected to the torso with the attachment at the SJC. The forearm segment was connected to the upper arm segment with the attachment at the EJC. The hand was connected to the forearm segment with the attachment point at the WJC. Once the hierarchy was described and the anthropometric information of each segment was entered a REACTION function solved the equations of motion of the segment taking into account all reactions applied to it by connected segments. The

following syntax was used in Bodylanguage to complete the reaction solutions of each segment:

$$\text{ReactionName} = \text{REACTION} (\text{SegmentName})$$

The REACTION function outputs a 3 x 3 matrix describing a combination of force (F_x , F_y , F_z), moment (M_x , M_y , M_z) and point of application (P_x , P_y , P_z) of the reaction on the specified segment:

$$\begin{array}{ccc} F_x & F_y & F_z \\ M_x & M_y & M_z \\ P_x & P_y & P_z \end{array}$$

The reaction matrix can then be decomposed into its separate components using the following syntax:

$$\text{Forcename} = \text{ReactionName} (1)$$

$$\text{Momentname} = \text{ReactionName} (2)$$

$$\text{Pointname} = \text{ReactionName} (3)$$

The BodyLanguage™ program is shown in Appendix A and the details of the kinetic chain are under the heading, Kinetics.

6.3 Kinetic Chain While Opening a Door

While opening a door, the terminal segment is the hand. To determine the forces and moments acting on the hand, an ATI™ force and torque (F/T) transducer described in Section 4.4 was used. The coordinate system of the F/T transducer was entered into the Vicon BodyBuilder program in relation to the global coordinate system. The segment hierarchy connected the torso to the upper arm, the upper arm to the forearm, the forearm to the hand and the hand to F/T transducer. The CONNECT function was used to apply

the reaction expression of the F/T transducer consisting of the force, moment and point of application to the hand.

6.4 Kinetic Chain While Lifting a Box

The box lift was a bilateral task. A box segment was created from 4 markers placed on the box (See Figure 6.1). The kinetic hierarchy was similar to the door kinetic chain from the torso down to the hand. However, for this case half the box mass was connected to the right hand and half of the box mass was connected to the left hand. Again the CONNECT function was used to connect the box reaction expression to the hands. The box reaction was defined using the weight of the box as the force.



Figure 6.1. Marker placements on the box during the bilateral lifting task.

6.5 Adjusted Inertial Properties for an Upper Limb Prosthesis

The anthropometrics data for the torso, and upper arm were defined the same as for the non-amputee group. However, the anthropometric data for the forearm and hand

segment had to be estimated and adjusted for the side of the prosthesis. The whole TRMP of each subject in the prosthesis user group was weighed prior to data collection. The mass of the terminal device (hand) of the TRMP was acquired from the manufacturer. Due to the difficulty of disassembling the TRMP of each subject, however, on average TRMP was used to determine the location of the center of mass of the hand and forearm as a proportion of the prosthesis. It was assumed that the prosthesis was symmetric as far as thickness and therefore the location of center of mass was reduced to two dimensions. Since these objects of the TRMP are of complex shape, each object was suspended from two different points in two planes. A plumb line was marked during each suspension and the intersection of these lines was estimated as the center of mass of the object. Once the proportion of center of mass location to length of principal axis of the forearm and hand segment of the general prosthesis was determined this ratio was used for each amputee subject. Normally, the moment of inertia of a geometrically complex object such as a prosthesis can be estimated by pendulum suspension method. However, in this case the radii of gyration were assumed to be similar to the human arm and the moment of inertia for the prosthesis was calculated using the following equation:

$$I = mr^2 \quad (6.1)$$

where m is the mass of the prosthesis and r is the radius of gyration of human arm [16].

This assumption should have minimal effect on the moment calculations because the small angular acceleration values during the tasks result in inertial torques that are much smaller than the torques due to gravity. An equivalent intact body mass of the PROS group was estimated by the following equation:

$$\text{Adjusted Body Mass} = \frac{(\text{BodyMass} - \text{Prosthesis Mass})}{1 - (\text{Normalized hand mass} + \text{Normalized forearm mass})} \quad (6.2)$$

where BodyMass = body mass including the mass of prosthesis measured using a scale

Normalized segment mass = proportion of normal body mass of the missing segments (hand and forearm) [16]

Prosthesis mass = mass of prosthesis measured from a scale

In the BodybuilderTM software, a table of anthropometric data based on the standards values published by Winter was used [16]. For subjects with a prosthesis a direct definition of mass properties was used in the following general form:

segmentS =[segments, SegmentMass, CenterOf MassPoint, Inertia]

where segmentS is the segment name

SegmentMass is a scalar quantity expressing the mass of the segment (in kg)

CenterOfMassPoint is the location of the center of mass of the segment in the local coordinate system and

Inertia is defined using three terms which correspond to the components of the moment of inertia.

Each subject had a corrected body mass and a mass of the prosthesis. A center of mass point was defined from a suspension test of a typical TRMP so the same value was used for all subjects (Figure 6.2). Table 6.1 shows these measurements calculated from the suspension test. The inertia term used was the same as published by Winter [16]. Appendix A under the Kinetics heading shows specifically how these corrections were implemented in the software program.



Figure 6.2. Suspension test on a typical TRMP to determine inertial properties.

Table 6.1. Inertial properties from a typical TRMP calculated from a suspension test.

| Segment of Prosthesis | Distance from distal end to CoM (cm) | Total Length | Proportion = Distance/Total |
|-----------------------|--------------------------------------|--------------|-----------------------------|
| Forearm | 19 | 28 | 0.68 |
| Hand | 10 | 17 | 0.59 |

6.6 Adjusted Inertial Properties with Added Mass

The amputee subjects completed the tasks with added mass proximally near the elbow and distally near the wrist. A 96 g mass was added using a wrist band measuring 7.5 cm along the principal axis on the forearm segment of the prosthesis.

To determine the new location of the center of mass as a proportion of the total length of the forearm (FA) the following equation was used:

$$\begin{aligned} \text{New } X_{\text{CoM of FA}} &= \frac{\sum \text{Moments}}{\sum \text{Mass}} \\ &= \frac{(X_{\text{CoM of FA}})(\text{Mass}_{\text{FA}}) + (X_{\text{CoM of Band}})(\text{Mass}_{\text{Band}})}{(\text{Mass}_{\text{FA}}) + (\text{Mass}_{\text{Band}})} \end{aligned} \quad (6.3)$$

- L_{Band} = Length of wrist band (added mass)
- L_{FA} = Length of forearm
- $X_{\text{CoM of FA}}$ = Position of center of mass of forearm
- $X_{\text{CoM of Band}}$ = Position of center of mass of wrist band

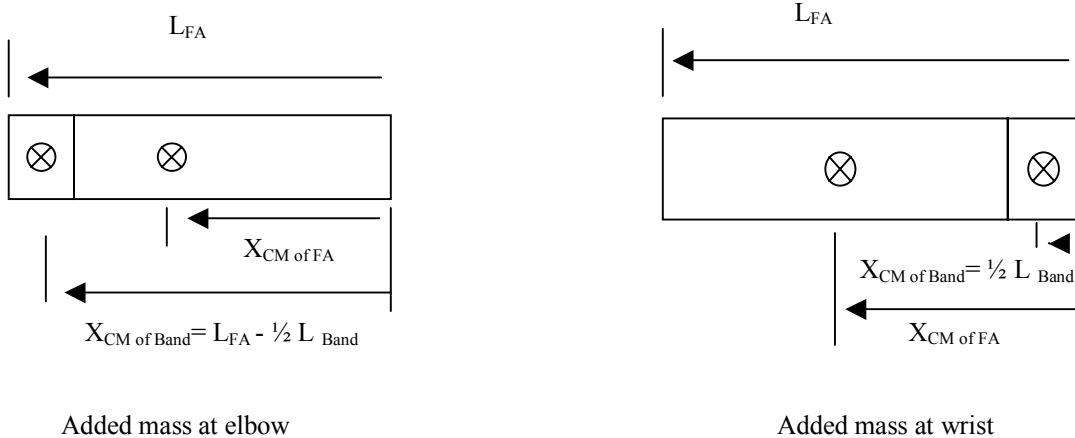


Figure 6.3. Depiction of the forearm (FA) with mass added at the elbow and at the wrist.

For each subject the distance from the distal end to the center of mass location was determined using the proportion determined from the suspension test on the average TRMP and the specific forearm lengths of the subjects using the following equation:

$$X \text{ cm} = (\text{length of forearm of prosthesis}) * (\text{proportion CoM location}) \quad (6.4)$$

where X cm = distance of CoM from distal end (wrist) and

length of forearm of prosthesis was measured for each subject and the

proportion of CoM location = 0.68 as measured from average TRMP as explained above. Table 6.2 shows the adjusted inertial properties for each of the amputee subjects with mass added at elbow and mass at wrist.

Table 6.2. Adjusted inertial properties of the prosthesis users with added mass.

| | Length of FA (cm) | Location of CoM as a proportion of FA length mass at elbow | Location of CoM as a proportion of FA length mass at wrist |
|-----------|-------------------|--|--|
| Subject 1 | 23 | 0.70 | 0.62 |
| Subject 2 | 23 | 0.70 | 0.62 |
| Subject 3 | 28 | 0.70 | 0.60 |
| Subject 4 | 29 | 0.70 | 0.62 |
| Subject 5 | 28 | 0.71 | 0.58 |
| Subject 6 | 31 | 0.70 | 0.61 |
| Subject 7 | 36 | 0.69 | 0.64 |

Chapter 7: Data Analysis

7.1 Validation

Validity is the degree to which a study accurately depicts the actual measurements examined. Numerous studies have validated the accuracy of motion analysis technique [50,51]

A validation study was conducted to determine the accuracy of the camera and marker placement as well as the Bodybuilder™ program (see Appendix A) that calculated angles written by the author. The same marker set described in Chapter 3 was used. The validity was first tested on a human volunteer. A plastic goniometer was used to position the subject's arm at various positions: shoulder flexion, shoulder abduction and elbow flexion at 30°, 60°, 90°, 120°, and 150°. The subject was asked to maintain these positions statically during recording. In a similar study, a universal goniometer was filmed in various static angular alignments in order to validate a Peak 5 motion analysis system [52].

Analysis of validity by linear regression was completed. Figure 7.1 depicts the relationship between the measuring devices during shoulder flexion. The difference between the means and standard deviations of the two measuring tool were computed. Pearson's *R* correlation, which describes the linear relationship between two variables, was also computed to compare the joint angles determined by the two modes of measurement [53]. The results of the validity testing comparing measurements from the

goniometer and from the ViconTM system during shoulder and elbow motion including the Pearson's *R* correlation are shown in Table 7.1.

Even though the results for the human subject elbow flexion showed a high correlation (Pearson's 0.99) a larger mean difference and standard deviation difference was shown, and therefore elbow flexion was also tested using a skeleton model. The skeleton model of the upper limb was used to dynamically flex the elbow to the following joint angles: 0°, 30°, 60°, 90°, 120°, and 150°. The arm was held in a neutral position and flexed at the elbow to the specified goniometer measurements and then back to the starting position. The results from the skeleton model validity test are shown in Table 7.2.

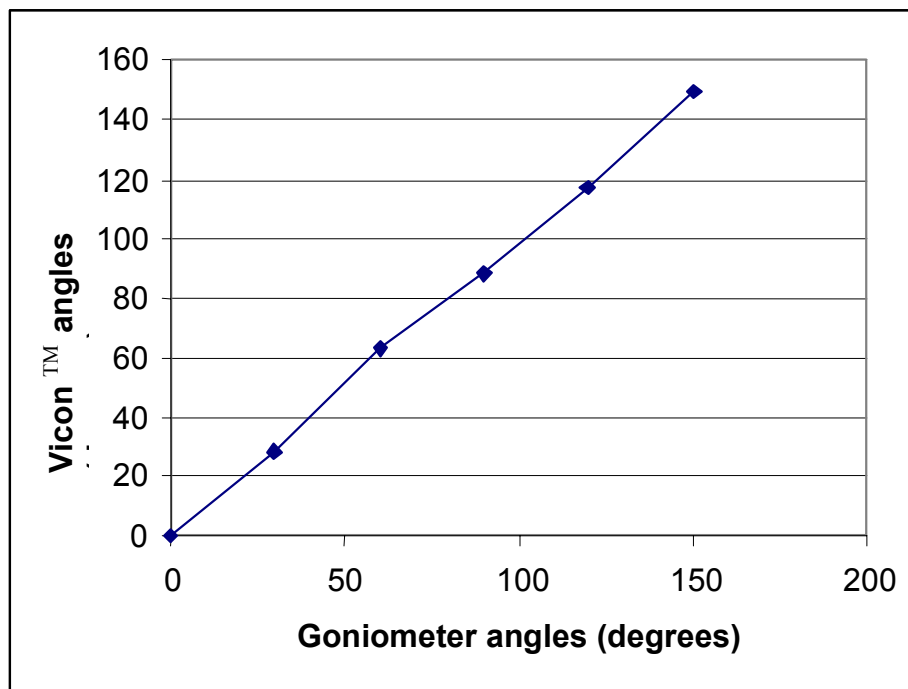


Figure 7.1. Linear regression between the goniometer and ViconTM for shoulder flexion.

Table 7.1. Measurements of shoulder and elbow angles from the goniometer and the Vicon™ system.

| | Shoulder Flexion | | Shoulder Abduction | | Elbow Flexion | |
|------------------|------------------|--------|--------------------|--------|---------------|--------|
| | Goniometer | Vicon™ | Goniometer | Vicon™ | Goniometer | Vicon™ |
| | 0 | 0.10 | 0 | 0 | 0 | 24.00 |
| | 30 | 28.50 | 30 | 33.90 | 30 | 47.30 |
| | 60 | 63.20 | 60 | 56.80 | 60 | 70.30 |
| | 90 | 87.80 | 90 | 82.90 | 90 | 95.20 |
| | 120 | 117.10 | 120 | 144.20 | 120 | 118.30 |
| | 150 | 149.20 | NA | NA | 150 | 140.90 |
| Mean Difference | 0.68 | | 3.6 | | 7.7 | |
| Stdev Difference | 0.72 | | 7 | | 12 | |
| Pearson's r | 0.99 | | 0.98 | | 0.99 | |

Table 7.2. Measurements of elbow flexion of skeleton model.

| Elbow flexion (Skeleton) | |
|--------------------------|------------------|
| Goniometer (degrees) | Vicon™ (degrees) |
| 30.00 | 54.30 |
| 60.00 | 60.80 |
| 90.00 | 95.30 |
| 120.00 | 117.00 |
| 150.00 | 148.40 |
| Mean difference = 1.6 | |
| Stdev. Difference = 3.6 | |
| Pearson's r = 0.985 | |

The validity results of the shoulder flexion show a 0.7 mean difference between the measurements taken and the results provided by Vicon™ system. The results of the shoulder abduction were much less conclusive. This was perhaps because of the subjective nature of taking measurements and/or the subject slightly changing position. These same limitations may explain the much higher mean difference in the elbow flexion of the human subject. However, the change in methodology and the usage of the skeleton as a subject provide for much more reassuring data with only a 1.6 mean difference.

7.2 Reliability

Reliability is the repeatability or consistency of a measurement. Reliability explains how reproducible and free from error a measurement is. Test-retest reliability describes the measurements consistency on two separate occasions keeping the testing conditions as stable as possible. Intrarater reliability refers the consistency of the data from one person over multiple trials one right after the other [53]. The intrarater reliability of the Vicon™ system in this case is more important since the trials on one subject were recording one right after each other on the same day. Figure 7.2 shows the average shoulder flexion with standard deviations of one subject while opening a door during 3 different trials. This graph indicates acceptable repeatability.

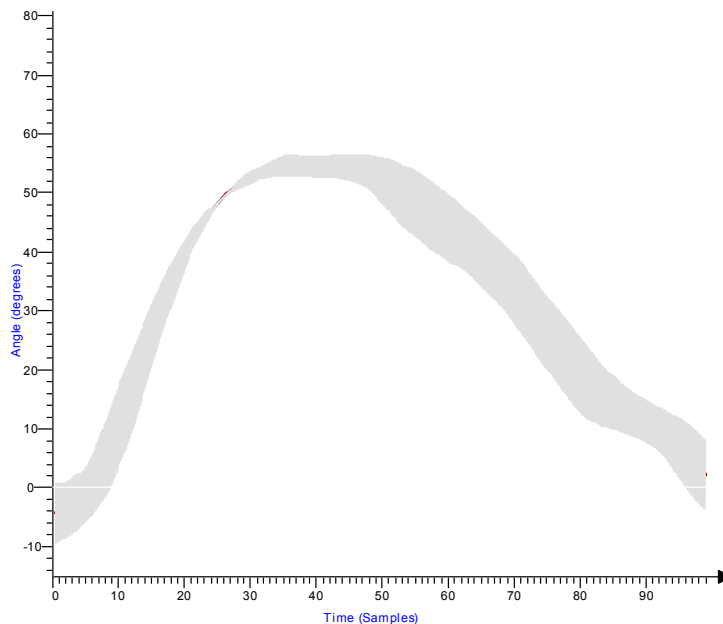


Figure 7.2. Average shoulder flexion with standard deviations shaded areas of one subject opening a door three times showing repeatability.

7.3 Kinematic Outcome Measures

The following kinematic outcome measures were calculated: range of shoulder flexion of glenohumeral joint, range of shoulder abduction, range of shoulder rotation, range of elbow flexion and torso sideways and forward bending. The range of motion was calculated by subtracting the minimum angle from the maximum angle. The maximum angle and total range of motion were then used in subsequent analyses.

For the drinking and door opening tasks, these measures were determined from the right (dominant) side for the control group and on the prosthesis side (6 subjects on the left side; 1 subject on the right side) for the PROS group. For the box lift and turning tasks, measures from both the right and left side were determined. The degree of asymmetry (DoA) between the right (dominant) side (R) and the left side (L) during the bilateral box lift task was calculated with the following equation:

$$\text{DoA} = \frac{(L - R)}{(L + R)} \quad (7.1)$$

The DoA was calculated for the range of shoulder flexion, shoulder abduction and elbow flexion. The value of zero represented perfect symmetry, a positive number and a negative number represented the left dominant asymmetry or increased range of motion of the left side and right dominant asymmetry respectively.

7.4 Kinetic Outcome Measures

The joint reaction forces and the joint moments of the glenohumeral joint, the elbow joint and the wrist joint were calculated. The forces in three directions (Fx, Fy, Fz) of the joints were calculated with Fx in the direction anteriorly to posteriorly, Fy,

medially to laterally and F_z in the vertical direction. The peak forces and moments were calculated and then divided by the individual subject body mass (N) to obtain values as a percentage of body mass in order to accurately compare between subjects. These peak forces and moment as expressed as % of body mass were used in the subsequent statistical analysis.

7.5 Statistical Analysis

7.5.1 Power Calculation to Determine Sample Size

There is a relatively small upper limb amputee patient population in the greater Tampa area, particularly when limited to TRMP users. As mentioned in Chapter 2, few studies have evaluated kinematic and kinetic data of the upper limb and even fewer have considered upper extremity prosthesis users. This fact makes estimating clinically relevant variability difficult. Murray et al. studied the joint angles, forces and moments at the shoulder and elbow on ten unimpaired subjects. They reported standard deviations ranging from 6° to 38° for shoulder flexion, 5° to 13° for shoulder abduction and 4° to 24° for elbow flexion among the ten tasks studied [34]. Changes smaller than 5° standard deviation will be too small to detect and changes in excess of 38° standard deviation is unrealistic expectations. Therefore standard deviation of 10° was chosen within the reported range of 5° to 38° of all movements.

The following power calculation was used to determine the sample size needed to show a

$$n = \frac{z_{\alpha/2} * \sigma}{E} \quad (7.2)$$

where $z_{\alpha/2} = 1.96$ at $\alpha = .05$

$\sigma = 10^\circ$ from 5° to 38° range reported [34]

$E = 7^\circ$ within the population mean, which is 4% of largest mean angle (164°) reported [34].

With this calculation it was determined that a sample size of seven would be sufficient to determine a statistical difference between groups. A power calculation to obtain a “norm” of a particular group would most likely produce a much higher sample size requirement. However, normal functional range of upper limb joints during feeding activities has been published with a sample size of ten [34].

7.5.2 Between Subject Analysis

Using SPSS software (Ver. 15 for Windows, Chicago, IL), a one-way analysis of variance (ANOVA) was performed on each maximum angle and range of motion for each of the four tasks separately between the three groups: non-braced (N-BR), braced (BR) and transradial prosthesis users (PROS). Since the N-BR and BR groups were the same subjects, a repeated measured ANOVA was conducted to determine differences between those two groups. A P value of less than 0.05 was considered significant with level of significance of $\alpha = 0.05$. A one-way ANOVA was also computed for the DoA for each range separately for the two bilateral tasks: lifting a box and turning a steering wheel. A Tukey post hoc comparison adjusted for unequal sample sizes was used to

determine between which two of the three groups the significant differences, if any, occurred [54,55].

7.5.3 With-In Subject Analysis

A within subject repeated measures design where each subject repeated tasks during the three levels: no mass added, mass added at elbow, mass at wrist was analyzed for the BR and PROS group. Again using SPSS software package package (Ver. 15 for Windows, Chicago, IL), a repeated measure analysis of variance (ANOVA) was performed on each maximum and range of motion for each task separately for the three interventions.

Chapter 8: Descriptive Observations

As explained in the previous chapter, average range of motions and maximum joint angles based on marker placement were collected and will be reported in Chapter 9. However, the marker set described in Chapter 3, was limited to the upper limbs and torso. During the study, compensatory motions were observed in other parts of the body such as the neck and legs but not analyzed due to the limitation of the marker set. For this reason and because only range and maximum angles were reported, this chapter is dedicated to descriptive observations of the completion of tasks.

8.1 Control Subjects

The control subjects were the ten non-amputee subjects that first completed the task with no brace and then completed the task with a brace limiting wrist and forearm movement. While drinking from the cup, all the control subjects followed a similar pattern of raising the cup to the mouth by mostly flexing the elbow. The door knob could be twisted to the right or to the left to be opened. All but one of the ten control subjects turned the door to the right by mostly supinating the forearm. The starting point of the forearm rotation varied, with some subjects starting in a neutral position and others starting with the forearm pronated. During the box lift, eight of the control subjects followed a three-part linear path: bringing the box straight toward the stomach in a horizontal line, lifting straight up to the level of the shelf in a vertical line and completing the task in a horizontal line. Two of the control subjects, brought the box toward stomach and upward at the same time in a more semi-circular motion.

Subjects were allowed to set the chair used during the turning task to a comfortable position that allowed two hands to remain on the steering wheel at a “10 and 2” position. This allowed for varying starting positions of the rest of the arm with some subjects keeping the elbow in a more extended position while others lowered and flexed the elbow. Spine posture also varied while turning a steering wheel with some subjects sitting up with the vertebral column straight and others sitting in a more slumped kyphotic position.

The guidelines described in Chapter 3 were given to the subjects, however, no instructions were given to the subjects on how to compensate for lack of wrist and forearm movements while braced. Braced subjects were observed forward bending the cervical spine (neck) to compensate while drinking from a cup. Movement of the cervical spine was not recorded and is non-quantified therefore limiting our ability to measure compensatory motions that may involve the neck in this study. The one control subject that turned the door to the left pronating his forearm turned the door to the right while braced. While using the brace, subjects were asked not to use the proximal interphalangeal (PIP) joints or the distal interphalangeal (DIP) joints of the fingers and instead hold the index and middle fingers straight moving only the metacarpophalangeal joints of these two fingers together in opposition to the thumb to simulate the one degree of freedom of a prosthetic hand. However, it seemed that two subjects were able to get some rotation of the door knob by flexing the PIP and DIP joints of the one or two fingers. Four of the subjects seemed to rely mostly on torso side bending for compensation, while two visibly internally rotated the shoulder and one awkwardly abducted the shoulder, to open the door while braced. During the box lift while braced,

all the subjects seemed to follow the same trajectory of the box (either linearly in three stages or a semi-circle) as with no brace, although some had to bend torso backwards to accommodate the same pattern. There were no visible obvious differences between braced and unbraced trials while turning a steering wheel.

8.2 Prosthesis Wearing Subjects

The subjects in the prosthesis wearing group had a wide range of techniques used to accomplish the tasks. As mentioned in Chapter 3 (3.3 Description of Tasks), the subjects were given limited guidelines for each task, and no specific instructions on how to complete the task that normally require forearm or wrist movement.

While drinking from a cup, five of the TRMP users had some forward bending of the cervical spine. One subject did not seem to bend the neck, rotate the torso to the left toward the side of the prosthesis to bring the cup up to mouth level. The other subject (Subject # 3, see Section 8.4) that did not use neck bending, abducted the shoulder to compensate for lack of wrist and forearm movement.

The compensatory motion of the TRMP users while opening a door seemed to be the most varied. All the TRMP users had some visible torso bending toward the side of the prosthesis. Two subjects bent the knees in a squatting position to open the door. One of these subjects squatted in such an exaggerated manner that he was eliminated from the analysis of the door task (see Chapter 9 Results). The other subject only bent slightly at the knees, and stood farther back from the door having to extend his arm greatly. Some of the TRMP users visibly bent the torso forward while one subject visibly bent the torso backward to open the door. One subject described in Section 8.4, positioned her body

perpendicular to the door (instead of facing toward the door) and seemed to hike her hip on the prosthetic side to complete the task.

Prior to lifting instead of bringing the box toward the chest and straight up, four of the subjects in the PROS group shifted the box toward the unaffected side and lifted the box following a horizontal semi-circular trajectory that differed from the vertical semi-circular path followed by a couple of the control subjects mentioned in Section 8.1. Without wrist extension, the prosthetic arm was unable to position the elbows out of the way to allow the box to be brought to the chest prior to lifting. The three TRMP users that did not use this circular pattern, seemed to rely more on the backward or side bending (toward the prosthetic side) of the torso. The majority (five of seven) of the PROS group chose to place the fingertips of the prosthetic hand on to the side of the box. The remaining two subjects placed the medial side of the thumb and index finger of the prosthetic hand on to the box.

8.3 Case Study of Prosthesis User Subject # 3

One subject was reported as a case study for the American Academy of Orthotics and Prosthetists Conference (Orlando, FL; Feb. 2008). This volunteer was a 53 year old female who was born with a congenital defect on the left arm that required surgical revision of a vestigial limb. She had been using the myoelectric transradial prosthesis with SensorHand (Otto Bock, Duderstadt, Germany) for sixteen years. Her prosthesis weighed 1.2 kg. In addition to completing the tasks with the prosthesis, this subject completed three of the simulated activities of daily living: drinking from a cup, opening a door, and turning a steering wheel with her sound hand also. For the steering wheel task,

the subject completed the task three times, first turning to the right (sound side) and then to the left prosthetic side. Table 8.1 shows the maximum, minimum and range of the shoulder, elbow and torso motion for each task. The wrist flexion and extension and forearm rotation (Table 8.1) were calculated for the sound arm only since the prosthesis did not allow for these motions.

While drinking from a cup with the sound arm, the subject used a total of 31 degrees of wrist flexion and extension and 24 degrees of forearm rotation. While using the prosthesis the subject used less elbow flexion and a greater peak shoulder abduction to compensate for the lack of wrist movement and forearm movement. Opening a door with the sound arm required 64 degrees of wrist flexion and extension and 123 degrees of forearm rotation. Compensation while completing the door opening task with a prosthesis occurred by bending the torso to the right side and by maintaining the elbow flexed at 87 degrees (Figure 8.1a-b). The steering wheel task also required wrist flexion (49 degrees) and forearm pronation (33 degrees) of the sound arm. With the lack of these movements on the prosthetic side, like during the door task the elbow remained mostly flexed, but the shoulder flexed and abducted more to compensate.

Table 8.1. The maximum, minimum and range of motions (in degrees) during each task for Subject # 3 of prosthesis users.

| Task | Motion (in degrees) | Left | | | Right | | |
|------|-------------------------------------|------|-----|-------|-------|-----|-------|
| | | Max | Min | Range | Max | Min | Range |
| Cup | | | | | | | |
| | Shoulder flexion | 71 | 25 | 46 | 73 | 25 | 48 |
| | Shoulder ab(+)/ad(-)duction | 21 | 18 | 3 | 12 | 3 | 9 |
| | Elbow flexion | 102 | 74 | 28 | 122 | 72 | 50 |
| | Wrist flexion (+)/extension(-) | N/A | N/A | N/A | 21 | -10 | 31 |
| | Forearm pronation(+)/supination (-) | N/A | N/A | N/A | 16 | -8 | 24 |
| Door | | | | | | | |
| | Shoulder flexion | 23 | 4 | 19 | 57 | 17 | 40 |
| | Shoulder ab(+)/ad(-)duction | 35 | 26 | 9 | -1 | -11 | 10 |
| | Elbow flexion | 87 | 80 | 7 | 58 | 5 | 53 |
| | Torso bend right | 16 | 3 | 13 | 9 | 5 | 4 |
| | Wrist flexion (+)/extension(-) | N/A | N/A | N/A | 25 | -39 | 64 |
| | Forearm pronation(+)/supination (-) | N/A | N/A | N/A | 46 | -77 | 123 |
| Turn | | | | | | | |
| | Shoulder flexion | 109 | 48 | 61 | 95 | 49 | 46 |
| | Shoulder ab(+)/ad(-)duction | 43 | 6 | 37 | 5 | -17 | 22 |
| | Elbow flexion | 88 | 76 | 12 | 83 | 48 | 35 |
| | Wrist flexion (+)/extension(-) | N/A | N/A | N/A | 49 | 0 | 49 |
| | Forearm pronation(+)/supination (-) | N/A | N/A | N/A | 33 | 0 | 33 |

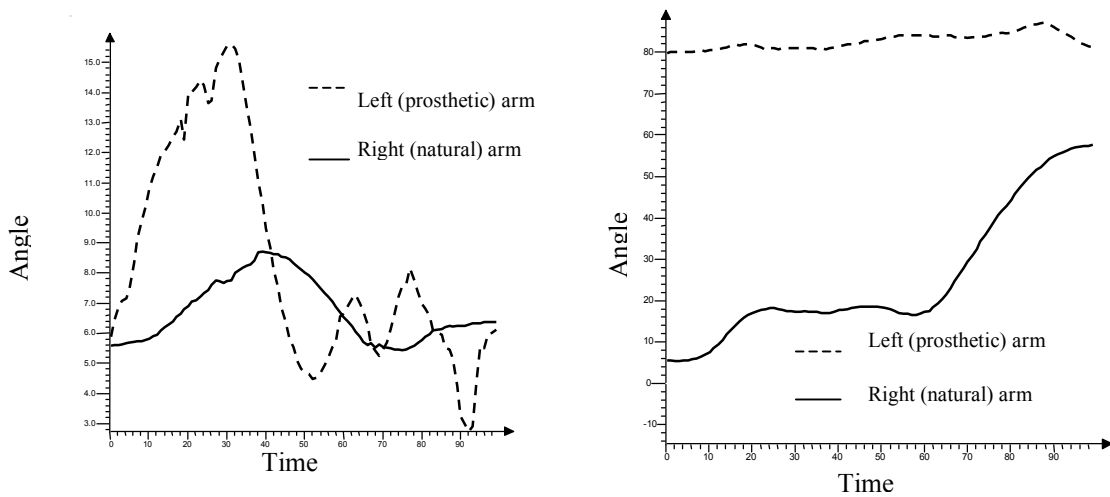


Figure 8.1.a. Torso right side bend during the door task. Figure 8.1.b. Elbow flexion during the door task.

In general when comparing the prosthetic and sound arm for this subject, an increase in peak shoulder abduction was shown in all tasks. The elbow of the sound side

and prosthetic side was also used differently either less or by maintaining a greater peak flexion. Opening the door required torso right side bending which was not predicted. This may have been due to the difficulty of grasping the door knob with prosthetic hand. It was difficult to recruit volunteers using a TRMP to complete this study so this type of comparison between the prosthetic and sound arm was not recorded and analyzed due to the extra time commitment it would have required from the subjects.

Chapter 9: Experimental Results

9.1 Range of Motion Results

Peak wrist flexion and extension and peak forearm pronation and supination required to complete the tasks by the non-impaired group are shown in Table 9.1. The BR group and the PROS group lacked forearm and wrist movements and used different parts of the upper limb kinetic chain as compensation to complete the tasks.

Table 9.1. Average and standard deviation (SD) peak wrist flexion and extension and peak forearm pronation and supination of right (dominant) side (in degrees) of control group during the four tasks.

| Task | Wrist flexion | | Wrist extension | | Forearm pronation | | Forearm supination | |
|------------|---------------|----|-----------------|----|-------------------|----|--------------------|----|
| | Angle(°) | SD | Angle(°) | SD | Angle (°) | SD | Angle (°) | SD |
| Cup | 7 | 7 | 25 | 7 | 11 | 8 | 2 | 8 |
| Door | 20 | 8 | 25 | 17 | 54 | 29 | 39 | 37 |
| Box lift | 8 | 11 | 70 | 12 | 0 | 0 | 70 | 18 |
| Right turn | 62 | 16 | 21 | 14 | 36 | 12 | 75 | 31 |

9.1.1 Between Group Results

The outcome measures between the three groups: non-braced (N-BR), braced (BR) and prosthesis user (PROS) were compared using a one way analysis of variance as explained in detail in Section 7.5. Tables 9.2-9.5 list the maximum (MAX) and range of motion (ROM) of the glenohumeral joint in the sagittal plane (GHsag), the frontal plane (GHfront), the transverse plane (Ghtran), the elbow flexion (Elflex) and in some cases the torso motion of the three groups during each task.

9.1.1.1 Drinking from a Cup

The mean maximum and total range of motions of the shoulder and elbow while drinking from a cup are shown in Table 9.2. Significant differences ($P < 0.05$; $\alpha = 0.05$) were found in the range of GHsag ($P = 0.04$) between the groups. Tukey post hoc comparisons showed the PROS group has a significantly less range of motion in the GH joint in the sagittal plane (Figure 9.1). The PROS group had the greatest range of elbow flexion (40 degrees) of the groups (Figure 9.2).

Table 9.2. The maximum and range of motion of the glenohumeral (GH) joint and the elbow joint of the three groups while drinking from a cup.

| CUP | N-BR | | | | BR | | | | PROS | | | |
|---------|------|----|-----|----|-----|----|-----|----|------|----|-----|----|
| Angle | Max | SD | ROM | SD | Max | SD | ROM | SD | Max | SD | ROM | SD |
| GHsag | 70 | 19 | 69 | 19 | 77 | 6 | 71 | 24 | 72 | 30 | 47 | 12 |
| GHfront | 28 | 8 | 10 | 7 | 31 | 12 | 13 | 9 | 23 | 13 | 9 | 7 |
| GHtran | 28 | 28 | 20 | 6 | 33 | 23 | 21 | 17 | 37 | 13 | 20 | 9 |
| ELflex | 123 | 10 | 31 | 13 | 115 | 8 | 30 | 11 | 112 | 16 | 40 | 9 |

Note: Max: maximum; ROM: range of motion; SD: standard deviation

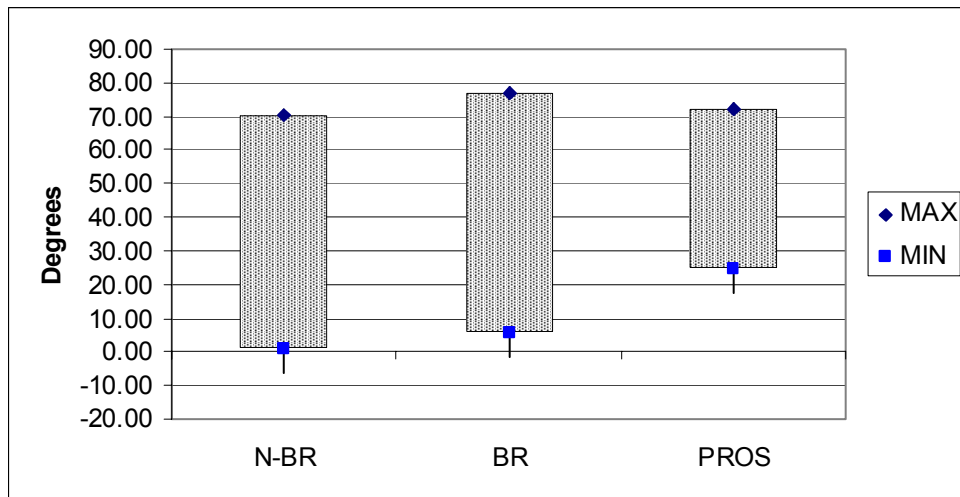


Figure 9.1. Average range of motion of the glenohumeral (GH) joint in the sagittal plane of the three groups while drinking from a cup.

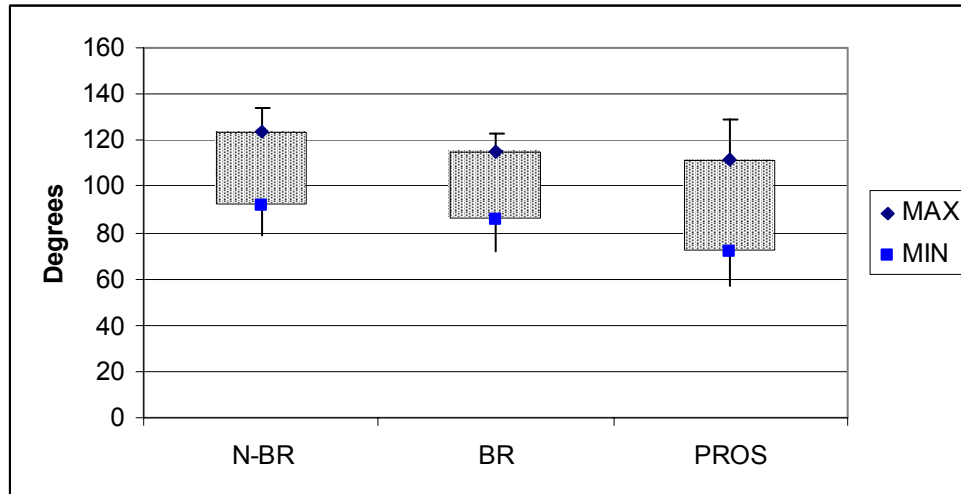


Figure 9.2. Average range of elbow flexion of the three groups while drinking from a cup.

9.1.1.2 Opening a Door

The mean maximum and total range of motions of the shoulder and elbow while opening a door are shown in Table 9.3. While opening a door, the PROS and BR group showed significantly greater range of shoulder rotation when compared to the N-BR group ($P = <.001$; $P=.046$). The PROS group has the largest internal shoulder rotation, while the N-BR showed external shoulder rotation (Figure 9.3). Significant differences were shown in the range of motion of the elbow flexion ($P=0.003$). Tukey post hoc comparisons showed that the PROS group had a significantly smaller range of elbow flexion than the N-BR group (Figure 9.4). Figure 9.5 shows the torso side bending toward the affected side of one subject from each group while opening a door. Only subjects that completed the door task without total knee bending were considered and therefore six subjects in the PROS were used for analysis of this task. Peak torso bending to the right and the range of torso right side bending was significantly greater ($P=0.002$; $P=0.009$ respectively) in the PROS group compared to the N-BR group (Figure 9.6). Although the

BR group showed a greater range of torso bending when compared to the N-BR group, this difference was not significant.

Table 9.3. Maximum and total range of motion of shoulder and elbow of the reference, braced and prosthetic side while drinking from a cup.

| DOOR | N-BR | | | | BR | | | | PROS | | | |
|---------------------|------|----|-----|----|-----|----|-----|----|------|----|-----|----|
| | Max | SD | ROM | SD | Max | SD | ROM | SD | Max | SD | ROM | SD |
| GHsag | 52 | 12 | 49 | 12 | 50 | 18 | 51 | 18 | 44 | 30 | 38 | 29 |
| GHfront | 29 | 7 | 15 | 7 | 35 | 11 | 17 | 5 | 30 | 12 | 20 | 12 |
| GHtran | -7 | 13 | 18 | 9 | 9 | 27 | 49 | 17 | 30 | 18 | 37 | 11 |
| ELflex | 66 | 14 | 53 | 14 | 61 | 15 | 41 | 16 | 73 | 16 | 24 | 16 |
| Torso Sideways Bend | 5 | 7 | 10 | 5 | 8 | 12 | 16 | 7 | 26 | 13 | 19 | 11 |

Note: Max: maximum; ROM: range of motion; SD: standard deviation

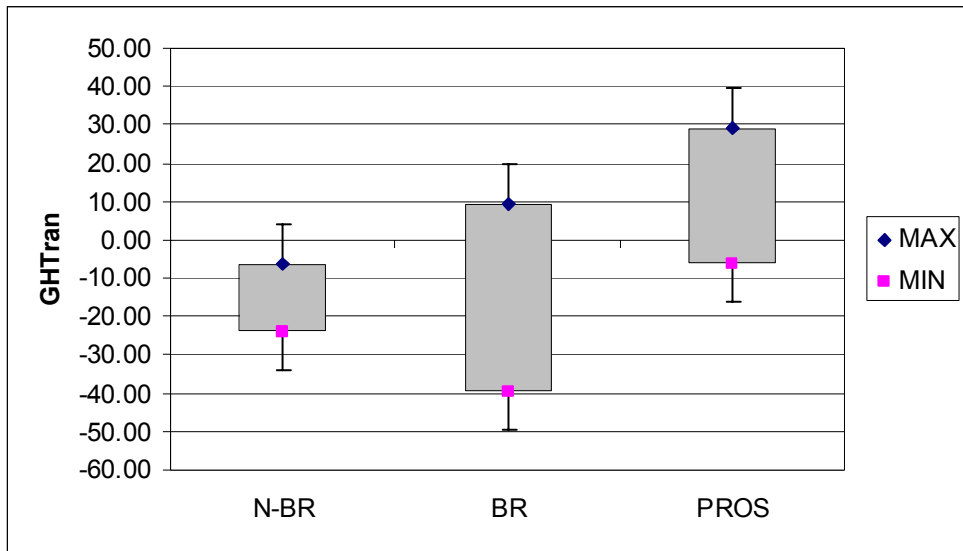


Figure 9.3. Average range of shoulder rotation of the three groups while opening a door.

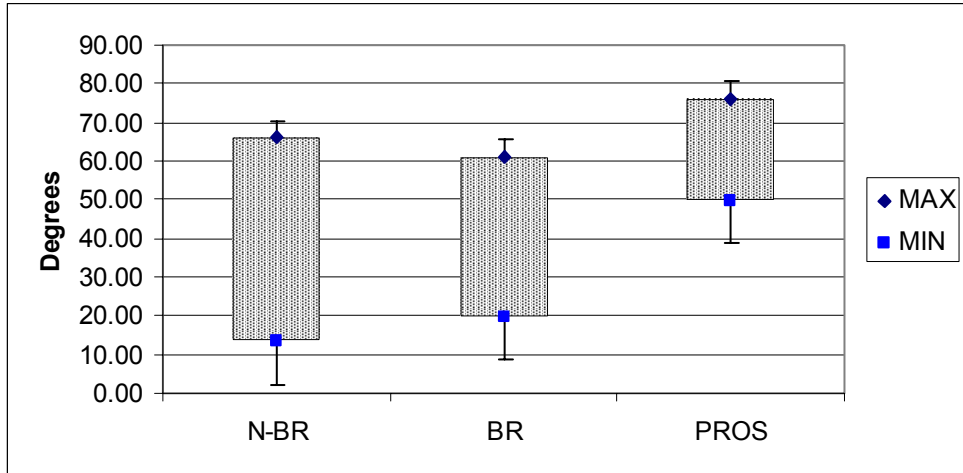


Figure 9.4. Average range of elbow flexion of the three groups while opening a door.

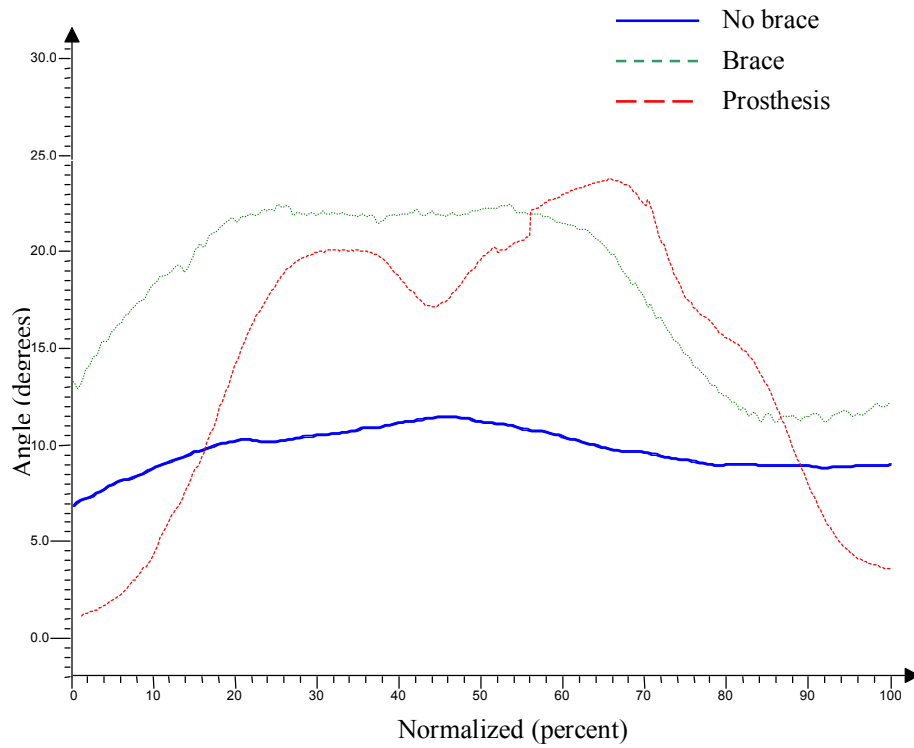


Figure 9.5. Torso side bending (toward affected side) of one subject from each group while opening a door.

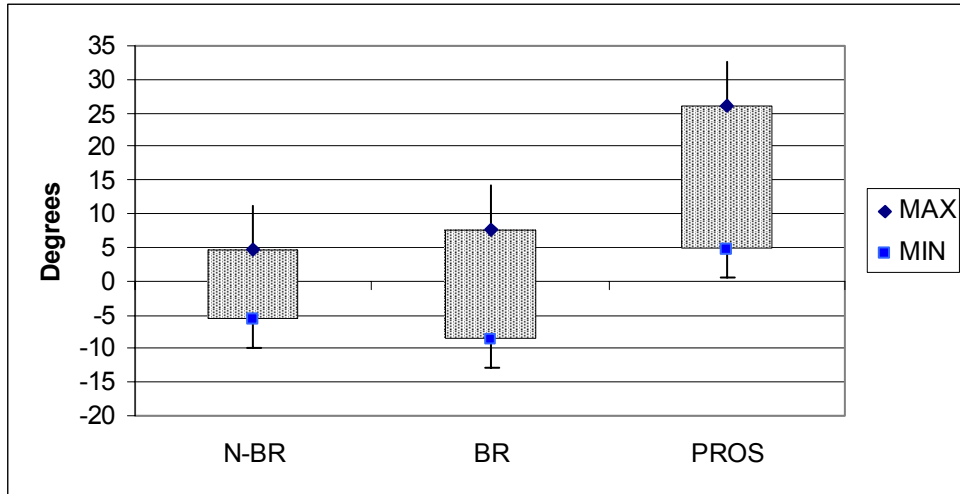


Figure 9.6. Average torso bending (affected side +; unaffected side -) during door opening of the three groups.

9.1.1.3 Lifting a Box

Significant differences were shown in the range of motion of the glenohumeral joint in both the sagittal plane ($P=.001$) and frontal plane ($P<.001$) and the range of motion of the elbow ($P<.001$) while lifting a box (Table 9.4). Tukey post hoc comparisons showed that the differences were between the N-BR and PROS groups and the BR and PROS groups. As shown in Figure 9.6, the PROS group showed a significantly greater maximum and range of torso forward bending during the box lift task when compared to the N-BR group ($P<0.001$) and the BR group ($P=0.010$). The PROS group also showed significantly increased maximum torso right side bending ($P<0.001$) when compared to N-BR and BR groups, although the difference in total range of torso side bending was not significant (Figure 9.8).

Table 9.4 Average maximum (Max) and range of motion (ROM) of the three groups while lifting a box.

| Box Lift | N-BR | | | | BR | | | | PROS | | | |
|------------|------|----|-----|----|-----|----|-----|----|------|----|-----|----|
| | Max | SD | ROM | SD | Max | SD | ROM | SD | Max | SD | ROM | SD |
| A GHsag | 88 | 13 | 82 | 17 | 89 | 20 | 70 | 12 | 85 | 16 | 42 | 22 |
| UA GHsag | 85 | 12 | 81 | 19 | 81 | 14 | 77 | 15 | 77 | 11 | 73 | 19 |
| A GHfront | 41 | 7 | 30 | 8 | 43 | 8 | 25 | 9 | 32 | 10 | 11 | 7 |
| UA GHfront | 44 | 10 | 28 | 8 | 42 | 10 | 28 | 7 | 27 | 14 | 23 | 12 |
| A GHtran | 23 | 13 | 25 | 14 | 31 | 44 | 34 | 11 | 42 | 30 | 22 | 10 |
| UA GHtran | 33 | 13 | 34 | 12 | 33 | 18 | 27 | 13 | 44 | 13 | 28 | 13 |
| A ELflex | 102 | 13 | 78 | 18 | 84 | 31 | 54 | 26 | 66 | 17 | 21 | 18 |
| UA ELflex | 108 | 7 | 78 | 19 | 90 | 30 | 71 | 22 | 82 | 21 | 56 | 29 |

Note: Max: maximum; ROM: range of motion; SD: standard deviation, A:affected side; UA:unaffected side

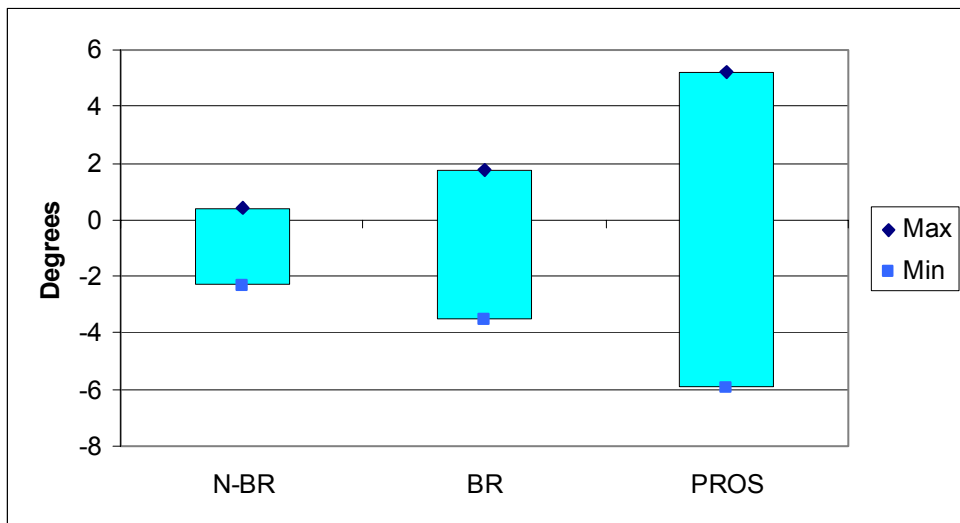


Figure 9.7. Average torso bending (forward + / backward-) while lifting a box.

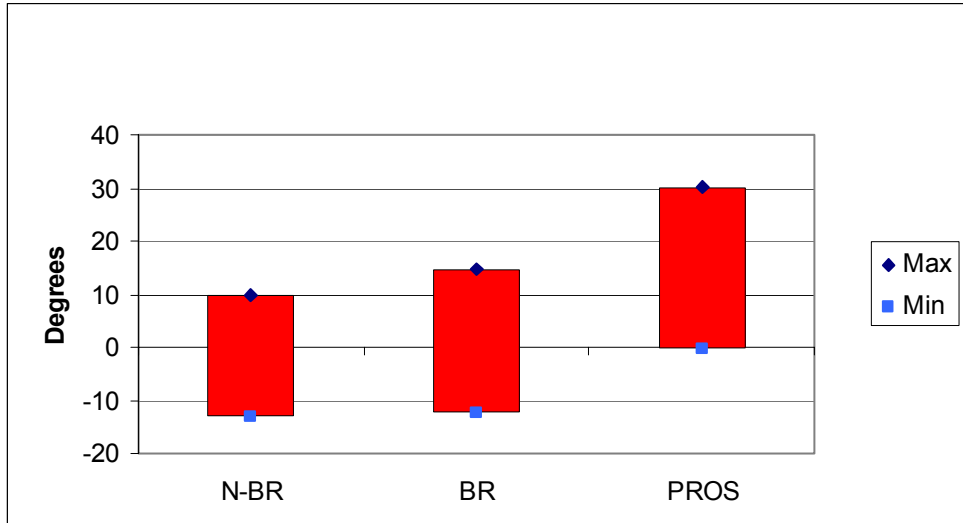


Figure 9.8. Average range of torso bending (Right side +; Left side -) while lifting a box.

The degrees of asymmetry of the range of motion of the glenohumeral joint in sagittal plane and the range of motion of the elbow also had significant differences between the N-BR and PROS group (GHSag: $P < .001$; ELFlex: $P < .001$) and the BR and PROS group (GHSag: $P < .001$; ELFlex: $P = .01$). Figure 9.9 shows that the PROS group had a greater dominance on the unaffected side while lifting a box.

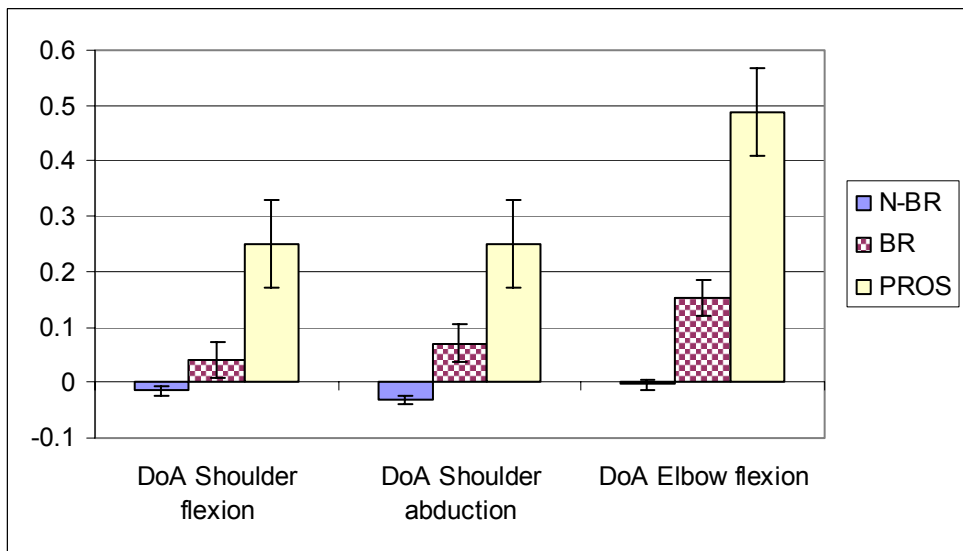


Figure 9.9. Degree of asymmetry during the box lift for each of the three groups.

Note: Positive DoA represents an unaffected side dominance.

9.1.1.4 Turning a Steering Wheel

Figure 9.10 shows an example of the shoulder flexion of one subject while turning a steering wheel non-braced and braced. It shows that during the braced condition the right (affected) shoulder moves through a greater range of flexion when compared to the non-braced trials. Oppositely, the left shoulder moves through a lesser range of flexion during the right arm braced trial when compared to the non-braced trial.

The PROS group showed a significantly greater maximum ($P=0.004$) and total range of elbow flexion ($P=0.008$) of the unaffected arm when compared to BR group although not significant when compared to the N-BR group (Figure 9.11). Asymmetry between the affected and unaffected side was shown in the BR and PROS groups although differently (Figure 9.12).

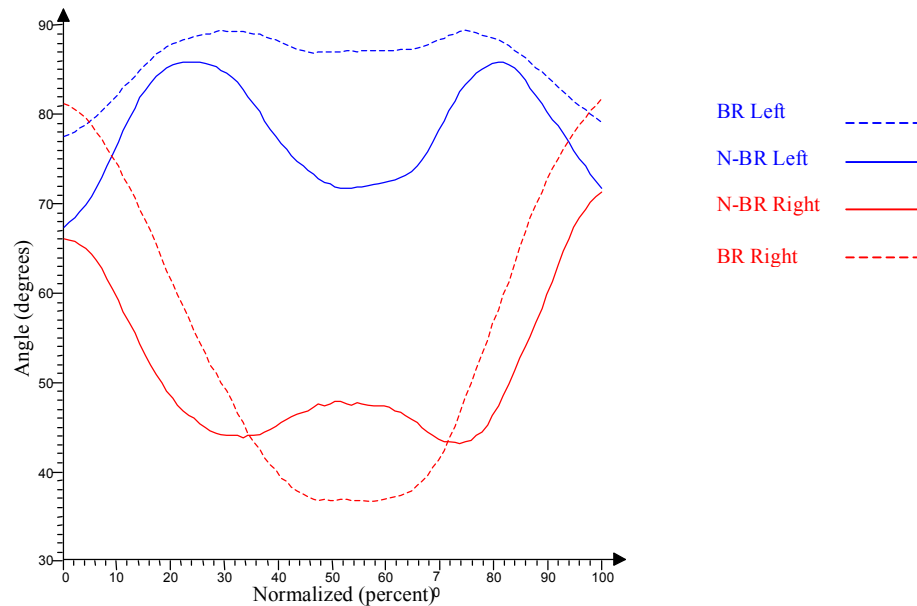


Figure 9.10. Right (affected) and left shoulder flexion of one subject during the non-braced and braced conditions while turning a steering wheel to the affected side.

Table 9.5 Average maximum (Max) and range of motion (ROM) of the three groups while turning a steering wheel to the affected side.

| Steering wheel turn | N-BR | | | | BR | | | | PROS | | | |
|---------------------|------|----|-----|----|-----|----|-----|----|------|----|-----|----|
| | Max | SD | ROM | SD | Max | SD | ROM | SD | Max | SD | ROM | SD |
| A GHsag | 78 | 12 | 39 | 8 | 86 | 18 | 49 | 5 | 73 | 11 | 36 | 14 |
| UA GHsag | 99 | 11 | 22 | 6 | 95 | 9 | 15 | 5 | 91 | 4 | 31 | 9 |
| A GHfront | 13 | 6 | 26 | 9 | 18 | 10 | 23 | 10 | 22 | 13 | 16 | 7 |
| UA GHfront | 15 | 9 | 31 | 7 | 15 | 13 | 27 | 10 | 3 | 4 | 17 | 6 |
| A GHtran | -18 | 13 | 22 | 8 | -4 | 16 | 28 | 10 | -23 | 21 | 30 | 17 |
| UA GHtran | 41 | 20 | 34 | 17 | 35 | 21 | 24 | 10 | 38 | 15 | 28 | 14 |
| A ELflex | 60 | 17 | 17 | 5 | 63 | 19 | 29 | 12 | 73 | 14 | 19 | 11 |
| UA ELflex | 40 | 14 | 29 | 13 | 30 | 13 | 14 | 8 | 58 | 19 | 31 | 12 |

Note: Max: maximum; ROM: range of motion; SD: standard deviation, A:affected side; UA:unaffected side

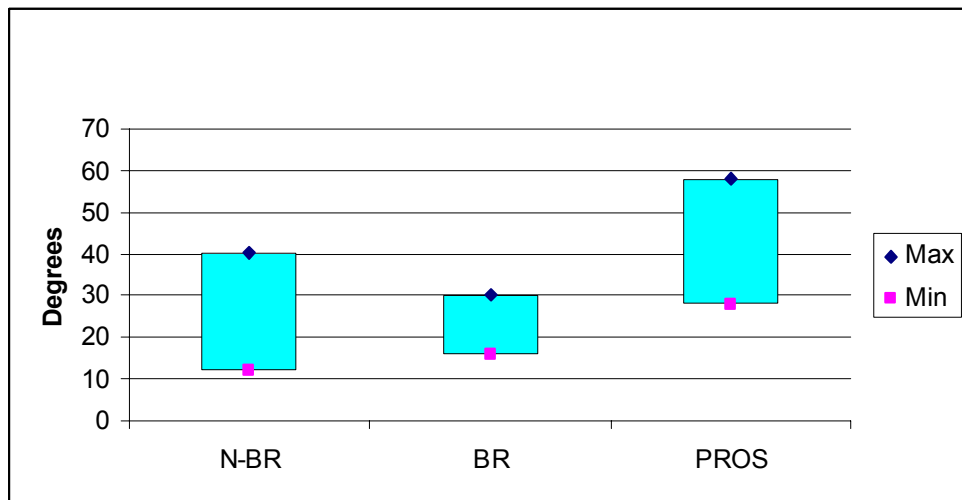


Figure 9.11. Average range of elbow flexion of the reference, braced and prosthetic side while turning a steering wheel to the affected side.

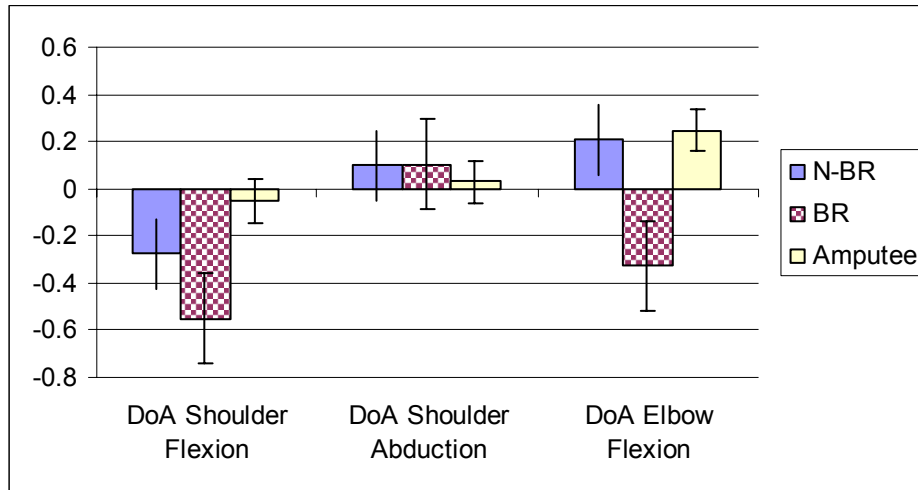


Figure 9.12. Degree of asymmetry of range of motions during the steering wheel right turn.

Note: Negative DoA represents affected side dominance.

Significant differences while turning a steering wheel were shown in all range of motions except in the affected glenohumeral joint in the frontal plane. Tukey post hoc comparisons showed that most of the differences occurred between the N-BR and BR group. Asymmetry between the affected and unaffected side was shown in the BR and PROS group although differently (Figure 9.13).

9.1.2 Braced Group With-In Subject Results

The average range of motion of the shoulder, elbow and in some cases torso while drinking from a cup, opening a door, lifting a box and turning a steering wheel with the different mass placements while the control group was braced are shown in Tables 9.6-9.9 respectively.

There were no significant differences between the three factor levels for shoulder motion while drinking from a cup (n=9).

Table 9.6. Maximum and range of motions of braced group while drinking from a cup during three mass conditions.

| CUP | BR | | | | BR -EL | | | | BR-WR | | | |
|---------|-----|----|-----|----|--------|----|-----|----|-------|----|-----|----|
| | Max | SD | ROM | SD | Max | SD | ROM | SD | Max | SD | ROM | SD |
| GHsag | 77 | 6 | 71 | 24 | 77 | 20 | 69 | 20 | 75 | 23 | 70 | 24 |
| GHfront | 31 | 12 | 13 | 9 | 31 | 9 | 10 | 6 | 33 | 14 | 13 | 13 |
| ELflex | 115 | 8 | 30 | 11 | 112 | 8 | 28 | 12 | 111 | 13 | 28 | 14 |

Note: Max: maximum; ROM: range of motion; SD: standard deviation

Table 9.7. Maximum and range of motions of the braced group while opening a door during three mass conditions.

| DOOR | BR | | | | BR-EL | | | | BR-WR | | | |
|---------|-----|----|-----|----|-------|----|-----|----|-------|----|-----|----|
| | Max | SD | ROM | SD | Max | SD | ROM | SD | Max | SD | ROM | SD |
| GHsag | 50 | 18 | 51 | 18 | 46 | 15 | 49 | 15 | 53 | 12 | 51 | 14 |
| GHfront | 35 | 11 | 17 | 5 | 36 | 9 | 18 | 8 | 36 | 10 | 18 | 7 |
| ELflex | 61 | 15 | 41 | 16 | 62 | 20 | 38 | 13 | 48 | 13 | 31 | 13 |

Note: Max: maximum; ROM: range of motion; SD: standard deviation

Although no significant differences were found between the different added mass positions: near the elbow (proximally) or near the wrist (distally), Figure 9.13 demonstrates the difference in degree of asymmetry of elbow flexion during the box lift during the four experimental conditions completed by the control group.

Table 9.8. Maximum and range of motions of braced group while lifting a box during three mass conditions.

| Box Lift | BR | | | | BR-EL | | | | BR-WR | | | |
|------------|-----|----|-----|----|-------|----|-----|----|-------|----|-----|----|
| | Max | SD | ROM | SD | Max | SD | ROM | SD | Max | SD | ROM | SD |
| A Ghsag | 89 | 20 | 70 | 12 | 89 | 20 | 69 | 11 | 87 | 23 | 69 | 15 |
| UA Ghsag | 81 | 14 | 77 | 15 | 80 | 11 | 81 | 15 | 79 | 14 | 79 | 17 |
| A Ghfront | 43 | 8 | 25 | 9 | 41 | 10 | 24 | 8 | 43 | 9 | 31 | 12 |
| UA Ghfront | 42 | 10 | 28 | 7 | 40 | 10 | 26 | 4 | 44 | 11 | 30 | 5 |
| A Elbow | 84 | 31 | 54 | 26 | 83 | 39 | 60 | 26 | 77 | 35 | 50 | 23 |
| UA Elbow | 90 | 30 | 71 | 22 | 94 | 60 | 71 | 22 | 97 | 55 | 77 | 30 |

Note: Max: maximum; ROM: range of motion; SD: standard deviation

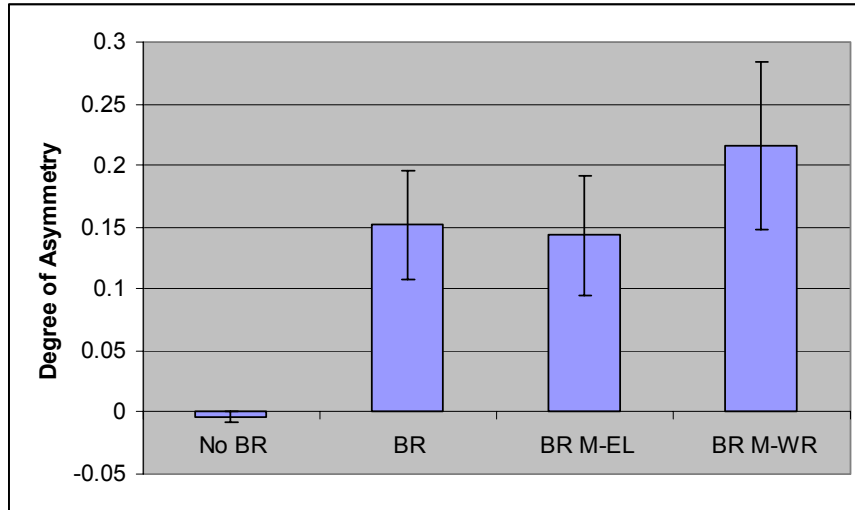


Figure 9.13. Degree of asymmetry of elbow flexion while lifting a box during four conditions.

Note: 0 is perfect symmetry; Negative DoA represents affected side dominance.

Table 9.9. Maximum and range of motions of braced group while turning a steering wheel during three mass conditions.

| Steering wheel turn | BR | | | | BR-EL | | | | BR-WR | | | |
|---------------------|-----|----|-----|----|-------|----|-----|----|-------|----|-----|----|
| | Max | SD | ROM | SD | Max | SD | ROM | SD | Max | SD | ROM | SD |
| A GHsag | 86 | 18 | 49 | 5 | 89 | 17 | 45 | 8 | 89 | 19 | 46 | 12 |
| UA GHsag | 95 | 9 | 15 | 5 | 98 | 11 | 14 | 5 | 98 | 12 | 16 | 6 |
| A GHfront | 18 | 10 | 23 | 10 | 16 | 8 | 18 | 9 | 18 | 9 | 20 | 9 |
| UA GHfront | 15 | 13 | 27 | 10 | 13 | 12 | 24 | 7 | 14 | 12 | 26 | 7 |
| A Elbow | 63 | 19 | 29 | 12 | 55 | 20 | 25 | 8 | 54 | 20 | 26 | 12 |
| UA Elbow | 30 | 13 | 14 | 8 | 33 | 15 | 18 | 11 | 32 | 14 | 18 | 11 |

Note: Max: maximum; ROM: range of motion; SD: standard deviation

9.1.3 Prosthesis Wearing Group With-In Subject Results

During the box lift, a significant difference ($p = .033$) was shown in the GHSag on the affected side. Bonferroni pairwise comparisons showed that range of GHSag was significantly greater ($p = .035$) with the prosthesis only when compared to using the prosthesis with added mass at the elbow. Using the prosthesis with added mass at the

wrist was not significantly different. A significant difference ($p = .003$) was also shown in the degree of asymmetry of the GHfront during the box lift. Bonferroni pairwise comparisons showed that the degree of asymmetry was more positive (representing an unaffected side dominance) for the PROS ($p = .016$) and PROS-WR ($p = .002$) when compared to the PROS-EL mass condition. No other significant differences were found in joint angles when comparing the three experimental set-ups: using a prosthesis, using a prosthesis with added mass at elbow, and using a prosthesis with added mass at wrist. The mean range of motions of the shoulder and elbow for the different added mass conditions are shown in Tables 9.10- 9.13.

Table 9.10. Maximum and range of motions of prosthesis users while drinking from a cup at three mass conditions.

| Cup | PROS | | | | PROS-EL | | | | PROS-WR | | | |
|---------|------|----|-----|----|---------|----|-----|----|---------|----|-----|----|
| | Max | SD | ROM | SD | Max | SD | ROM | SD | Max | SD | ROM | SD |
| GHsag | 72 | 31 | 47 | 12 | 67 | 31 | 46 | 14 | 72 | 31 | 47 | 12 |
| GHfront | 23 | 14 | 9 | 7 | 23 | 13 | 10 | 7 | 23 | 14 | 8 | 6 |
| ELflex | 112 | 17 | 40 | 9 | 103 | 11 | 32 | 9 | 107 | 8 | 37 | 13 |

Note: Max: maximum; ROM: range of motion; SD: standard deviation

Table 9.11. Maximum and range of motions of prosthesis users while opening a door at three mass conditions.

| Door | PROS | | | | PROS-EL | | | | PROS-WR | | | |
|-----------------|------|----|-----|----|---------|----|-----|----|---------|----|-----|----|
| | Max | SD | ROM | SD | Max | SD | ROM | SD | Max | SD | ROM | SD |
| GHsag | 44 | 30 | 38 | 29 | 43 | 27 | 41 | 24 | 42 | 23 | 44 | 24 |
| GHfront | 30 | 12 | 20 | 12 | 29 | 13 | 17 | 10 | 31 | 13 | 22 | 9 |
| ELflex | 73 | 16 | 24 | 16 | 72 | 17 | 26 | 17 | 72 | 18 | 24 | 11 |
| Torso side bend | 26 | 13 | 19 | 11 | 22 | 18 | 22 | 18 | 19 | 20 | 19 | 20 |

Note: Max: maximum; ROM: range of motion; SD: standard deviation

Table 9.12. Maximum and range of motions of prosthesis users while lifting a box at three mass conditions.

| Box Lift | PROS | | | | PROS-EL | | | | PROS-WR | | | |
|------------------|------|----|-----|----|---------|----|-----|----|---------|----|-----|----|
| | Max | SD | ROM | SD | Max | SD | ROM | SD | Max | SD | ROM | SD |
| Angle | | | | | | | | | | | | |
| A GHsag | 85 | 16 | 42 | 8 | 81 | 13 | 36 | 9 | 84 | 17 | 37 | 8 |
| UA GHsag | 77 | 11 | 73 | 19 | 77 | 10 | 64 | 22 | 75 | 12 | 70 | 22 |
| A GHfront | 32 | 10 | 12 | 7 | 33 | 11 | 13 | 4 | 32 | 10 | 9 | 4 |
| UA GHfront | 27 | 14 | 23 | 12 | 22 | 14 | 19 | 10 | 24 | 14 | 21 | 10 |
| A Elbow | 66 | 17 | 21 | 18 | 66 | 15 | 20 | 16 | 70 | 22 | 25 | 22 |
| UA Elbow | 82 | 21 | 56 | 29 | 80 | 25 | 57 | 33 | 84 | 24 | 57 | 29 |
| Torso Bend Right | 5 | 4 | 11 | 6 | 5 | 5 | 12 | 6 | 3 | 6 | 10 | 6 |
| Torso Bend Front | 30 | 11 | 31 | 10 | 31 | 8 | 29 | 11 | 32 | 11 | 34 | 12 |

Note: Max: maximum; ROM: range of motion; SD: standard deviation

Table 9.13. Maximum and range of motions of prosthesis users while turning a steering wheel at three mass conditions.

| Steering Wheel Turn | PROS | | | | PROS-EL | | | | PROS-WR | | | |
|---------------------|------|----|-----|----|---------|----|-----|----|---------|----|-----|----|
| | Max | SD | ROM | SD | Max | SD | ROM | SD | Max | SD | ROM | SD |
| Angle | | | | | | | | | | | | |
| A GHsag | 73 | 11 | 36 | 14 | 70 | 13 | 35 | 13 | 74 | 12 | 37 | 11 |
| UA GHsag | 91 | 4 | 31 | 9 | 92 | 5 | 31 | 10 | 93 | 3 | 31 | 10 |
| A GHfront | 22 | 13 | 16 | 7 | 22 | 13 | 16 | 6 | 23 | 13 | 18 | 4 |
| UA GHfront | 3 | 4 | 17 | 6 | 4 | 7 | 15 | 7 | 4 | 6 | 16 | 6 |
| A Elbow | 73 | 14 | 19 | 11 | 76 | 10 | 17 | 14 | 72 | 15 | 21 | 12 |
| UA Elbow | 58 | 19 | 31 | 12 | 53 | 25 | 24 | 12 | 53 | 22 | 26 | 14 |
| Torso Bend Right | 11 | 6 | 4 | 3 | 12 | 3 | 5 | 3 | 13 | 3 | 6 | 2 |

Note: Max: maximum; ROM: range of motion; SD: standard deviation

9.2 Kinetic Results

As described in Chapter 3 and Chapter 7, the kinetic data were collected and analyzed for one unilateral task, opening a door, and one bilateral task, lifting a box.

9.2.1 Between Group Kinetic Results

The kinetic data were compared between non-braced (NB) control group and the prosthesis wearing (PROS) group. Figure 9.14 shows the peak joint forces acting at the shoulder, elbow and wrist between the two groups while opening a door. There were no significant differences in the peak joint forces or moments between the two groups while opening a door. Figures 9.15-9.17 show the peak forces bilaterally at the shoulder, elbow and wrist respectively while lifting a box. The non-braced control group showed significantly greater ($p=.028$) a shoulder joint force in the medial/lateral direction on the unaffected (non-dominant side of control; sound side of amputees). The non-braced group also showed a significantly greater ($p=.048$) elbow joint force along the forearm of the affected side (dominant side of controls; prosthetic side of amputees). Figures 9.18-9.20 show the degrees of asymmetry between the unaffected side and the affected side of the peak forces at shoulder, elbow and wrist joint respectively. Figure 9.21 depicts the moments at the shoulder and elbow joint between the two groups.

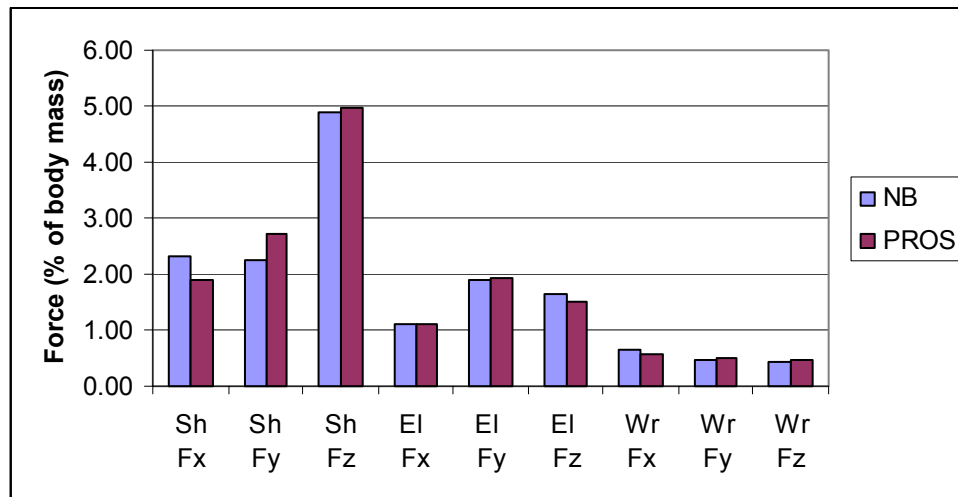


Figure 9.14. The peak external joint forces of the non-braced (NB) group and the prosthesis user (PROS) group while opening a door.

Note: Sh: shoulder; El: elbow; Wr: wrist.

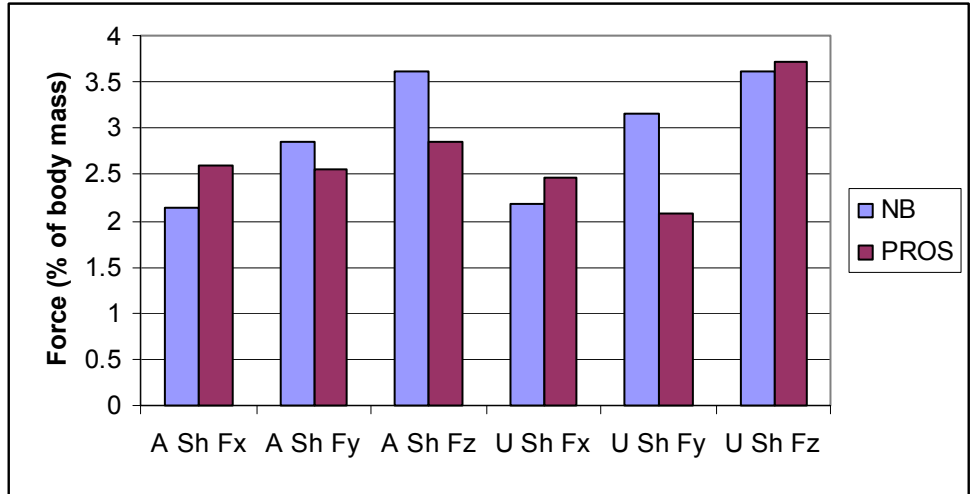


Figure 9.15. The peak shoulder joint forces of the non-braced (NB) group and the prosthesis user (PROS) group while lifting a box.

Note: A Sh; Affected shoulder; U Sh: Unaffected shoulder.

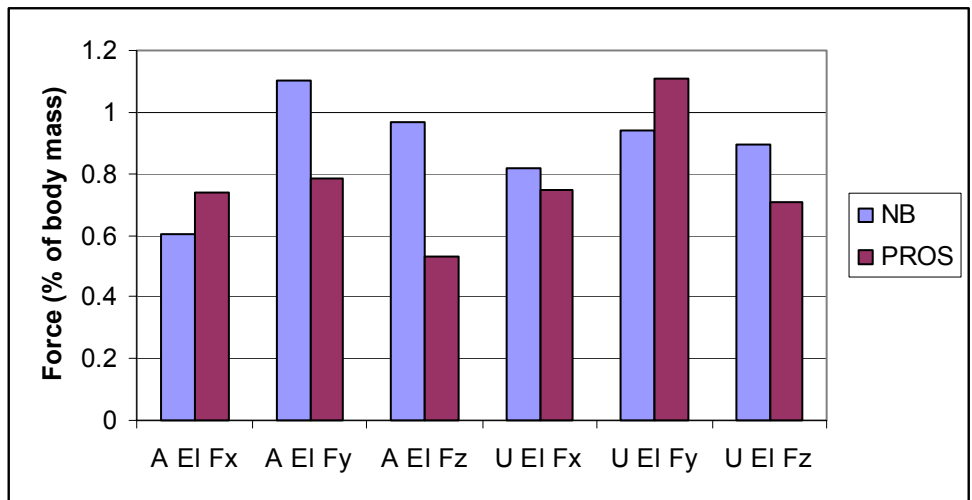


Figure 9.16. The peak elbow joint forces of the non-braced (NB) group and the prosthesis user (PROS) group while lifting a box.

Note: A El: Affected elbow; U El: Unaffected elbow.

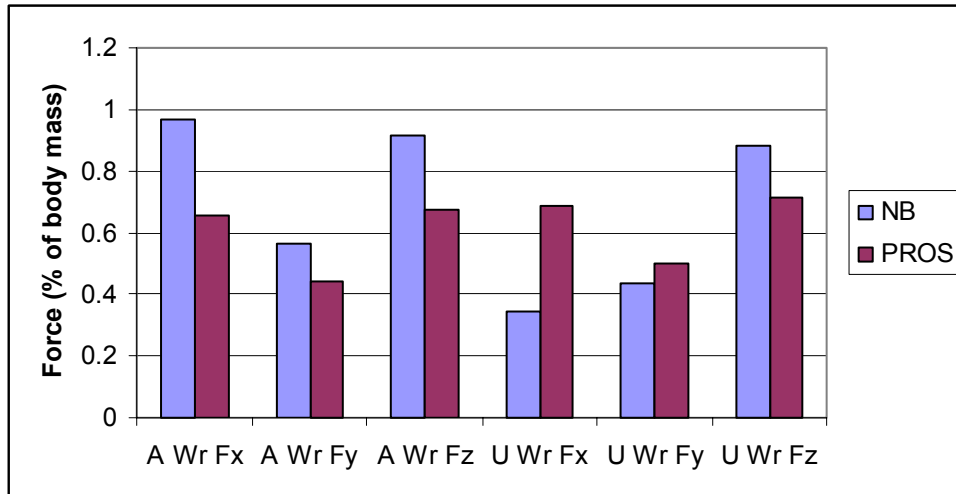


Figure 9.17. The peak wrist joint forces of the non-braced (NB) group and the prosthesis user (PROS) group while lifting a box.

Note: A Wr: Affected wrist; U Wr: Unaffected wrist.

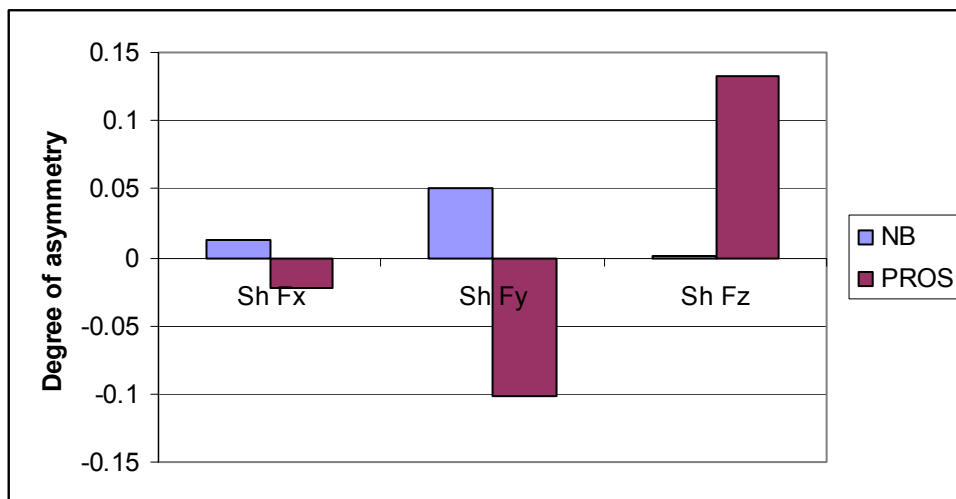


Figure 9.18. Degree of asymmetry of the peak shoulder joint forces between the non-braced (NB) group and prosthesis wearing (PROS) group.

Note: 0: perfect symmetry; Positive value represents unaffected side dominance.

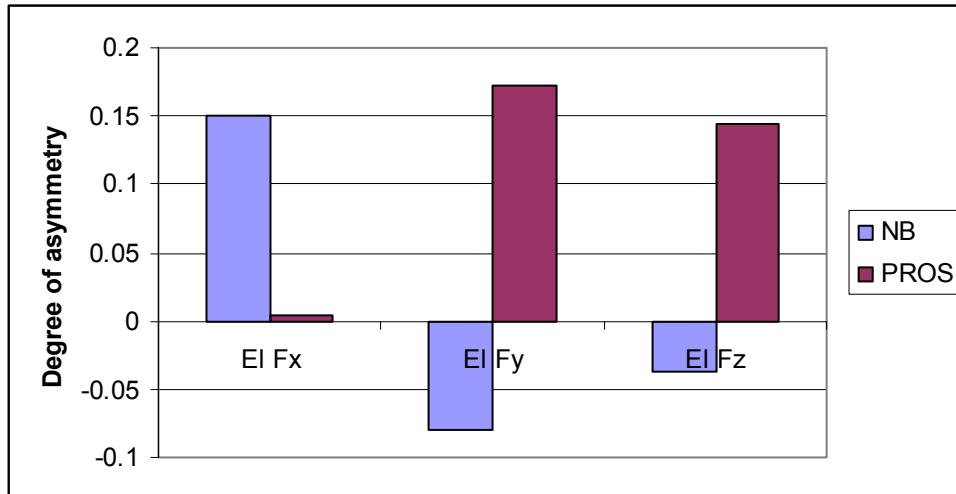


Figure 9.19. Degree of asymmetry of the peak elbow joint forces between the non-braced (NB) group and prosthesis wearing (PROS) group.

Note: 0: perfect symmetry; Positive value represents unaffected side dominance.

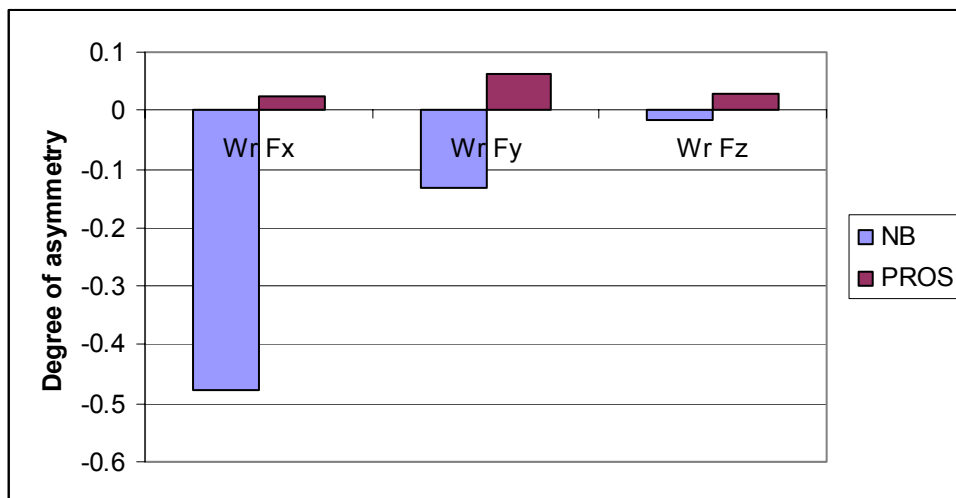


Figure 9.20. Degree of asymmetry of the peak wrist joint forces between the non-braced (NB) group and prosthesis wearing (PROS) group.

Note: 0: perfect symmetry; Positive value represents unaffected side dominance.

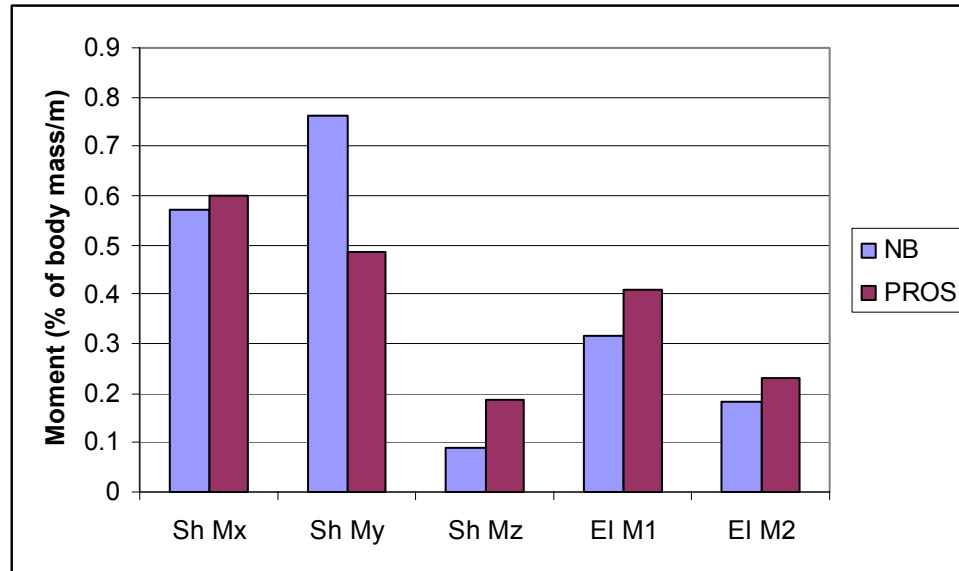


Figure 9.21. Shoulder (Sh) and elbow (El) joint moments between the non-braced (NB) group and prosthesis wearing (PROS) group while opening a door.

9.2.2 Prosthesis Wearing Group With-In Subject Results

Force and moment data were calculated with in the three mass conditions of the prosthesis wearing group. Kinetic data of the different mass conditions of the braced group were not reported because it was determined that the added mass of 96g was too small to make a difference in persons with an intact limb. Figure 9.22 shows the peak joint forces and Figure 9.23 shows the peak joint moments while opening a door under the three mass conditions: no mass; added mass at the elbow and added mass at the wrist. Figures 9.24-9.26 show bilaterally the peak joint forces of the shoulder, elbow and wrist respectively while lifting a box among the mass conditions. Figures 9.27 and 9.28 illustrates the peak moments acting bilaterally on the shoulder and elbow respectively while lifting a box.

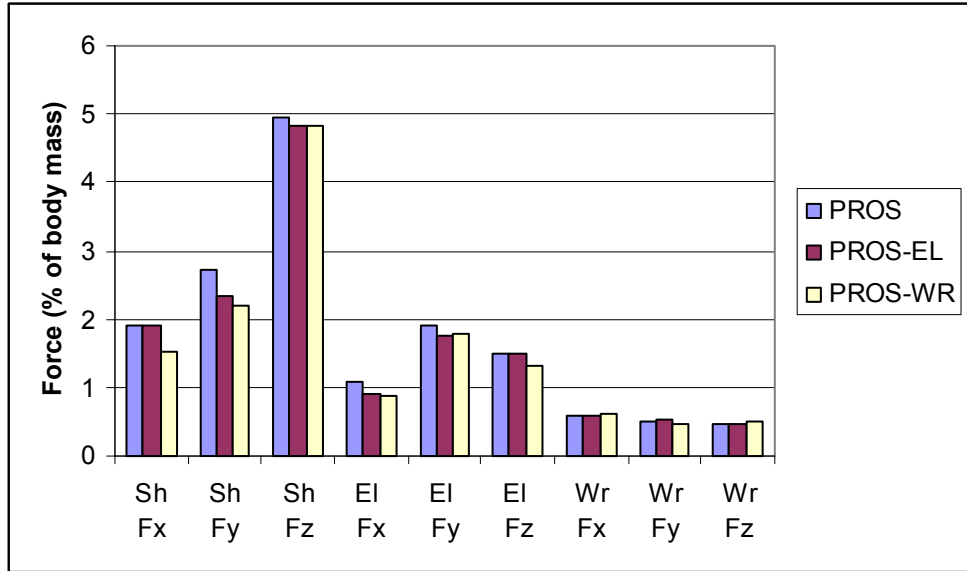


Figure 9.22. Peak joint forces while opening a door during three mass conditions.

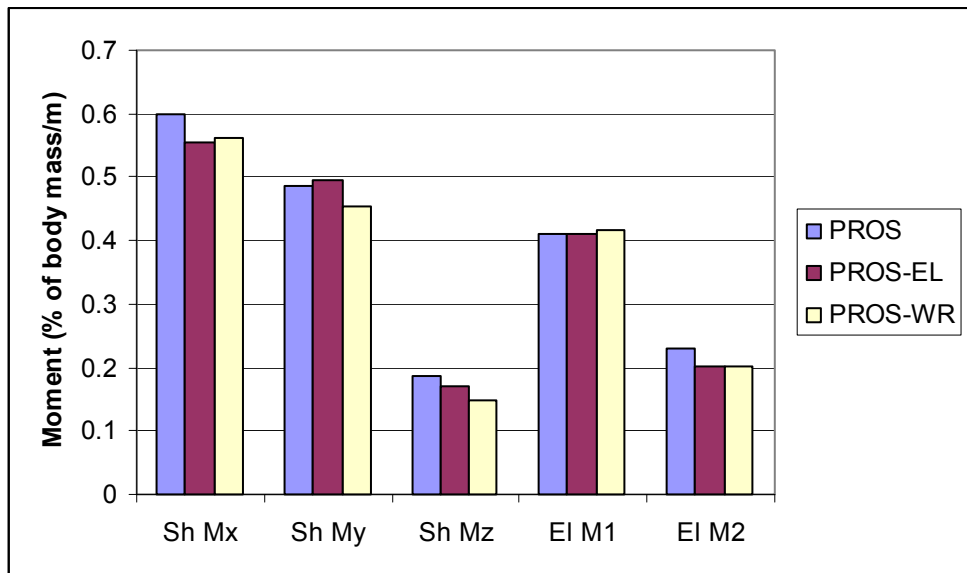


Figure 9.23 Peak shoulder (Sh) and elbow (El) moments while opening a door during three mass conditions.

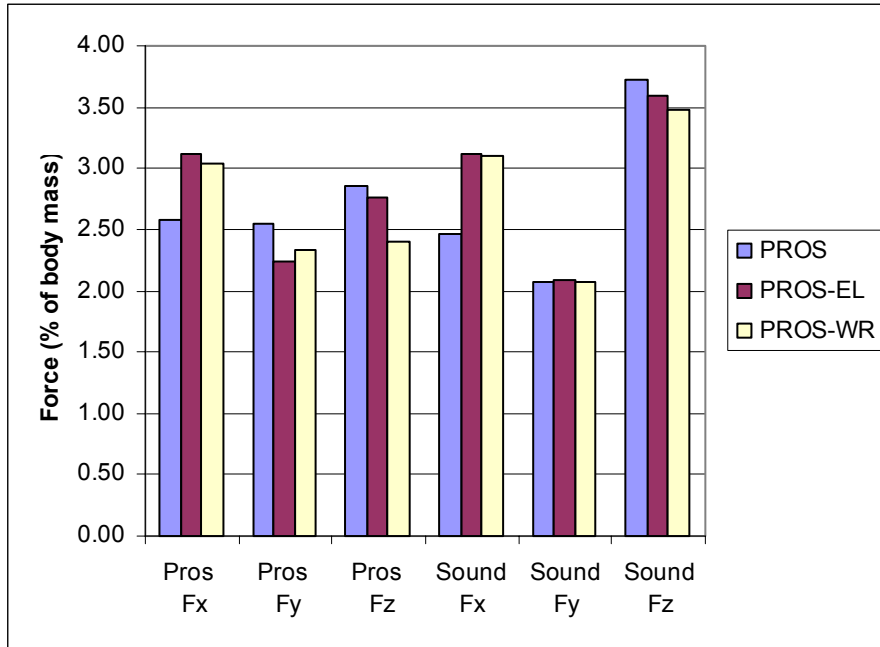


Figure 9.24. Peak external forces acting on the shoulder joint while lifting a box during three mass conditions.

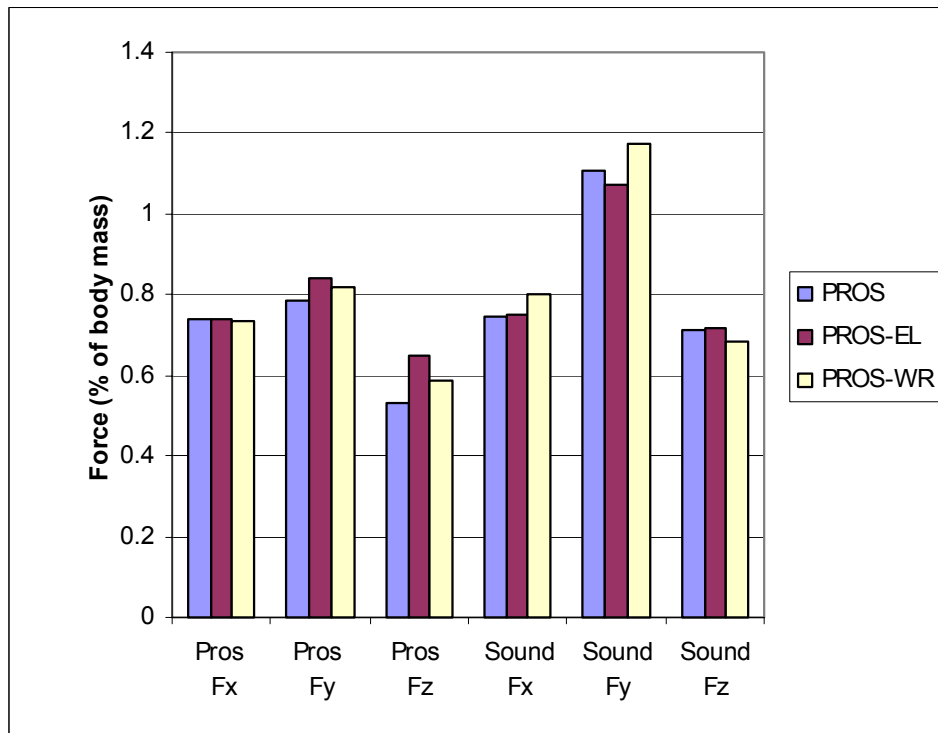


Figure 9.25. Peak external forces acting on the elbow joint while lifting a box during three mass conditions.

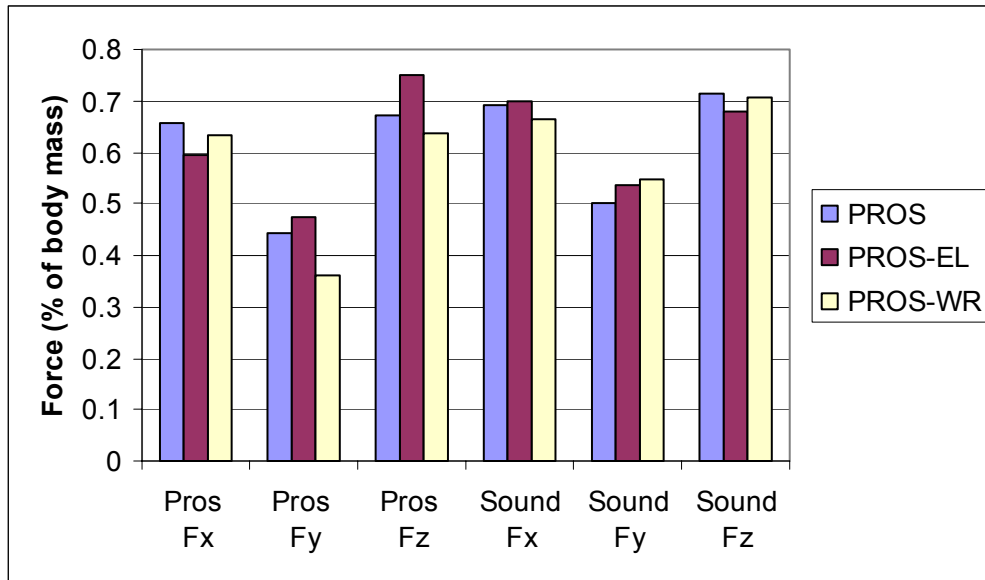


Figure 9.26. Peak external forces acting on the wrist joint while lifting a box during three mass conditions.

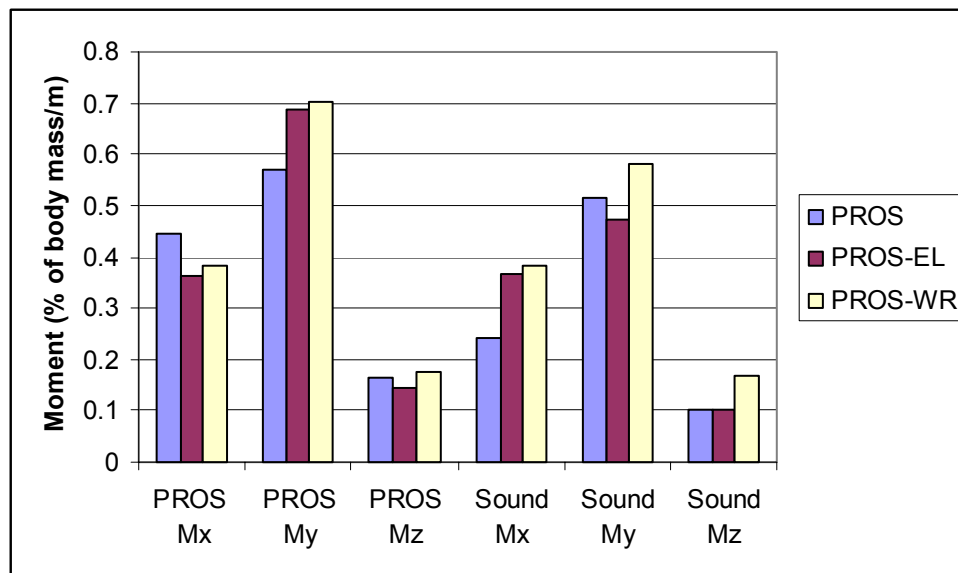


Figure 9.27. Peak moments acting at the shoulder while lifting a box during three mass conditions.

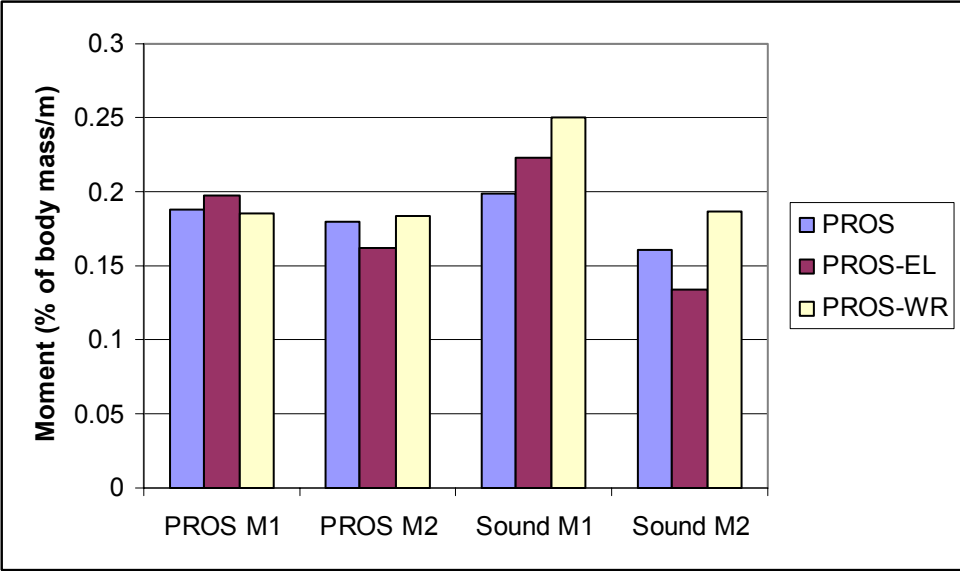


Figure 9.28. Peak moments acting at the elbow while lifting a box during three mass conditions.

Chapter 10: Discussion

The discussion of the results will include limitations of the study, comparison of findings of similar studies, and a review of significant findings and hypotheses. This chapter will also give some suggested recommendations regarding TRMP design, fitting and training.

10.1 Limitations of the Study

As with most research, this study had limitations. As mentioned in Chapter 2, there were assumptions made about the human body such as the arm is a completely rigid body, and that joints are frictionless. Such assumptions are necessary in order to simplify the equations of motions involved in the human motion and are accepted in the field of biomechanics.

Motion analysis, in general, has some limitations. There is a certain margin of error associated with marker placement, skin movement and camera capturing capabilities. Due to the difficulty of calculating movements of the scapula, GH and scapular rotations were combined. Sequence of rotations of Euler angles could also create errors. Efforts were made to minimize human error associated with marker placement and movement by using bone landmarks and requiring tight fitting clothing, however, eliminating marker movement completely is presently not possible and can lead to small joint angle error. The upper limb motions performed and analyzed in this study were larger gross movements not affected by small (less than 0.5 mm) marker movement.

Chapter 7 explained the validity study conducted on the system as it was used in this study. Bracing only limited the wrist and forearm movement, but did not simulate loss of musculature, change in lever arm or difference in arm center of mass that occurs after an amputation. It was also assumed that the braced forearm did not rotate and that hand motions within the brace were negligible.

It was hypothesized that compensatory motion would occur mostly in the shoulder and elbow, and therefore the marker set used to collect movements was limited to the upper limbs and torso. However, it was observed that TRMP users also compensated for lack of wrist and forearm movement by bending the cervical spine and in some cases using a knee flexion or hiking of the hip to complete a task. Since markers were not placed on the lower limbs or head, these movements were not quantified.

Additionally, because the selected tasks were performed in a laboratory setting, performance may not be ecologically valid as the laboratory setting can never replicate each subject's living environment and conditions. Markers were placed on the person and the objects, also limited the fully realistic completion of the tasks. Furthermore, the activities examined in this study are merely four of an innumerable quantity of tasks that the upper extremity performs on a day to day basis.

Bracing an intact extremity is always an attractive comparative condition for simulating prosthetic function but does not completely simulate prosthetic use/function. Although the brace satisfied the objective of restricting forearm and wrist movement, simulating prosthetic terminal device prehension was not possible under these conditions. A brace may be helpful in the collection of preliminary data to help determine where compensation may occur in order to develop a marker set prior to testing prosthesis users.

Bracing appears to cause compensations but these may not be the exact compensations experienced by prosthetic users.

The study was also limited by the assumptions made for completing inverse dynamics calculations. The anthropometrics of the prosthesis was estimated. Due to the difficulty of finding prosthesis wearing subjects as well as considering the time constraint, each individual prosthesis was not disassembled to complete a center of mass location calculation. However as explained in Chapter 6, each prosthesis was weighed. Also an estimation of the anthropometrics of the residual limb of the amputee subjects was not completed. An estimation of the residual limb mass could have been estimated by creating a water filled bag the same shape and size as each individual limb. The bag could have been weighed to complete the estimate of the weight of the residual limb since the specific gravity of water is similar to that of the human body. Generalizations of anthropometrics of the human body are often made in the field of biomechanics since it is impossible to weigh each segment of the body separately. Inverse dynamics also require acceleration data calculated by taking the second derivative of the marker position data. This calculation is also limited but a weighted average type filter was used to smooth the data.

The number of subjects was also limited. Although a power calculation was completed that allowed for comparisons to be made with only seven subjects in each group, a larger number of subjects would provide statistical strength to the generalizations made from data collected in this study. Many studies discussed in Chapter 2 that reported on upper limb motions of unaffected subjects have also been limited to ten subjects [36], six subjects [39], five subjects [32], and four subjects [35].

When studying actual upper limb prosthesis wearers the number of subjects decreases to three subjects [46] or case studies involving only one prosthesis user [53]. Due to the complexity of the upper limb motions, and the difficulty of successfully capturing and analyzing common upper limb tasks, the sample size in upper limb studies is often small.

10.2 Comparison of Results to Similar Studies

The cup task was chosen to allow comparison with other studies. In this study, subjects were asked to start in a neutral position with the elbow flexed to approximately 90 degrees. In similar studies, reaching for the cup was also included in the task [34, 37]. These previous investigations reported a maximum shoulder (glenohumeral) flexion of 43°, maximum shoulder abduction 31°, and maximum elbow flexion of 129° which are comparable to our intact, N-BR group's averaged (n=10) maximum shoulder and elbow motions: shoulder flexion 70°, maximum shoulder abduction 28°, and maximum elbow flexion 123°, with exception of shoulder flexion. Landry reported a maximum shoulder (glenohumeral) flexion of 61° which is more comparable to our findings [37]. The smaller values of shoulder flexion reported by Safaee-Rad et al. [34] could be the result of using only two cameras and a smaller marker set.

Our study also quantified forearm and wrist movement while dinking from a cup. The control group, on average, used a total of 32° of wrist movement (flexion/extension) and 13° of forearm rotation (pronation/supination). Morrey et al. [35] reported an elbow flexion range of approximately 22° to 58° and Romilly 42° to 76° during a door opening task. We found a mean range of elbow flexion of 57° (13-66°). The difference may be

because Morrey et al. [35] used an electrogoniometer to determine range of motion at the elbow and Romilly [40] used a stereo image analysis system. We additionally looked at wrist and forearm movement of the control group that showed an average range of wrist motion (flexion/extension) of 45° and forearm rotation (pronation/supination) of 93 degrees.

During the box lift, the N-BR group, on average, required 70° of supination and 70° of wrist extension. Anglin and Wyss [39] studied healthy subjects lifting a 5 kg. box with both hands, but reported the upper limb and torso angles at peak external moments. Our study examined peak and range of joint angles with a 2.27 kg box so a comparison between the two studies was not made.

As mentioned in Chapter 2, Section 2.4.2, studies have analyzed the external joints and moments of the upper limbs [35, 38-39]. However, none of these studies were similar enough to make direct comparisons to the results of these studies. Chadwick looked at the contact forces of the elbow and wrist during tasks such as answering the telephone and opening a jar, but did not have any ADLs similar to the four chosen for this study [38].

Murray et al. [35] studied ten common tasks which included drinking from a mug, a task similar to drinking from a cup in this study. The peak external forces and moments were calculated for the shoulder and elbow for each task, but only the task that showed the maximum force and moment value was reported. The drinking from a mug task never reported a maximum force or moment value. The maximum force of shoulder occurred along the longitudinal axis of the upper arm and the maximum force of the elbow occurred along the longitudinal axis of the forearm [35]. These maximums

reported were collected while raising a block to head height and so can not be compared to the results of the study discussed in this dissertation. However, our study also found the maximum forces occurring in the vertical directions while opening a door and lifting a box for the non-amputee group.

As mentioned earlier, the Anglin study examined the lifting of a 5 kg box and reported the total hand load of 3% of body weight mostly occurred in the vertical direction. The total moment (box load moment + gravitational moment of the upper arm, forearm and hand) in all directions was reported as 21.8 Nm. Although again it is difficult to make a direct comparison to the hand load lifting 5 kg box, the study described in this dissertation found maximum loads up to 3.5% of body mass at each shoulder while lifting a box about half the mass as the one described by Anglin.

10.3 Discussion of Results

A complete description of all the results was given in Chapter 9. Tables 10.1 (unilateral tasks) and 10.2 (bilateral tasks) review the significant kinematic findings between groups that will be discussed here.

Table 10.1. A review of statistically significant findings during the unilateral tasks.

| | Cup Task | | Door Task | |
|-----------------|-----------|----------------|---------------|---------------|
| | Max Angle | ROM | Max Angle | ROM |
| GHsag | * | N-BR, BR >PROS | * | * |
| GHfront | * | * | * | * |
| GHtran | * | * | PROS>N-BR,BR | PROS,BR>N-BR |
| ELflex | * | * | * | N-BR >PROS |
| Torso side bend | NA | NA | PROS>N-BR, BR | PROS>N-BR, BR |

Note: An * indicates no significant difference; NA: Not applicable.

Table 10.2. A review of statistically significant findings during the bilateral tasks.

| | Box Task | | Turning Task | |
|--------------------|-----------------|------------------------------|--------------|---|
| | Max Angle | ROM | Max Angle | ROM |
| A GHsag | * | N-BR, BR > PROS | * | BR> N-BR, PROS |
| A GHfront | BR > PROS | N-BR, BR > PROS | * | * |
| A GHtran | * | * | * | * |
| A ELFlex | N-BR > PROS | N-BR > BR > PROS | * | BR> N-BR, PROS |
| UA GHsag | * | * | * | N-BR>BR>PROS |
| UA GHfront | N-BR, BR > PROS | * | N-BR>PROS | N-BR>PROS |
| UA GHtran | * | * | * | * |
| UA ELFlex | NS | * | PROS>BR | PROS,N-BR>BR |
| Torso side bend | PROS>N-BR, BR | * | * | * |
| Torso forward bend | PROS>N-BR | PROS>, N-BR, BR | * | * |
| DoA GHSag | NA | PROS affected side dominance | NA | PROS similar asymmetry as N-BR; BR greater dominance on affected side |
| DoA GHFront | NA | * | NA | * |
| DoA ELFlex | NA | PROS affected side dominance | NA | PROS similar asymmetry as N-BR showing dominance on unaffected side; BR group showed dominance on affected side |

Note: An * indicates no significant difference; NA: Not applicable.

10.3.1 Drinking from a Cup

The PROS group had less range of the glenohumeral joint in the sagittal plane while drinking from the cup compared to the control group. With less flexion at the shoulder and no wrist or forearm motion available, braced and prosthesis using subjects were observed forward bending the cervical spine (neck) to compensate. As mentioned earlier, movement of the cervical spine was not recorded and is therefore non-quantified represents a limitation in this study.

10.3.2 Opening a Door

The loss of forearm and wrist movement in the braced and prosthesis wearing groups was compensated by side bending of the torso and increased internal shoulder rotation while opening a door. We hypothesized that compensatory motion would most likely occur in the shoulder abduction during the door task, however, it occurred in torso bending and shoulder rotation. The unaffected group with the elbow extended, slightly externally rotated the shoulder while rotating the forearm to twist the door knob and open the door. It was thought that the PROS group would have trouble rotating the shoulder joint without the ability to rotate the forearm. However, the PROS group held the elbow in a flexed position that allowed for internal rotation of the shoulder. The location of compensation may not always be obvious, which demonstrates the importance of studying transradial prosthesis user's motion..

The PROS group had a greater shoulder joint force acting in the medial/lateral direction mostly due to the acceleration sideways while bending the torso to complete the task. The PROS group also had greater moments with the exception of the shoulder moment around the medial/lateral axis. This is probably because the PROS group relied on the bending of the torso instead of the rotation of the shoulder joint.

10.3.3 Lifting a Box

The PROS group compensated for the lack of wrist and forearm movement by bending the torso forward and sideways. The BR group showed greater use of the torso also although not significantly different than the N-BR group. The BR group did not require as much compensation in the torso as the PROS group due to greater although

still limited use of the terminal device (hand) for gripping. The N-BR group was observed pulling the box toward the chest symmetrically by extending the wrist allowing for the positioning of the elbows laterally and then lifting it linearly up to the shelf. The right and left sides of the N-BR group are close to symmetric (Figure 9.9) for all motions, with showing a slight right side dominance ($DoA = -0.03$) of range of motion probably due to all subjects being right-handed. The braced group shows a trend towards a right-left positional asymmetry toward the affected side despite this task being considered symmetrical although not significantly different than the N-BR group. The PROS group shows the greatest dominance statistically on the unaffected side for all three ranges of motion. Prior to lifting instead of bringing the box toward the chest and straight up, the PROS group shifted the box toward the unaffected side and lifted the box following a circular trajectory. Without wrist extension, the prosthetic arm was unable to position the elbows out of the way to allow the box to be brought to the chest prior to lifting. This caused a greater range of motion on the sound side. The PROS group showed a significantly greater dominance of the unaffected side in terms of shoulder force in the vertical direction when compared to the N-BR group (Figure 9.17). For the wrist forces, the N-BR favored the right (dominant) hand during the box lift while the PROS group showed a slight degree of asymmetry toward the unaffected side (Figure 9.19). Kinetically, in the vertical direction the PROS group tended to rely more on the sound or non amputated side during the box lift which is in agreement with the kinematic findings.

While lifting a box, the added mass conditions (PROS-EL, PROS-WR) showed greater peak shoulder forces in the anterior/posterior direction and greater elbow forces in most directions when compared to the PROS group with no added mass (Figure 9.24,

Figure 9.25). The PROS-WR condition experienced the greatest shoulder moments bilaterally and elbow moments on the sound side (Figure 9.27). This suggests with added mass, the center of mass of the prosthesis changes enough to increase the forces and moments at the shoulder and elbow. If this type of task is done repetitively, it may injure the intact joints or create a reason for rejection or lack of use of the prosthesis. However, in general, the location of such a small mass had little effect.

10.3.4 Turning a Steering Wheel

For the steering wheel task, the second bilateral activity, the braced subjects were required to use the affected side more for GHSag and elbow angle motion although not for GHFront motion. However, the PROS group was similar to the N-BR group. Turning a steering wheel to the right requires flexing and abducting the shoulders to hold the hands on the wheel. It also requires rotation of the forearms, and flexion of the wrist and elbow to produce the rotation of the wheel. Basic transradial myoelectric prostheses do not allow for pronation or supination of the forearm that is used to rotate the end effectors (hands) attached to the steering wheel. Only the right turn was analyzed under normal conditions and this required a greater range of motion (not peak) of the right shoulder during flexion and greater range of left elbow flexion. The BR group showed a similar but greater right (affected) side range of motion dominance as the N-BR group. However, the left elbow of the BR group did not show dominance or flex more than the right side (Figure 9.10). This demonstrates that the affected (simulated prosthetic use) side can change the kinematics of the unaffected (sound) side. However the PROS group DoA profile was similar to the N-BR. The PROS group showed a significantly greater

elbow flexion maximum and range compared to the BR group (Figure 9.11). The BR group may have had a different grip or may have felt that elbow range of motion was restricted by the brace during this task even though the brace allowed a full range of elbow motion in flexion/extension. This is a case when bracing was a good simulation for prosthetic use.

No differences were found between the different added mass positions: near the elbow (proximally) or near the wrist (distally) of the braced group or of the prosthesis wearing group kinematically while turning a steering wheel.

10.3.5 Review of Hypotheses

The first hypothesis stated that there would be significant differences in the motions of the shoulder, elbow and torso between the control group and the prosthesis users. This was true for all tasks with the exception of the steering wheel turning task. During this task the prosthesis users had similar shoulder flexion as the non-amputee subjects, but differed in shoulder abduction and elbow flexion. The turning task was also the activity where the braced and prosthesis groups were the most dissimilar, suggesting that bracing is not always a good method for determining compensatory motions.

The second and third hypotheses predicted that the range of motions and forces and moments of the joints would differ during three mass conditions: no mass, mass added at elbow and mass added at wrist. The mass conditions had little effect on the door task, but some minimal changes were found during the box lift task.

10.4 Recommendations

By looking at four tasks, it has become obvious that TRMP users must compensate for lack of wrist and forearm movement. However, depending on the task the compensation occurs in different segments of the body. It is difficult to make overall recommendations regarding improvements of an upper limb prosthesis since it can be used in such varied tasks. However, in general it seemed that awkward bending of the torso provided the compensation in most of the four tasks studied. Flexing the elbow to position the end-effector differently was also a compensatory strategy used. This shows the necessity of using a wrist component that allows pronation and supination of the forearm and in some cases wrist flexion and extension. The prosthesis users seemed to not change the degree of elbow flexion much throughout the task. This could be caused by the difficulty either mentally or physically to use the biceps brachii to both control elbow flexion and to control the opening and closing of the myoelectrically controlled terminal device. A new wrist component design should be lightweight and easy to control.

It is also recommended that more time be spent on determining how the residual limb and body mass affects compensatory motion. It is recommended that a quick modeling of the residual limb and its characteristics be done by measurements and calculations of the volume of the stump. Adding a wrist component to the prosthesis may decrease compensatory motion, but for an amputee with a short residual limb and small body mass it may not be worth the added function. For upper limb prosthesis users without a wrist component, it is recommended that therapists demonstrate a more optimal technique to compensate depending on task.

The process of fitting an amputee with a prosthesis and teaching its optimal usage is an arduous task that requires many experts. An amputee must get a prescription of a prosthesis from a physician, fitting various components by a prosthetist, provide justification of component choices to an insurance company or government agency in order to receive monetary reimbursement, receive training from a therapist and deal with psychological implications of limb loss. These decisions that are required for prosthesis use can sometimes be made based on biased unconfirmed claims from manufacturers, subjective choices of prosthetists and limited funding options. All these variables can lead to improper fitting and use of an upper extremity prosthesis or worse, overprescription and rejection. Therefore, it is recommended that a more individualized and quantitatively driven process be developed and implemented for a prosthesis from prescription to expert use. This kind of process can be started by developing a kinematic simulated model of an upper limb prosthesis explained in Section 11.2, Future Studies. It may also be helpful to catalog the inertial properties of each basic prosthetic component. With information such as the center of mass and moment of inertia of a hand component or of a wrist component could be implemented into a simulated biomechanical model to help prosthetists with component selection based on patient parameters.

When studying prosthesis users certain aspects should be considered for the testing protocol. For one thing, the whole body should be studied since it may not be obvious where compensation due to limitations of the prosthesis occurs.

The following testing procedure is recommended when studying the motions of upper limb prosthesis wearers in particular for design changes:

- Survey prosthesis users about difficult movements and design flaws
- Survey prosthetists, therapists about compensatory motion of patients
- Record motions of non-amputee population for comparative purposes
- Record motions of non-amputee population limiting degrees of freedom similar to the prosthesis to determine possible areas of compensation
- Determine appropriate marker set to fully capture these areas of compensation
- Record motions of one prosthesis user including the inertial properties of the prosthesis
- Make sure that pseudo joints within the prosthesis don't affect motion analysis – that is that each segment can be assumed to be a rigid body
- Compare non-amputee motion to prosthesis user motion
- Determine design changes based on these differences
- Implement design change
- Test prosthesis users with and without design change and compare motions

It is important to include users, surgeons, prosthetists, therapists and engineers in the testing protocol.

Chapter 11: Summary and Conclusions

11.1 Contributions

This work has provided many contributions to the biomechanics, prosthetic design and physical medicine fields. One important aspect of studying human problems is to have a set of control data to use for comparison. This work has documented kinematic data of the upper limb during four common tasks and this can be used for a comparison when studying many upper limb problems or injuries. Quantitative data as shown has justified the necessity of providing more degrees of freedom such as a properly designed wrist component to a transradial prosthesis. From this study, a general testing protocol for studying prosthesis users was developed.

This work has started to bridge the gap between the technological innovation of the engineering field and the clinical astuteness of the clinicians that are in contact with the prosthetic users on a daily basis. Through this study, an interdisciplinary group from the University of South Florida's Department of Mechanical Engineering and the School of Physical Therapy and Rehabilitation Sciences; the St. Petersburg College of Orthotics and Prosthetics; and West Coast Brace and Limb, a prosthetics and orthotics fitting service has been developed and shown that collaborative work can be accomplished.

11.2 Future Studies

In general, future studies should include more subjects, specifically different levels of amputees such as transhumeral and shoulder disarticulation. The upper limb is

capable of a wide variety of tasks, so other tasks should also be considered in future studies. Particularly, bilateral tasks should be investigated because these activities definitely require the use of the prosthesis. Electromyography should be studied along with the motion analysis to determine if TRMP users limit range of elbow flexion because of muscle contractions are also used to control the opening and closing of the terminal device.

11.2.1 Biomechanical Model

A biomechanical simulation for transradial prosthesis users will be created by a mechanical engineering graduate student using data from this study. This future study will use the compensatory motion data from this dissertation to create a simulated biomechanical model that can select the best prosthesis for a given user. This simulation program could also be used to design and test prostheses that are more effective at strategic tasks. Kinematic data from actual body motions will be used to test and evaluate the accuracy of this upper limb prosthetic model. A comparative analysis of experimental data to model predicted data can be completed to determine the robustness of the model. Based on the experimental data collected and studied here, weight coefficients can be given to specific parameters of the upper limb prosthetic model. Subject inputs such as length of residual limb, height, and weight and task preference can be entered into the model. Parameters of the prosthesis such as a range of movement, component selection, degrees of freedom, grip angle(s), weight, and geometry will also be inputs for the model. Task inputs will include information on joint constraints, and a trajectory which the hand or limb must follow. Joint locations necessary to accomplish

the task with a given configuration will be outputted and simulated from the biomechanical model. Figure 11.1 explains the simulation model in a schematic form. The simulation will allow for wrist rotation given by the prosthesis, elbow flexion, three degrees of rotation at the shoulder joint, movements of the shoulder joint about the sternoclavicular joint, and bending and rotation of the torso. All joints will have a restricted range of motion that will be determined by subject data, prosthesis, and task

Once a reasonable upper limb model is created, kinematic and kinetic simulations as well as individual patient parameters can be used to fit the amputee with the proper prosthesis. This simulation can also help to individualize training and therapy associated with a prosthesis.

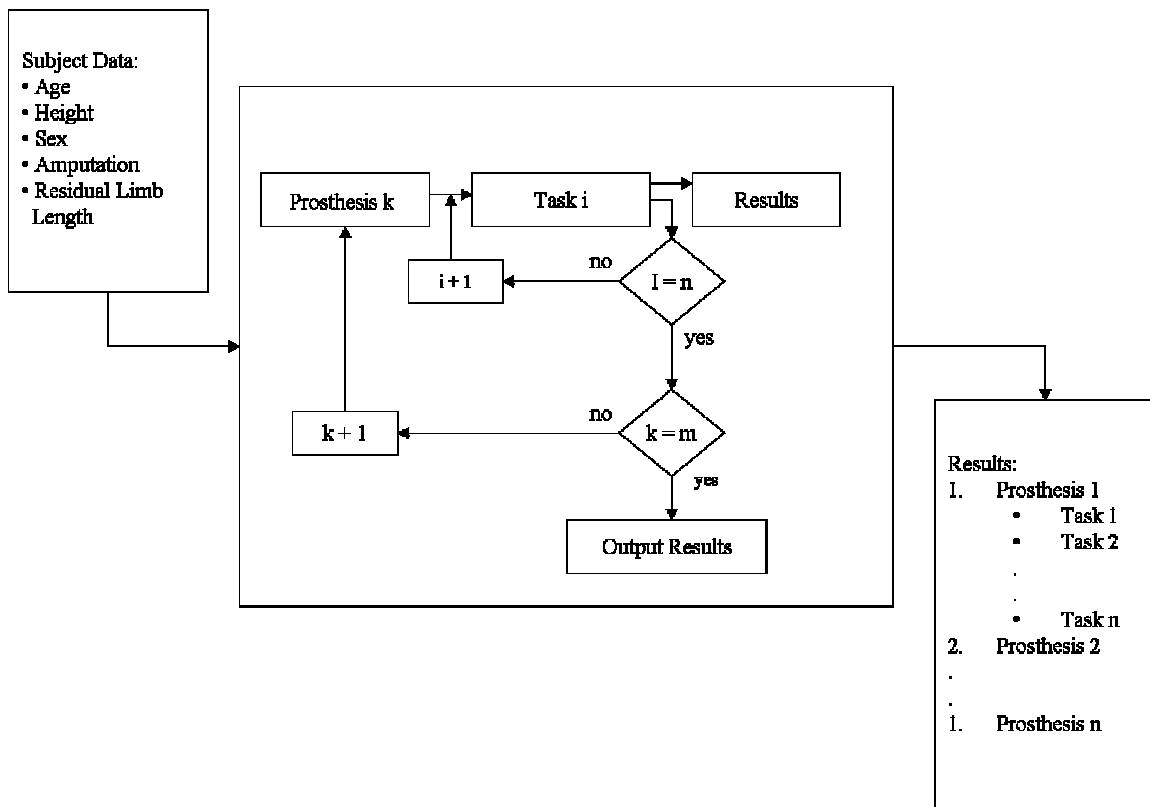


Figure 11.1. Schematic of biomechanical simulation model for compensatory motion of transradial prosthesis users created by Derek Lura.

11.2.2 Prosthetic Component Design Testing

Having a baseline data of unaffected as well as amputee data can also contribute to the testing phase of new designs of components of the upper limb prosthesis. For example, a new powered prosthetic St. Petersburg (SPC) wrist with two degrees of freedom was presented at the 12th World Congress of the International Society for Prosthetics and Orthotics [57]. For the clinical testing phase of the SPC wrist, motion analysis can be used to determine if using the wrist decreases the compensatory motion used by upper limb prosthesis users during common tasks without increasing force and moments of the intact joints. With the computer programming completed in this dissertation that includes anthropometric changes to account for a prosthesis, this kind of study showing the benefits of a new design can be easily implemented. Completing the biomechanical model mentioned above, some preliminary design considerations can be tested in simulation before complete prototypes are fabricated.

11.3 Conclusions

This study compared the compensatory motion of persons using a transradial prosthesis without wrist motion to that of non-amputees under an unrestricted and restricted forearm rotation (braced) conditions while performing four ADL's; drinking from a cup, opening a door, lifting a box and turning a steering wheel. It also looked at the effects of added mass on the prosthesis users' motions. This study adds to the kinematic and kinetic database of upper limb movements needed to understand how a person with amputation of the forearm/hand using a prosthesis lacking forearm rotation will compensate relative to non-amputees. While opening a door and lifting a box, tasks

that require a significant amount of forearm rotation and wrist flexion, persons with transradial amputation compensated predominantly with movements of the torso side bending toward affected side. The door task also required rotation of the shoulder. During the steering wheel task, amputees used more elbow flexion to accommodate for the lack of forearm rotation. While drinking from a cup, a task that does not require as much forearm rotation or wrist movement as the other tasks, the location of compensation was not determined. Bending in the cervical spine was anecdotally observed while drinking from a cup but was not analyzed in this study. With the exception of turning the steering wheel, the braced group seemed to compensate similarly to the amputee group although to a lesser degree. This suggests that studies using bracing to simulate a transradial prosthesis may be helpful to make preliminary generalizations about the potential type, quantity and origin of awkward, compensatory motions caused by functional prosthetic limitations, but that actual prosthesis users need to be studied to more accurately locate and quantify compensatory motion especially during tasks that depend largely on prehension. Added mass had the most effect during the bilateral lifting task. This suggests the importance of keeping a wrist component light or developing a component with a more evenly distributed mass. It also emphasizes the importance of considering bilateral tasks when considering improvements of an upper limb prosthesis. Compensatory motion should also be studied to develop a kinematic and kinetic model specifically for upper limb prosthesis users and to help with design, prescription and training of prostheses.

List of References

- [1] Anonymous, 2007, "Amputee Coalition of America," http://www.amputee-coalition.org/nllic_faq.html, 2007(Aug.).
- [2] Delpalma, R., Daughtery, P. J., Flood, K. M., 2006, "Traumatic Amputation and Prosthetics. Independent Study Course," http://www1.va.gov/vhi/docs/amputation_www.pdf, 2007(Aug.).
- [3] Sherman, R. A., 1999, "Utilization of Prostheses among US Veterans with Traumatic Amputation: A Pilot Survey," *Journal of Rehabilitation Research and Development*, **36**(2), pp. 100-108.
- [4] Jacobsen, S. C., Knutti, D. F., Johnson, R. T., 1982, "Development of the Utah Artificial Arm," *IEEE Transactions on Bio-Medical Engineering*, **29**(4), pp. 249-269.
- [5] Silcox, D. H., 3rd, Rooks, M. D., Vogel, R. R., 1993, "Myoelectric Prostheses. A Long-Term Follow-Up and a Study of the use of Alternate Prostheses," *The Journal of Bone and Joint Surgery. American Volume*, **75**(12), pp. 1781-1789.
- [6] Kay, H. W., and Newman, J. D., 1975, "Relative Incidence of New Amputation," *Orthotics and Prosthetics*, **29**(2), pp. 3-16.
- [7] Sears, H. H., and Shaperman, J., 1991, "Proportional Myoelectric Hand Control: An Evaluation," *American Journal of Physical Medicine & Rehabilitation / Association of Academic Physiatrists*, **70**(1), pp. 20-28.
- [8] Wright, T. W., Hagen, A. D., and Wood, M. B., 1995, "Prosthetic Usage in Major Upper Extremity Amputations," *The Journal of Hand Surgery*, **20**(4), pp. 619-622.
- [9] Lamb, D. W., 1993, "State of the Art in Upper-Limb Prosthetics," *Journal of Hand Therapy: Official Journal of the American Society of Hand Therapists*, **6**(1), pp. 1-8.
- [10] Uellendahl, J. E., 2000, "Upper Extremity Myoelectric Prosthetics" *Physical Medicine and Rehabilitation Clinics of North America*, **11**(3), pp. 639-652.
- [11] Light, C. M., Chappell, P. H., Hudgins, B., 2002, "Intelligent Multifunction Myoelectric Control of Hand Prostheses," *Journal of Medical Engineering & Technology*, **26**(4), pp. 139-146.

- [12] Kyberd, P. J., Davey, J. J., and Morrison, J. D., 1998, "A Survey of Upper-Limb Prosthesis Users in Oxfordshire," *Journal of Prosthetics and Orthotics*, **10**(4), pp. 85-91.
- [13] Buckley, M. A., Yardley, A., Johnson, G. R., 1996, "Dynamics of the Upper Limb during Performance of the Tasks of Everyday Living--a Review of the Current Knowledge Base," *Proceedings of the Institution of Mechanical Engineers. Part H, Journal of Engineering in Medicine*, **210**(4), pp. 241-247.
- [14] Atkins, D. J., Heard D., and Donovan, W. H., 1996, "Epidemiologic Overview of Individuals with Upper-Limb Loss and their Reported Research Priorities," *Journal of Prosthetics and Orthotics*, **8**(1), pp. 2-11.
- [15] Ling, G., 2005, "PROSTHESIS 2007," <http://www.darpa.mil/baa/baa05-19mod5.htm> , **2005** (Aug.).
- [16] Winter, D.A., 1990, *Biomechanics and Motor Control of Human Movement*, University of Waterloo, Ontario, Canada, pp. 56-57.
- [17] Winter, D.A., 1979, *Biomechanics of Human Movement*, John Wiley & Sons, New York, pp. 202.
- [18] Craig, J.J., 2005, *Introduction to Robotics Mechanics and Control*, Pearson Prentice Hall, Upper Saddle River, New Jersey, pp. 400.
- [19] Nordin, M., and Frankel, V.H., 2001, *Basic Biomechanics of the Musculoskeletal System*, Lippincot Williams & Wilkins, New York.
- [20] Clarkson, H.M., 2005, *Joint Motion and Function Assessment: A Research Based Practical Guide*, Lippincot Williams & Wilkins, New York, pp. 278-279.
- [21] Morrey, B. F., Askew, L. J., and Chao, E. Y., 1981, "A Biomechanical Study of Normal Functional Elbow Motion," *Journal of Bone and Joint Surgery. American Volume*, **63**(6), pp. 872-877.
- [22] Neumann, D.A., 2002, *Kinesiology of the Musculoskeletal System: Foundations for Physical Rehabilitation*, Elsevier Health Sciences, New York, pp. 624.
- [23] Martinez, K., and Mipro, R. C., 2006, "Upper Limb Prosthetics," *Physical Medicine and Rehabilitation*, http://www.emedicine.com/pmr/topic174.htm#section~terminal_device, **2007**.
- [24] Cuccurullo, S., 2004, "Physical Medicine and Rehabilitation Board Review," Demos Medical Publishing, Inc., New Jersey.
- [25] Fillauer, K., 2007, "Upper Extremity High-Level Amputation and Myoelectric Prosthesis," http://www.fillauer.com/education/ED_myoelectric.html, **2008** (Jan.).

- [26] Miguelez, J. M., 2002, "Critical Factors in Electrically Powered Upper-Extremity Prosthetics," *Journal of Prosthetics and Orthotics*, **14**, pp. 36-38.
- [27] Miguelez, J. M., 2006, "Our Services, Expedited Delivery," <http://www.darpa.mil/baa/baa05-19mod5.htm>, 2007 (Jan.).
- [28] Rietman, J. S., Postema, K., and Geertzen, J. H., 2002, "Gait Analysis in Prosthetics: Opinions, Ideas and Conclusions," *Prosthetics and Orthotics International*, **26**(1), pp. 50-57.
- [29] Twiste, M., and Rithalia, S., 2003, "Transverse Rotation and Longitudinal Translation during Prosthetic Gait--a Literature Review," *Journal of Rehabilitation Research and Development / Veterans Administration, Department of Medicine and Surgery, Rehabilitation R&D Service*, **40**(1), pp. 9-18.
- [30] Tokuno, C. D., Sanderson, D. J., Inglis, J. T., 2003, "Postural and Movement Adaptations by Individuals with a Unilateral Below-Knee Amputation during Gait Initiation," *Gait & Posture*, **18**(3), pp.158-169.
- [31] Anglin, C., and Wyss, U. P., 2000, "Review of Arm Motion Analyses," *Proceedings of the Institution of Mechanical Engineers. Part H, Journal of Engineering in Medicine*, **214**(5), pp. 541-555.
- [32] Yang, N., Zhang, M., Huang, C., 2002, "Synergic Analysis of Upper Limb Target-Reaching Movements," *Journal of Biomechanics*, **35**(6), pp. 739-746.
- [33] Yang, N., Zhang, M., Huang, C., 2002, "Motion Quality Evaluation of Upper Limb Target-Reaching Movements," *Medical Engineering & Physics*, **24**(2), pp. 115-120.
- [34] Safaee-Rad, R., Shwedyk, E., Quanbury, A. O., 1990, "Normal Functional Range of Motion of Upper Limb Joints during Performance of Three Feeding Activities," *Archives of Physical Medicine and Rehabilitation*, **71**(7,) pp. 505-509.
- [35] Murray, I. A., and Johnson, G. R., 2004, "A Study of the External Forces and Moments at the Shoulder and Elbow while Performing Every Day Tasks," *Clin.Biomech.(Bristol, Avon)*, **19**(6), pp. 586-594.
- [36] Murgia, A., Kyberd, P. J., Chappell, P. H., 2004, "Marker Placement to Describe the Wrist Movements during Activities of Daily Living in Cyclical Tasks," *Clin.Biomech.(Bristol, Avon)*, **19**(3), pp. 248-254.
- [37] Landry, J. S., 2000, "Optimal Fixed Wrist Alignment for Below-Elbow, Powered, Prosthetic Hands," *Master's thesis*pp. 1-80.
- [38] Chadwick, E. K., and Nicol, A. C., 2000, "Elbow and Wrist Joint Contact Forces during Occupational Pick and Place Activities," *Journal of Biomechanics*, **33**(5) pp. 591-600.

- [39] Anglin, C., and Wyss, U. P., 2000, "Arm Motion and Load Analysis of Sit-to-Stand, Stand-to-Sit, Cane Walking and Lifting," *Clinical Biomechanics*, **15** pp. 441-448.
- [40] Romilly, D. P., Anglin, C., Raymond, G. G., 1994, "A Functional Task Analysis and Motion Simulation for the Development of a Powered Upper-Limb Orthosis," *IEEE Transactions on Rehabilitation Engineering*, **2**, pp. 119-129.
- [41] Perry, J. C., Rosen, J., and Burns, S., 2007, "Upper-Limb Powered Exoskeleton Design," *IEEE/ASME Transactions on Mechatronics*, **12**(4), pp. 408-417.
- [42] Rosen, J., Perry, J. C., Manning, N., 2005, "The Human Arm Kinematics and Dynamics during Daily Activities toward a 7 DOF Upper Limb Powered Exoskeleton," *Advanced Robotics*, 12th International Conference on Advanced Robotics Proceedings, pp. 532-539.
- [43] Stavdahl, O., 2002, "Optimal Wrist Prosthesis Kinematics: Three-Dimensional Rotation Statistics and Parameter Estimation," Ph.D. thesis, Norwegian University of Science and Technology, Norway.
- [44] Mell, A. G., Childress, B. L., and Hughes, R. E., 2005, "The Effect of Wearing a Wrist Splint on Shoulder Kinematics during Object Manipulation," *Archives of Physical Medicine and Rehabilitation*, **86**(8) pp.1661-1664.
- [45] Weeks, D. L., Wallace, S. A., and Anderson, D. I., 2003, "Training with an Upper Limb Prosthetic Simulator to Enhance Transfer of Skill Across Limbs," *Archives of Physical Medicine and Rehabilitation*, **84**(3), pp. 437-443.
- [46] Highsmith, M. J., Carey, S. L., Koelsch, K. W., 2007, "Kinematic Evaluation of Terminal Devices for Kayaking with Upper Extremity Amputation," *Journal of Prosthetics and Orthotics*, **1**, pp. 84-90.
- [47] Black, N., Biden, E. N., and Rickards, J., 2005, "Using Potential Energy to Measure Work Related Activities for Persons Wearing Upper Limb Prostheses," *Robotica*, **23**, pp. 319-327.
- [48] Woltring, H.J., 1980. "Planar Control in Multi-Camera Calibration for 3-D Gait Studies," *Journal of Biomechanics*, **13**, pp.39-48.
- [49] Martin, 1997. *Vicon BodyBuilder for Biomechanics Manual* Version 3.5, Oxford Metrics Ltd, pp. 1-182.
- [50] Lowe, B.D., 2004, "Accuracy and Validity of Observational Estimates of Shoulder and Elbow Posture," *Applied Ergonomics*, **35**, pp.159-171.
- [51] Small, C.F., Bryant, J.T., Dwosh, I.L., Griffiths, P.M., Pichora, D.R., Zee, B., 1996, "Validation of a 3D Optoelectronic Motion Analysis System for the Wrist Joint," *Clinical Biomechanics*, **11**(8), pp.481-483.

- [52] Selfe, J., 1998, "Validity and Reliability of Measurements Taken by the Peak 5 Motion Analysis System," *J Med Eng Technol.*, **22**(5), pp. 220-225.
- [53] Portney, L.G., Watkins, M.P., 2000, *Foundations of Clinical Research Applications to Practice*, Prentice Hall Health, New Jersey, 2nd edition, Chapter 5, pp. 61-75.
- [54] Tukey, J.W., 1968. "The problem of multiple comparisons," Ditto, Princeton University, 1953; cited in Roger E. Kirk, *Experimental Design: Procedures for the Behavioral Sciences*, Brooks/Cole, Pacific Grove, CA.
- [55] Spjøtvoll, E., Stoline, M.R., 1971. "An extension of the T-Method of multiple comparison to include the cases with unequal sample sizes." *Journal of the American Statistical Association.* **68**, pp. 975-78.
- [56] Cutti, A. G., Garofalo, P., Janssens, K., 2007, "Biomechanical Analysis of an Upper Limb Amputee and His Innovative Myoelectric Prosthesis: A Case Study Concerning the Otto Bock "Dynamic Arm."," *Orthopaedie-Technik Quarterly*, (1) pp. 6-15.
- [57] De Laurentis, K. J., and Phillips, S. L., 2007, "Design of a powered two-DOF prosthetic wrist," 12th World Congress of the International Society for Prosthetics and Orthotics. Vancouver, Canada.

Appendices

Appendix A: Bodybuilder™ Software Program for Upper Limb Calculations

```
{*=====*}  
{*Start of macro section*}  
{*=====*}
```

```
{*Display of segment axes*}  
{*-----*}
```

```
Macro AXISVISUALISATION(Segment)  
ORIGIN#Segment=O(Segment)  
AXISX#Segment={100,0,0}*Segment  
AXISY#Segment={0,100,0}*Segment  
AXISZ#Segment={0,0,100}*Segment  
output(ORIGIN#Segment,AXISX#Segment,AXISY#Segment,AXISZ#Segment)  
Endmacro
```

```
{*Replace a missing marker from set of 4 in a segment*}  
{*-----*}
```

```
macro REPLACE4(p1,p2,p3,p4)  
s234 = [p3,p2-p3,p3-p4]  
p1V = Average(p1/s234)*s234  
s341 = [p4,p3-p4,p4-p1]  
p2V = Average(p2/s341)*s341  
s412 = [p1,p4-p1,p1-p2]  
p3V = Average(p3/s412)*s412  
s123 = [p2,p1-p2,p2-p3]  
p4V = Average(p4/s123)*s123  
{* Now only replaces if original is missing 11-99 *}  
p1 = p1 ? p1V  
p2 = p2 ? p2V  
p3 = p3 ? p3V  
p4 = p4 ? p4V  
endmacro
```

```
{*=====*}  
{*End of macro section*}  
{*=====*}
```

Appendix A (continued)

```
{*=====*}  
{*Initialisations*}  
{*=====*}
```

```
{*Define optional marker points*}  
{*-----*}
```

```
OptionalPoints(RBAK,RSHO,RELB,  
RELBM,RWRA,RWRB,RFIN,LSHO,LELB,LELBM,LWRA,LWRB,LFIN)  
OptionalPoints(CLAV,C7,STRN,T10,BOXR,BOXL,BOXC)
```

```
{*Define the Global Origin*}  
{*-----*}  
Gorigin = {0,0,0}  
Global = [Gorigin, {1,0,0}, {0,0,1},xyz]
```

```
{*=====*}  
{*VIRTUAL POINTS*}  
{*=====*}
```

```
{*Calculate the joint centers*}  
{*-----*}
```

```
{*Torso*}
```

```
Replace4 (C7,T10,CLAV,STRN)  
UTorso = (C7+CLAV)/2
```

```
If Exist (STRN) Then  
  LTorso = (T10+STRN)/2  
  FTorso = (CLAV+STRN)/2  
Else  
  LTorso = (T10+CLAV)/2  
  FTorso = CLAV  
ENDIF
```

```
BTorso = (C7+T10)/2
```

```
Torso = [UTorso,UTorso-LTorso,BTorso-UTorso,zyx]
```

Appendix A (continued)

{*Shoulder joint centers*}

{*Temporary local coordinate system*}

TempRClav = [RSHO,UTorso-RSHO,1(Torso),zyx]

TempLClav = [LSHO,UTorso-LSHO,1(Torso),zyx]

If \$Static == 1 Then

RSJC = RSHO+{0,0,-\$RShoulderDepth}*Attitude(Torso)

LSJC = LSHO+{0,0,-\$LShoulderDepth}*Attitude(Torso)

\$_RSJC = RSJC/TempRClav

\$_LSJC = LSJC/TempLClav

PARAM(\$_RSJC)

PARAM(\$_LSJC)

EndIf

{*From local coordinate system to global*}

RSJC = \$_RSJC*TempRClav

LSJC = \$_LSJC*TempLClav

{*Elbow joint centers*}

{*Temporary local coordinate system*}

TempRArm = [RELB, RELB-RUPA,RSHO-RUPA,zyx]

TempLArm = [LELB, LELB-LUPA,LSHO-LUPA,zyx]

If \$Static == 1 Then

REJC = (RELBM + RELB)/2

LEJC = (LELBM + LELB)/2

\$_REJC = REJC/TempRArm

\$_LEJC = LEJC/TempLArm

PARAM(\$_REJC)

PARAM(\$_LEJC)

EndIf

REJC = \$_REJC*TempRArm

LEJC = \$_LEJC*TempLArm

Appendix A (continued)

```
{*Wrist joint centers*}  
RWJC=(RWRA+RWRB)/2  
LWJC=(LWRA+LWRB)/2
```

```
{*Hand offsets*}  
RHandOS = ($MarkerDiameter + $RHandThickness)/2  
LHandOS = ($MarkerDiameter + $LHandThickness)/2
```

```
{*=====*}  
{*KINEMATICS*}  
{*=====*}
```

```
{*Segments*}  
{*-----*}
```

```
If Exist (STRN) Then  
Torso = [UTorso,UTorso-LTorso,BTorso-UTorso,zyx]  
Else  
Torso = [UTorso,UTorso-T10,BTorso-UTorso,zyx]  
ENDIF
```

```
If Exist (T10) Then  
Torso = [UTorso,UTorso-LTorso,BTorso-UTorso,zyx]  
Else  
Torso = [UTorso,UTorso-STRN,C7-UTorso,zyx]  
ENDIF
```

```
RUpperarm = [REJC,RSJC-REJC,RUPA-REJC,zxy]  
LUpperarm = [LEJC,LSJC-LEJC,LUPA-LEJC,zxy]
```

```
RForearm = [RWJC,REJC-RWJC,REJC-RSJC,zxy]  
LForearm = [LWJC,LEJC-LWJC,LEJC-LSJC,zxy]
```

Appendix A (continued)

RWrist = [RWJC,REJC-RWJC,RWRA-RWRB,zyx]

LWrist = [LWJC,LEJC-LWJC,LWRA-LWRB,zyx]

RHJC = RFIN + (RHandOS*RWrist(1))

LHJC = LFIN - (LHandOS*LWrist(1))

RHand = [RWJC,RWrist(3),RHJC-RWJC,yxz]

LHand = [LWJC,LWrist(3),LHJC-LWJC,yxz]

```
{*=====*}  
{*Joint Angles*}  
{*=====*}
```

```
{*Caculated Euler floating angles*}
```

TorsoAngles = -<Global,Torso,xyz>

RShoulderAngles = <Torso,RUpperarm,yxz>

LShoulderAngles = <Torso,LUpperarm,yxz>

RElbowAngles = <RUpperarm,RForearm,yxz>

LElbowAngles = <LUpperarm,LForearm,yxz>

RWristAngles = -<RForearm,RHand,yxz>

LWristAngles = -<LForearm,LHand,yxz>

```
{* Forearm pronation and supination*}  
{* Rotation around the z-axis so consider z component (3)*}  
RForearmRotation = -<RForearm,RWrist,yxz>  
LForearmRotation = -<LForearm,LWrist,yxz>
```

```
{*KINETICS*}  
{*=====*}
```

```
{*Upper Body Anthropometric Data*}
```

```
{*This data is from Winter (1990) Chapter 3 Anthropometry, Biomechanics and Motor  
Control of Human Movement, Second Edition*}
```

```
{*University of Waterloo, Ontario, Canada, pages: 56, 57*}
```


Appendix A (continued)

AnthropometricData

AnthroHand 0.006 0.6205 0.223 0

AnthroForearm 0.016 0.57 0.303 0

AnthroUpperarm 0.028 0.564 0.322 0

AnthroTorso 0.355 0.63 0.31 0

EndAnthropometricData

{*Define the hierarchy for the Upper Body Kinetics*}

Torso = [Torso, AnthroTorso]

RUpperarm = [RUpperarm,Torso,RSJC, AnthroUpperarm]

LUpperarm = [LUpperarm,Torso,LSJC, AnthroUpperarm]

RForearm = [RForearm,RUpperarm,REJC,AnthroForearm]

LForearm = [LForearm,LUpperarm,LEJC,AnthroForearm]

RHand = [RHand,RForearm,RWJC,AnthroHand]

LHand = [LHand,LForearm,LWJC,AnthroHand]

{*Adjust for Prosthesis weight(SC122707)*}

{* If statement to allow definition of prosthesis on right or left side*}

{* CoM of forearm and hand portion of the prosthesis calculated from one sample prosthesis using the suspension test*}

{* CoM location = length from distal end of principal axis of segment/ total length of segment*}

{* CoM of forerarm = 19/27; CoM of hand = 10/17*}

{* Direct definition of mass properties used *}

{* Moment of inertia data the same as in table above from Winter but adjusted to fit direct definition format*}

{* $I = mr^2$; therefore Mass of prosthetic segment * (radius of gyration (from table above-3rd number) 2 *)}

{* If \$Prosthesis == 1 Then

 If \$ProsthesisR == 1 Then

 RForearm =

 [RForearm,RUpperarm,REJC,\$ProsthesisForearmMass,{0,0,\$CoMForearm},\$ProsthesisForearmMass*{0,0.091809,0}]

 RHand =

 [RHand,RForearm,RWJC,\$ProsthesisHandMass,{0,0,\$CoMHand},\$ProsthesisHandMass*{0,0.049729,0}]

 Else

 LForearm =

 [LForearm,LUpperarm,LEJC,\$ProsthesisForearmMass,{0,0,\$CoMForearm},\$ProsthesisForearmMass*{0,0.091809,0}]

Appendix A (continued)

```
LHand =  
[LHand,LForearm,LWJC,$ProsthesisHandMass,{0,0,$CoMHand},$ProsthesisHandMass  
*{0,0.049729,0}]  
  EndIf  
EndIf* }
```

```
{*Create reaction for Door force transducer*}  
{*Set a variable in marker file to determine right or left handed*}
```

```
OptionalReactions(ForcePlate1)  
If $Lefthanded ==1
```

```
  DoorTransducer=ForcePlate1(2)
```

```
  ForceDirect=[LHCM,LSJC-LHCM,LWRA-LWJC,zxy]
```

```
  DoorTransducerNew={DoorTransducer(1),DoorTransducer(2),DoorTransducer(3  
)}*Attitude(ForceDirect)  
  ForcePlate1=|DoorTransducerNew,ForcePlate1(2),{LHCM(1),LHCM(2),LHCM(  
3)}|  
  CONNECT(LHand,ForcePlate1,1)
```

```
ELSE
```

```
  DoorTransducer=ForcePlate1(2)
```

```
  ForceDirect=[RHCM,RSJC-RHCM,RWRA-RWJC,zxy]
```

```
  DoorTransducerNew={DoorTransducer(1),DoorTransducer(2),DoorTransducer(3  
)}*Attitude(ForceDirect)  
  ForcePlate1=|DoorTransducerNew,ForcePlate1(2),{RHCM(1),RHCM(2),RHCM(  
3)}|  
  CONNECT(RHand,ForcePlate1,1)
```

```
Endif
```

```
{*Create a Reaction for box*}  
{*The dummy force must be entered in the .mp file or subject measurements if run  
through Plug In Modeller*}  
{* Box is 5 lbs which converts to 2.268 kg*}
```

```
DummyForce = {0,0,2.268*(9.81)}  
DummyMoment = {0,0,0}
```

Appendix A (continued)

{*This relates the force to the Body Segments:ReactionForce is the force applied*}
{* to the segment, and the ScalarTest set on with a value of 1. *}

ReactionRWrist = REACTION(RHand)
ReactionRElbow = REACTION(RForearm)
ReactionRShoulder = REACTION(RUpperarm)

ReactionLWrist = REACTION(LHand)
ReactionLElbow = REACTION(LForearm)
ReactionLShoulder = REACTION(LUpperarm)

{*ReactionBox=|DummyForce,DummyMoment,BOX|*}

{*CONNECT(BOX,ReactionBox,1)*}

{*OUTPUT*}

{*Joint Centers*}
OUTPUT (RSJC,LSJC,REJC,LEJC,RWJC,LWJC,RHJC,LHJC)

{*Angles*}
OUTPUT (TorsoAngles)
OUTPUT (RShoulderAngles,LShoulderAngles,RElbowAngles,LElbowAngles)
OUTPUT (RWristAngles,LWristAngles,RForearmRotation,LForearmRotation)

{*Output Joint Forces (1) and Moments (2)*}

RWristForce = ReactionRWrist(1)
RWristMoment = ReactionRWrist(2)
LWristForce = ReactionLWrist(1)
LWristMoment = ReactionLWrist(2)

RElbowForce = ReactionRElbow(1)
RElbowMoment = ReactionRElbow(2)

LElbowForce = ReactionLElbow(1)
LElbowMoment = ReactionLElbow(2)

RShoulderForce = ReactionRShoulder(1)
RShoulderMoment = ReactionRShoulder(2)

Appendix A (continued)

```
LShoulderForce = ReactionLShoulder(1)
LShoulderMoment = ReactionLShoulder(2)
Output(RWristForce,LWristForce,RElbowForce,LElbowForce,RShoulderForce,LShoulderForce)
Output(RWristMoment,LWristMoment,RElbowMoment,LElbowMoment,RShoulderMoment,LShoulderMoment)
```

```
{*DISPLAY*}
{*This calls up the macro to display the segments*}
AXISVISUALISATION(Torso)
AXISVISUALISATION(RUpperarm)
AXISVISUALISATION(LUpperarm)
AXISVISUALISATION(RForearm)
AXISVISUALISATION(LForearm)
AXISVISUALISATION(RHand)
AXISVISUALISATION(LHand)
AXISVISUALISATION(Global)
```

Appendix B: Solution to an Open Chain 2D Example Problem

- no resistance to motion at the terminal segment
- forces only due to gravity and occur at center of mass of each segment \otimes
- based on a 150 lb. (68.04kg = BM) person with the following measurements:
 $L_{\text{humerus}} = 0.22 \text{ m}$; $L_{\text{forearm}} = 0.20 \text{ m}$; $L_{\text{hand}} = 0.18 \text{ m}$
- $g = \text{gravity} = 9.8 \text{ m/s}$
- uses anthropometrics from D.A. Winter [17,18]: humerus:0.28BM; forearm:
 0.016 BM ; hand: .006BM
- drawing not to scale

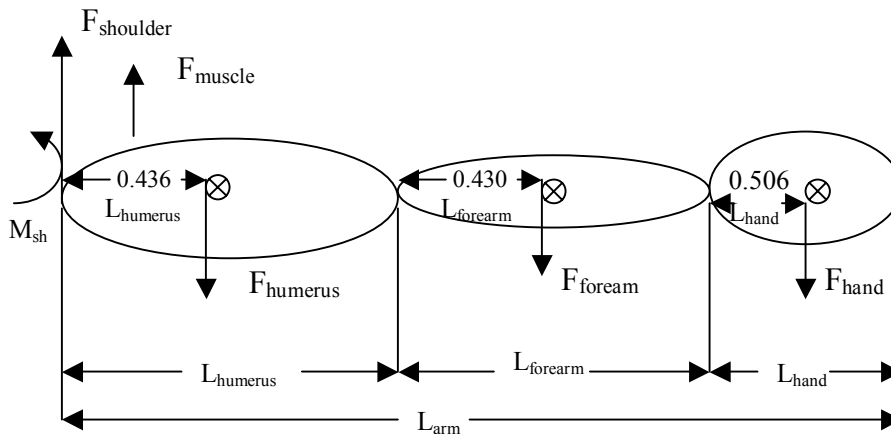


Figure B.1. A free body diagram of the arm.

$$L_{\text{arm}} = L_{\text{humerus}} + L_{\text{forearm}} + L_{\text{hand}}$$

$$M_{\text{shoulder}} = F_{\text{humerus}} (0.436 L_{\text{humerus}}) + F_{\text{forearm}} (L_{\text{humerus}} + 0.430 L_{\text{forearm}}) + F_{\text{hand}} (L_{\text{humerus}} + L_{\text{forearm}} + 0.506 L_{\text{hand}})$$

$$M_{\text{shoulder}} = (18.68)(0.09595) + (10.67)(0.306) + (4.00)(0.51108)$$

$$M_{\text{shoulder}} = 7.1017 \text{ N/m}$$

$$F_{\text{shoulder}} = F_{\text{humerus}} + F_{\text{forearm}} + F_{\text{hand}} - F_{\text{muscle}}$$

$$F_{\text{humerus}} = .028(\text{BM})g$$

$$F_{\text{forearm}} = .016(\text{BM})g$$

$$F_{\text{hand}} = .006(\text{BM})g$$

$$F_{\text{shoulder}} = 18.68 + 10.67 + 4.00 = 33.35 \text{ N}$$

From static trial, of person with the subject parameters used in this calculation

$$F_{\text{shoulder}} \text{ in x-direction} = 33.55 \text{ N}$$

About the Author

Stephanie Lutton Carey received a Bachelor's degree in Engineering Science from the University of Florida in 1996, and a Master's degree in Biomedical Engineering from the University of Miami in 2000. She worked for the Miami Project to Cure Paralysis as a research associate. Stephanie was married to Craig Carey in October 2000, and worked as a customer trainer and systems engineer for Peak Performance Technologies, Inc., a motion analysis company in Colorado. She also taught various mathematics courses at Front Range Community College in Boulder. She started at the University of South Florida in the fall of 2003. She taught Foundations of Engineering each semester while pursuing her doctoral degree and gave birth to son, Jack, in September of 2004 and to daughter, Amelia, in April of 2007. While attending USF, she has presented her research at several conferences for both engineering and prosthetics.